



(51) International Patent Classification:

G01N 33/48 (2006.01) **C12Q 1/68** (2006.01)
G01N 35/00 (2006.01)

(21) International Application Number:

PCT/US2009/054781

(22) International Filing Date:

24 August 2009 (24.08.2009)

(25) Filing Language:

English

(26) Publication Language:

English

(30) Priority Data:

61/091,036 22 August 2008 (22.08.2008) US

(71) **Applicants** (for all designated States except US): **AZTE ARIZONA TECHNOLOGY ENTERPRISES** [US/US]; Sky Song, 1475 North Scottsdale Road, Suite 200, Scottsdale, AZ 85257 (US). **THE UNIVERSITY OF WASHINGTON** [US/US]; 4311 11th Avenue NE, Suite 500, Seattle, WA 98105 (US).

(72) Inventors; and

(75) **Inventors/Applicants** (for US only): **HOLL, Mark** [US/US]; 1522 E. Southern Avenue, #1146, Tempe, AZ 85282 (US). **MELDRUM, Deirdre** [US/US]; 3902 E. Bronco Trail, Phoenix, AZ 85044 (US). **ANIS, Yassir** [EG/US]; ASU Biodesign Institute, Center for Ecogenomics, 1001 S. McAllister Avenue, Tempe, AZ 85287

(US). **ASHILI, Shashanka** [—/US]; ASU Biodesign Institute, Center for Ecogenomics, 1001 S. McAllister Avenue, Tempe, AZ 85287 (US). **HOUKAL, Jeff** [US/US]; 1013 W. 17th Place, Tempe, AZ 85281 (US). **JOHNSON, Roger** [US/US]; 1331 E. Townley Avenue, Phoenix, AZ 85020 (US). **KELBAUSKAS, Laimonas** [LT/US]; 889 E. Stottler Drive, Gilbert, AZ 85296 (US). **LI, Yongzhong** [CN/US]; 3689 E. Sundance Avenue, Gilbert, AZ 85297 (US). **MERZA, Saeed** [—/US]; ASU Biodesign Institute, Center for Ecogenomics, 1001 S. McAllister Avenue, Tempe, AZ 85287 (US). **NANDAKUMAR, Vivek** [IN/US]; 1265 E. University Drive, #3004, Tempe AZ 85281 (GB). **SMITH, Dean** [—/US]; ASU Biodesign Institute, Center for Ecogenomics, 1001 S. McAllister Avenue, Tempe, AZ 85287 (US). **YOUNG, Cody** [US/US]; 117 E. Loma Vista Drive, Tempe, AZ 85282 (US). **TIAN, Xanqing** [CN/US]; 900 N. Rural Road, #1094, Chandler, AZ 85226 (US). **ZHU, Haixin** [CN/US]; 4144 W. Bart Drive, Chandler, AZ 85226 (US). **CHAO, Joseph** [—/US]; ASU Biodesign Institute, Center for Ecogenomics, 1001 S. McAllister Avenue, Tempe, AZ 85287 (US).

(74) **Agent:** **WEBSTER, Mary, S.**; Nixon Peabody LLP, 401 9th Street, N.w. Suite 900, Washington, DC 20004 (US).

(81) **Designated States** (unless otherwise indicated, for every kind of national protection available): AE, AG, AL, AM, AO, AT, AU, AZ, BA, BB, BG, BH, BR, BW, BY, BZ,

[Continued on next page]

(54) **Title:** INTEGRATED, AUTOMATED SYSTEM FOR THE STUDY OF CELL AND TISSUE FUNCTION

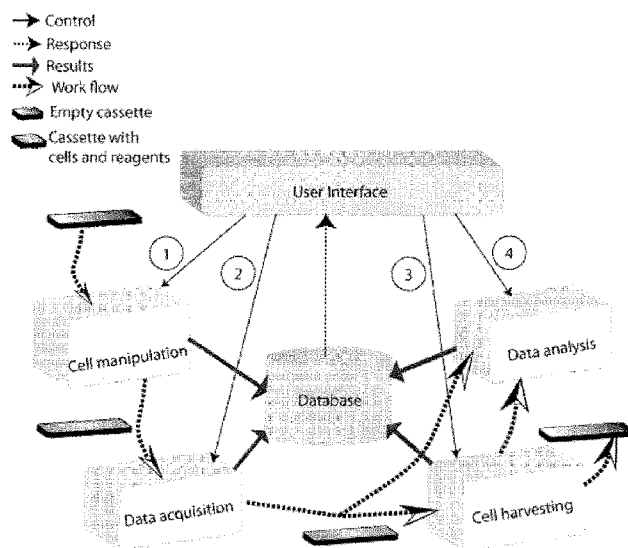


Figure 1A

(57) **Abstract:** The present invention provides for an automated, high-throughput, multi-parameter integrated analysis system to monitor, in parallel, cellular parameters descriptive of cell function and associated physiology both singly and in interactions with other cells in tissues. Parameters may be measured with cell or tissue samples confined in arrays of chambers microfabricated in cassettes. System variants provide for cell or tissue harvesting for (optionally destructive) further analysis. The present invention relates to a system for biological laboratory automation, providing for full automation of cell manipulation using capillary micropipettes and associated robotics. This invention provides a robust and flexible technology that can be deployed in research and corporate laboratories, enabling new experimental protocols. Applications include microinjection and high-throughput, single- to multi-cell, multi-parameter monitoring of parameters such as respiration rates, moiety of interest concentrations, metabolic fluxes, chemotactic gradients, gene expression and transcription, translation to proteins (intracellular, membrane, and extracellular), membrane integrity, and cellular ion gradients.



CA, CH, CL, CN, CO, CR, CU, CZ, DE, DK, DM, DO, DZ, EC, EE, EG, ES, FI, GB, GD, GE, GH, GM, GT, HN, HR, HU, ID, IL, IN, IS, JP, KE, KG, KM, KN, KP, KR, KZ, LA, LC, LK, LR, LS, LT, LU, LY, MA, MD, ME, MG, MK, MN, MW, MX, MY, MZ, NA, NG, NI, NO, NZ, OM, PE, PG, PH, PL, PT, RO, RS, RU, SC, SD, SE, SG, SK, SL, SM, ST, SV, SY, TJ, TM, TN, TR, TT, TZ, UA, UG, US, UZ, VC, VN, ZA, ZM, ZW.

(84) Designated States (*unless otherwise indicated, for every kind of regional protection available*): ARIPO (BW, GH, GM, KE, LS, MW, MZ, NA, SD, SL, SZ, TZ, UG, ZM,

ZW), Eurasian (AM, AZ, BY, KG, KZ, MD, RU, TJ, TM), European (AT, BE, BG, CH, CY, CZ, DE, DK, EE, ES, FI, FR, GB, GR, HR, HU, IE, IS, IT, LT, LU, LV, MC, MK, MT, NL, NO, PL, PT, RO, SE, SI, SK, SM, TR), OAPI (BF, BJ, CF, CG, CI, CM, GA, GN, GQ, GW, ML, MR, NE, SN, TD, TG).

Published:

— *without international search report and to be republished upon receipt of that report (Rule 48.2(g))*

INTEGRATED, AUTOMATED SYSTEM FOR THE STUDY OF CELL AND TISSUE FUNCTION

5 FEDERAL FUNDING LEGEND

This invention was made with government support under Grant 5 P50 HG002360 awarded by the National Institutes of Health NHGRI Centers of Excellence in Genomic Science. The U.S. government has certain rights in the invention.

10 RELATED APPLICATIONS

This application claims the benefit of U.S. Patent Application Ser. No. 61/091,036, filed August 22, 2008, incorporated herein in its entirety.

FIELD OF THE INVENTION

15 The present invention relates to automated laboratory equipment. More specifically, the present invention provides for the full automated framework for cell manipulation and analysis using microfluidics, optics or other sensors, and associated robotics, allowing for high-throughput assessment of cell physiology in multiple contexts and formats with high precision and minimal invasive artifacts.

20

BACKGROUND OF THE INVENTION

Laboratory automation is a classic instance of high throughput automation. It is a rapidly developing technology which poses several difficult challenges such as high throughput, efficient information management, and multi-disciplinary automation tasks, to name a few.

25 Analysis of cell physiology at all levels stands to benefit from laboratory automation. More specifically, research on single cells includes high throughput procedures such as cell selection, real-time data acquisition for stimulus/response experiments, and end point analyses such as PCR. These analyses require high precision in operation and measurement, and generate large volumes of data. In order to achieve these objectives it is essential that the development effort
30 for a high throughput automated system for single cell analysis be based on a well-defined architectural approach, and be implemented within a clearly defined framework.

In general, commercially available automation systems provide for microplate-based cell culture, microplate-based measurements, and microplate-based fluidic manipulations. These comparatively massive fluidic volume systems are well suited to bulk cell culture screening.

35 They are notably ill-suited, however, to a broad class of critical research and development

activities that examine the intricacies of cell function at the range of related complexities, from single cells to tissues.

Commercially available cell manipulation systems provide a limited degree of automation and integration through the ability to assign programmed operations to destination rows and columns within microwells on a microplate. This macro-scale programmability of protocols using the microplate format is utilized to assemble large-scale robotic platforms for the pipetting of fluids, incubation, and readout of a response. For bulky measurement of averaged responses to changes in environmental stimuli having larger averaged response times, such systems are suitable. There remains a need, however, for biological laboratory instruments that offer superior automation for high throughput assessment of cell physiology in multiple contexts and formats with high precision and minimal invasive artifacts.

SUMMARY OF THE INVENTION

The present invention provides for a systematic approach to implement a sophisticated automation pipeline for high-throughput analyses of living cells. The invention is embodied in the form of a system architecture that has been designed to perform high-throughput analysis of single cells in which each cell may be considered as an individual sample for investigation. Enabled by the single cell analysis function, the system also addresses creation and analysis of structured small populations of similar or differing cell types. The described system architecture is designed to be modular, extensible and flexible, with well-defined specifications for flow of control and information management. These benefits enable development, maintenance and enhancements of the integrated system. The architecture is generic and broadly applicable to laboratory automation, providing a core technology that enables novel analysis systems for interrogation of living systems.

Although this technology has broad applicability, one demonstration of its utility can be to address biological questions that probe cellular heterogeneity. Heterogeneity underlies most failures of current therapies for cancer. In order to realize the promise of genomics in curing major diseases, it is necessary to develop precise tools for multi-parameter analysis of single cells, and apply these tools to the understanding of biological questions characterized by cellular heterogeneity. The process of discovery required can be enabled with high-throughput multi-parameter integrated systems to monitor in parallel cellular parameters such as respiration rates, gene expression, protein expression, cytokine expression, membrane integrity, and ion fluxes and gradients, for example.

The embodiments of the invention provide for system architectures useful for the characterization of single cells and cell-cell interactions using an automated system capable of performing tasks with minimal operator interaction in a high-throughput manner, and providing for the analysis of cell's responses to stimuli. The described hardware and software system architectures are designed to be modular, extensible and flexible, with well-defined specifications for flow of materials, control, and information management. High-throughput automation demands a well-defined paradigm for system integration. The software required for hardware operation and data acquisition, storage and analysis needs to be efficient with regard to memory consumption and execution time. These objectives can be achieved by having a well-defined software hierarchy that incorporates structured programming concepts and methods along with clearly defined hardware-software interactions.

One embodiment of the invention provides a system comprising an analysis cassette, a cell loading module, a multi-parameter analysis module, and an end-point analysis module. In this embodiment of an application that uses the integrated pipeline for the study of cell and tissue function, an analysis cassette is prepared for cell loading. The cell loading module selects and loads individual cells or a plurality of cells into an analysis cassette; cell selection may be based on any number of parameters of interest for the purpose of study design. Generally, the loaded cassettes are then incubated to rest the cells before analysis to remove any residual loading effects from the subsequent study. The cassettes are then placed in the multi-parameter stimulus/response analysis system module for automated analysis. Full fluidic stimulus control is automated, as are all scan and data acquisition and storage. After the multi-parameter analysis is complete, the cassettes are transferred to the end-point analysis module. Interfaces for end-point analyses are automated in this example module. As an example, two end-point analyses such as: (a) quantitative PCR, for example LATE-PCR, and (b) capillary-based 2-D electrophoresis might be automated. The analysis cassettes may then be recycled or disposed of according to good laboratory practices.

Another embodiment of the present invention provides for closed-loop feedback control to fully automate cell manipulation using capillary micropipettes and associated robotics. In this embodiment, cell selection, cell-micropipette positioning, placement, and release are fully automated. This technology fulfills a fundamental need in the biological laboratory automation arena: allowing high-throughput analysis of cell physiological response extending from individual living cells, 2-D and 3-D cell structures (artificial tissues), and tissue biopsies in a highly controllable micro-environmental context. The invention addresses configurations that enable the study of intercellular communication via signaling molecules. It is a robust and

flexible technology that can be deployed in research and corporate laboratories, enabling new experimental protocols.

Still another embodiment provides for an automated system that places one or more cells in chambers that can alternately be opened or closed. An array of chambers is included as an element of an analysis cassette. The chambers can be perfused when open with any media or stimulus of choice. When closed, the chambers are sealed, and the depletion or accumulation of moieties of interest can be observed using sensors or sensor chemistries within the chambers. The chamber enables the measurement of metabolic rates of production and consumption of chosen analytes. For example, when the chamber materials are impermeable to oxygen and other gases, gas consumption and production rates can be measured. In other embodiments, the chamber and lid materials may be permeable to gases and impermeable to other molecules of interest (e.g., extracellular proteins) and can be used to measure the accumulation or depletion of these with appropriate sensor selections.

The present invention thus provides an automated system that measures, in parallel, the stimulus response of cells in structured populations down to the single cell level. A distinguishing characteristic of this parallel measurement platform is that each cell in the population may be isolated within a closed volume only a few times larger than the cell itself. The same approach applies to small microscale simulated tissues or organized cell structures. This technique enables the rapid quantification of a variety of molecules without the need to label the cell, avoiding any labeling-related effect on cell behavior. The instrument does not, however, preclude the use of standard labeling methods which may be used in conjunction with cell isolation.

DESCRIPTION OF THE DRAWINGS.

Figures 1A - 1F relate to architectural models and work flow for embodiments of the present invention. These models for implementing the automation incorporate modularity, extensibility, platform independence, and user-friendliness. Figure 1A includes steps that may be used in this embodiment: (1) select and load cells; (2) acquire multi-parameter data; (3) harvest cells and perform end-point analyses; and (4) analyze acquired data. Figure 1B presents one possible automation framework for single-cell analysis. Figure 1C, panel (a) coarse entity classification; panel (b) fine entity classification; panel (c), module and device constitution; panel (d) protocol between entities; and panel (e) control hierarchy for modules and devices in an embodiment of the invention.

Figure 1D depicts a generic system architecture for automated, high throughput, multi-process systems. Figure 1D illustrates the modular design and the structured arrangement of hardware and software, based on Developmental view model of UML. Figure 1E shows an example flow of control for a constituent sub-system for any/every automation task. The high-level instruction is given by the end user at the User Interface. This is processed by the Automation manager which routes the instruction to the relevant Engine in the appropriate sub-system. The Engine operates the necessary devices using a toolbox. Figure 1F illustrates details of an example system model of the present invention, including (a) The various entities, (b) Logical view illustrating the composition of a module and a device, (c) Logical views depicting the interaction paradigm for the system model.

Figures 2A-2K show examples and aspects of a robotic workstation for cell selection and placement. Figure 2A is a schematic showing the front view of the system depicting main hardware components for a particular embodiment. Figure 2B shows a side view of the cell selection workstation as seen from the direction "←A" of Figure 2A. Figure 2C is a model view of a multi-parameter stimulus/response analysis system platform showing: piston and related motion stages, fluid manifold and related motion stages, fluid delivery and full integration with a microscopy-based optics interface. Figure 2D shows a photo of the system platform from Figure 2C. Figure 2E shows a fluid manifold that interfaces with an analysis cassette. Two tangs located on either end of the jaws constrict upon the cassette when engaging and both align and hold the cassette against its fluid gasket. A cylindrical motor drives the jaws together via rack and pinion assembly. Figure 2F is a photo of the fluid manifold holding a cassette. The clear fluid management block mounted to the top of the manifold allows for delivery of selected stimuli into different macro-wells of the cassette independently. Figure 2G is a photo of the piston and driver motors. The square motor at the top drives the piston and subsequent lid, into contact with the cell containing chamber. A force gauge, located in line between the motor and the piston, delivers feed back control to the software which controls the force on the lower substrate of the cell chamber. Figure 2H is a photo of the piston block containing the force gauge and piston rotation motor. The force gauge wire-bundle comes out near the top of the photo. The cylindrical object to the right side of the piston is the rotation motor. This allows for subsequent rotation of the lid. Figure 2I is a photo of the motor that lifts the fluid manifold and cable routing tray that manages wiring bundles during automated motions. Figure 2J is a photo of the fluid delivery pump and selector valves. The peristaltic pump supplies a constant flow rate to the fluid and manifold, and thus the analysis cassette. The selector valves allows selection of different stimuli (shown here between one and eight). Figure 2K is a photo of the analysis

region. The small hole in the plate provides access to optical train for microscopy-based photon excitation and subsequent multi-parameter signal emission collection. The small opening size provides maximum chamber substrate support when clamping forces are applied.

Figures 3A-3D depict various contemplated embodiments of cell containers (e.g., analysis cassettes holding microwells) useful in the present invention. Figure 3A is a photo of analysis cassette and a close up of a microwell-array. The fully assembled cassette contains bonded halves, a cell chamber microwell-array containing substrate, fluid interface gasket, and associated bonding means. Figure 3B shows a model of unassembled cassette, top view. Channels in lower half of cassette allow for fluid transport. Small strip gasket in upper part of picture is adhered using pressure sensitive adhesive. The cell chamber microwell-array containing substrate in the lower part of picture is bonded to cassette using UV curing adhesive. Figure 3C shows a model of unassembled cassette, bottom view, and close-up of macro-wells. Rectangular notches in cassette allow for alignment. Raised strips on lower cassette half allow for optical planarity and management of loads and moments of the cassette in relation to the optical excitation and detection trains. Macrowells provide a fluid chamber above the microwell-arrays. Macrowell geometry allows for bubble purge and fluid exchange. Figures 3D shows more detailed construction of an example analysis cassette also incorporating provision for electrical analytic means.

Figures 4A-4E show various possible embodiments of microwell arrays. Figure 4A is an embodiment of a microwell array with nine microwells, showing example dimensions. Figure 4B depicts a magnified view of each compartment showing 81 microwells and a sample oxygen measurement configuration using a Platinum-porphyrin sensor. Molter et al., *Algorithm advancements for the measurement of single cell oxygen Consumption Rates*, in PROC. IEEE-CASE, 386-91 (2007). Figure 4C depicts a microwell array with a gasket, cover, and piston configured to allow parameter analysis via the quartz window aligned with the chip holder. Figure 4D is an illustrated sectional view of an example microwell holding a single cell for analysis. The Example in Figure 4D illustrates a glass barrier lid that is impermeable to gas transport. Figure 4E shows a schematic of a fused silica substrate, fixed to the bottom of a petri dish. The substrate includes nine microwell arrays, each consisting of nine microwells.

Figures 5A-5D are illustrations of several example chamber concepts suitable for containing and analyzing cells in the present invention. These chambers include lid structures for hermetically sealing the subject chamber, creating a chamber in which individual cells may be sealed from external exposure using a microwell-array base, lid, and piston system. Also shown are means of sensor detection (optical, electronic) and thermal control. Figure 5A shows

a lid structure comprising the actuator, a compliance layer, an impermeable layer, and a permeable layer with embedded bead-based sensors; and a base comprising microfabricated thermal heaters and in-chamber microelectrodes for detection of cell response.

Figure 5B shows a lid with rigid actuator, compliance layer, and impermeable barrier layer (shown as gold); and a base with features identical to those of Figure 5A with an optical sensor added to the cell chamber. Figure 5C shows a simplified base having a stress-concentrating well circumference structure with an optical sensor. Figure 5D shows the same configuration as Figure 5C minus the stress concentrating circumferential ridge.

Figures 6A-6F show several example embodiments of components of a multi-parameter analysis system, that includes a cell manipulation and loading module. Figure 6A is an example of LabVIEW-based GUI control software that enables both manual and automated control of the cell pickup and placement processes, showing the different software controls. Figure 6B is an example of image processing and object recognition sequence of operations for microparticle selection and positioning, showing both the micropipette tip and microparticles in the same horizontal plane: (a) is a grayscale 8-bit monochrome image; (b) shows morphological image processing; (c) shows recognized microparticles in the image plane; (d) shows a microparticle positioned at the pipette tip. Figure 6C depicts a 3×3 array of microwells loaded with eight live cells. Diamonds enclose these live cells. Figure 6D shows a 3×3 microarray of microwells loaded with one polystyrene bead in each microwell. Figure 6E is a flow chart presenting the automated cell placement sequence of cell selection, positioning, aspiration, and dispensing. Figure 6F is a block diagram of the automated cell-micropipette positioning control system using vision feedback. Figure 6G is a concept illustration of the device in action as a series of steps.

Figure 7 is a schematic of an example micropipette capillary tip, showing example dimensions, useful to aspirate and deposit single living cells.

Figure 8 is a system hardware schematic illustrating the physical connections between hardware components in a particular embodiment. Several types of communications cables are used, but they all feed into the personal computer to be controlled by the automation software. The hashing indicates the environmental chamber space. The optical path is also discernable: beginning with the light source and ending at the camera.

Figure 9 is a diagram illustrating the optical train of a possible embodiment of the multi-spectral imaging platform. AOTFs may be used to replace the discrete filter wheels.

Figure 10 shows the software organization for an automation program implemented using the aforementioned system architecture. Each hardware device is controlled by a C# object

which is an instantiation of an engine. The Experiment Engine object is an instance of the Automation Manager. The Experiment Designer object is part of the GUI and is used to aid the user in outlining experimental procedures. The arrows indicate the flow of control for the various objects.

5 Figure 11 is a drawing showing hardware placement in an embodiment of the present invention.

Figure 12 shows a schematic representing the control of fluids to and from the analysis cassette in an embodiment of the invention.

Figure 13 presents an example control of fluids for cell extraction for end-point analysis.

10 Figure 14 is an exploded internal side view of a particular embodiment of a fluid routing and control cassette that interfaces with the analysis cassette and method of manufacture and materials thereof.

Figure 15 shows an example of how an analysis cassette may be moved through an automated system such that individual, single cells are analyzed at the end of the experiment for their instantaneous composition (e.g., mRNA or protein content).

Figure 16 represents an example of automation robotics with fluid control devices and additional hardware that comprise the multiparameter analysis instrument module.

Figure 17 presents an overview of an example architecture that allows for automated living cellular assays.

20 Figure 18 is a flow chart description of example instrumentation and software associated with a platform for an automated living cellular assay.

Figures 19A and 19B are flow diagrams for the assembly processing for embodiments of an analysis cassette. Figure 19B shows an assembly process utilized in cassette assembly for cassette of Figure 3A thru 3C.

25 Figures 20 presents an example logic flow for conducting an automated analysis of a single biological cells in cell microwell-array analysis configurations.

Figure 21 is a fluorescence microscope image of a 3 x 3 array with a Pt-OEP sensor, showing the position of the wells and stress-concentrating circumferential ridges of the chambers.

30 Figure 22 is a fluorescence microscope photograph of a 3 x 3 array with a Pt-OEP sensor and wells containing cells.

Figure 23 depicts an alternative embodiment of a LabVIEW-based GUI control software that enables both manual and automated control of the cell pickup and placement processes, showing the different software controls.

Figure 24 is a flow chart presenting automated cell placement sequence of operations with cell positioning, aspiration, and dispensing inner loops in an embodiment of the present invention.

Figure 25 shows the planes for automatic system calibration showing the substrate plane, p_s , the micropipette plane, p_t , and the microscope object plane, p_o .

Figures 26 is a flow charts presenting the automated sequence of operations for cell selection, micropipette positioning, and aspiration of a biological cell.

Figure 27 is a block diagram of the automated cell-micropipette positioning control system using vision feedback in an embodiment of the invention.

Figure 28 is a flow chart presenting the automated sequence of operations for cell dispensing in an embodiment of the invention.

Figures 29A-29D are micrographs showing the automated selection and positioning of single live cells in a culture dish. Figure 29A is a bright field image of a micropipette tip and three BE cells; Figure 29B is a thresholding, image subtraction and processing; Figure 29C depicts cells recognition; Figure 29D is the positioning cell at tip orifice.

Figures 30A-30F are micrographs showing steps in the automated dispense of a single cell into a microwell. Figure 30A shows an empty well where a cell is to be dispensed. Figure 30B shows the micropipette orifice lowered into the empty microwell. Figure 30C shows a cell being dispensed. Figure 30D shows the micropipette being displaced upwards. Figure 30E shows image processing to inspect the presence of a cell. Figure 30F shows that a single cell is detected in the well.

Figure 31 is a micrograph of a 3 x 3 microwell array in which each microwell is occupied by one cell.

Figure 32 presents micrographs relating to the effect of the incubation time on a single cell, showing stretching and adhesion to the substrate: indicating cell viability. Panel 32A before incubation; Panel 32B after 30 minutes; Panel 32C after 2 hours.

Figures 33A and 33B reflect oxygen consumption measurements derived from single biological cells. Figure 33A: Eight CP-C cells were loaded in a 3 x 3 array of microwells and incubated for 16 hr under physiological conditions prior to and during the experiment. Figure 33B shows an example data processing and analysis: a bi-dose-response fit to one of the curves shown. The calculated bi-dose-response rates for O_2 consumption are 0.17 fmol/min/cell and 1.32 fmol/min/cell. Figure 33B-Bottom: Residuals from the fit.

Figure 34A and 34B show oxygen consumption measurements in single cells. Insets in Figure 34A are micrographs of corresponding microwells containing CP-C cells (the structures

Figure 35 shows p53 gene transcription in single-cell qRT-PCR in CP-C cells. Figure 35A presents real time RT-PCR running curve; Figure 35B shows PCR samples and their corresponding threshold Ct values in Figure 35A; Figure 35C is an image of an agarose gel analysis of the Figure 35A PCR mixture.

15 DETAILED DESCRIPTION

As used herein and in the claims, the singular forms “a,” “an,” and “the” include the plural reference and equivalents known to those skilled in the art unless the context clearly indicates otherwise. Other than in the operating examples, or where otherwise indicated, all numbers expressing quantities of ingredients or reaction conditions used herein should be understood as modified in all instances by the terms “about” or “approximately.”

10

applicants and do not constitute any admission as to the correctness of the dates or contents of these documents.

5 The present invention provides for a robotic manipulation system for automated selection and transfer of living cells, or an individual living cell, of interest to analysis locations in a series of operational components comprising an integrated system for the analysis of cell metabolism and gene expression at the single cell level. The present embodiments address a specific set of integrated system requirements comprising the placement of single cells in analysis locations, the analyses of these cells throughout application of external stimuli, and post stimuli end-point analyses of these same cells. The same framework and integrated system can be directly
10 extended to automate cell-to-cell, multiple cell, and tissue analyses. In one embodiment, the system control software and the automation manager system backbone was developed using principles from Unified Modeling Language (UML) to maximize potential for integration with other standard laboratory automation systems. Figure 1A presents an overview of desired automation pipeline for single-cell analysis from end user's perspective.

15 In examining the intricacies of cell functions and cell-to-cell interactions, an integrated and automated system for cell selection, placement, environmental control, and analysis is required. This system presented herein has fundamental attributes that enable such high-fidelity procedures to be performed at the single-cell level. By extension, and using the unique capabilities of the invention disclosed herein, one-cell after the next may be selected and placed
20 at desired locations with high precision, thereby enabling assembly of cell-to-cell interaction studies, and by extension micro-scale simulated tissues for examination of normal- and disease-state responses to drug or antagonist compounds, as one example. Further applications of the claimed system logically extend its novelty to tissue dissection at single-cell spatial dimensional scales. Notable examples of merit include for example, microsurgery on mouse oocytes for
25 single cell extractions, microsurgery on microtumors or segments of tumors for study of the genetic of clonal expansions, and so forth. For such surgical operations the need to target (analytically select) and perform precise manipulations (surgical extractions) rapidly and with minimal invasive artifacts is critical. The invention disclosed herein, and substantially reduced to fully functional form, defines within clear boundaries a new and unique system capability of
30 broad and deep scientific merit and practical applied impact.

As an example of how the present invention differentiates from current and common technology, we examined in general traditional methods of microplate-based cell manipulations and analysis. As noted previously, some commercially available cell manipulation systems provide limited automation and integration based on programmed well destination locations

within microplates. For the measurement of large cell populations' averaged responses to changes in a particular stimulus, such systems are reliable, rugged, and appropriate. The present invention, while most certainly maintaining the requirements of reliability and rugged performance in continued use, is distinctly different from all commercial solutions available in the following ways of direct contrast. The present system has, by design, the ability to drive both spatial manipulation control, temporal stimulus control, and temporal measurement resolution one or two orders of magnitude below that of existing systems. Therefore, the present invention is transformational in its impact and by definition highly novel in design and protocol enablement capability. Such protocol enablement is only possible within a well defined and carefully conceived architecture, designed specifically for full closed-loop integrated, automated control.

Effective automation requires the design of an architectural model of the system to be automated. As used herein, the nomenclature for *system architecture* and *framework* along with the details of the system model, are important for an understanding of the several embodiments. The terms *architecture* and *framework* are defined along the lines of the definitions in the IEEE standard on systems and software engineering, *Systems & software engineering - Recommended practice for architectural description of software-intensive systems*, ISO/IEC 42010 IEEE Std 1471-2000 (2007). Thus, as used herein, *Architecture* is a structured arrangement of components with well-defined functionality along with the protocols that define their interactions. An *architecture* can be either software or hardware architecture, or a combination of both. A *framework* is a design that utilizes a set of well-defined components to accomplish a specific task according to a well-defined methodology. A framework instantiates an architecture to accomplish a specific task.

According to this architecture, the integrated system of the present invention is broadly modeled as a structured organization of hardware and software entities (see Figure 1F). Hardware entities are either components or devices, while software entities are either modules or methods (Figure 1C, panel b). All these entities are heritable, i.e., they can be used repeatedly and simultaneously by multiple other entities. A *component* is a hardware unit which forms the token element of architecture. Every component has a definite function and is identified by a set of control parameters that define its operation. An experimental procedure may involve one or more components; a *device* is a collection of components, and is associated with a specific experimental procedure. Every experimental procedure that is performed by a device consists of a set of tasks, each of which is performed by a component; a *method* is a software construct that directs a hardware component of the architecture to perform a specific task. A method may

either control the physical operation of a component (for instance, as a device driver), or manipulate the function of a component (for instance, as an algorithm) by altering its control parameters. A component may have one or more methods associated with it; a *module* is a collection of similar or interrelated methods, and hence is also a software entity. A module
5 encapsulates all the methods to control a device and accomplish a specified procedure. A module may also drive another module; a *protocol* is a set of rules prescribing how two entities communicate or interact with each other. This protocol is also defined in methods. These guidelines demonstrate the application of structured programming principles which are a standard for software systems development and are also applied herein in principle to hardware
10 systems design.

An embodiment of the system architecture (*see* Figure 1D), a framework, is structured using the Developmental and Physical views from UML 2.0. Miles & Hamilton, Learning UML 2.0 (O'Reilly Media, 2006). The Developmental view details the organization of a system into its constituent components, while the Physical view describes the system design. The
15 integrated system is organized into independent sub-systems. Each sub-system has a well-defined functionality, consisting of the devices (hardware) and their associated modules (software) to execute the tasks that define functionality. The integrated system for biological cell analyses can be realized by customizing the generic architecture in order to seamlessly integrate the different hardware and software tools (Figure 1B). The devices within each sub-system are
20 operated by methods defined in a module referred to as Engine. For example, as in Figure 1B, the integrated system consists of four sub-systems: the cell-manipulation system, the real-time data-acquisition system, the analysis system, and the cell-harvesting system. Additional sub-systems can be added to this architecture if needed, without affecting the overall system.

The tasks to be performed by a sub-system are defined in methods that are present in
25 another module known as a Toolbox. The Engine accesses the appropriate method (as per the instructions from the user) from the Toolbox and accordingly drives the relevant device of the sub-system to execute the given task. The data associated with a sub-system is stored in a database (a module). Data can be either control data (to operate a device) or result data (generated from a device). The data manipulation to- and from the database is performed by the
30 Engine. The various constituent sub-systems are managed by a two-tier software. This software consists of two modules: a Graphical User Interface (GUI) which serves as the interface for the end user to communicate with the system, and an automation manager that routes the specifications given by the user via the GUI to the relevant sub-system to perform the required tasks. More specifically, the automation manager provides the necessary control signals to the

appropriate engine to execute the instruction(s). The GUI is the only module that is accessible to the end user (as denoted by the user abstraction layer in Figures 1B, 1D and 1E); the rest of the modules are abstracted. An example flow-of-control for this architecture is illustrated in Figure 1D.

5 Various sub-systems may constitute the architecture (shown in Figure 1B) for single-cell analyses. Functional specifications guide the development of the respective sub-systems. A cell manipulation sub-system consists of the tools needed to move, sort and place the cells in the appropriate positions, and to introduce appropriate quantities of reagents and other essential media into the analysis cassette. The hardware may include, for example, pumps, valves, mixers,
10 motion stages, optics, and glass micropipettes. Optical tweezers or micropipettes, etc., are also suitable approaches for cell manipulation. The pumps and valves are used to control fluid (media) flow in the cassette, the mixer mixes the reagents and the cells according to the stipulations of the experiment, and the micropipette or optical trap is used to move and place the cell in the appropriate locations on the cassette. All these devices are controlled by the cell
15 manipulator engine and its toolbox. The toolbox consists of algorithms for identifying, sorting and placing cells at the appropriate locations on the cassette. It may also include algorithms for generating specific patterns for reagent deposition on, and cell removal from, the cassette. A particular embodiment of this subsystem is described in detail below, providing an example of specific subsystem elements that may be suitable for other dependent sub-systems.

20 A data acquisition sub-system contains the tools needed to provide appropriate excitation signals, and subsequently capture and process data from the experimental procedures. The toolbox for this sub-system contains methods for signal generation, cassette movement, data acquisition, and environment regulation around the cell-containing cassette. The hardware devices may in the most general configuration include: signal sources (e.g., chemical, electrical,
25 photonic) to generate control/excitation signals, environmental-control to sustain the cells (by regulating temperature, gas concentrations and humidity around the cassette), positioning stages, optical measurement instrumentation (e.g., microscope, excitation/emission filters), and data acquisition devices (e.g., data acquisition cards, electronic cameras or PMTs to capture images, sensors to measure oxygen/ion/pH concentration, and patch clamps for electrophysiological
30 measurements). The data-acquisition devices are controlled by a data-acquisition engine, which also stores the collected data in the central database, from whence it can be retrieved for either analysis or visualization. Data may be in the form of digital images, or digitized analog data from sensors (electrical or optical measurements), or could be from any of the hardware devices

including those that are used in the post-processing stage (such as PCR). The toolbox for this system contains all the algorithms for acquiring data.

As an example embodiment, experiment level, highly interactive semi-automation has been demonstrated to record oxygen consumption from live cells maintained in the cassette.

5 Molter et al., Proc. IEEE-CASE, 386-91 (2007). Full automation embodiments are presented herein. Automation for generation of photonic excitation signals, cassette motion and manipulation (e.g., microwell sealing), and the acquisition of data from microscopes and sensors in the vicinity of the cell in the cassette are useful additions to this module.

An analysis sub-system may contain only software modules. The constituent engine
10 performs analyses on the data (raw or preprocessed) generated by the data-acquisition sub-system from the experimental procedures. It executes the algorithms stored in the analysis toolbox. Such analysis may be performed either online or offline. The analysis toolbox forms the core module for data analysis. It contains all the functions necessary to analyze the data acquired from the experimental assay. Functions include mathematical operations (such as regression,
15 curve-fitting, and optimization), statistical computations; algorithms for signal and image processing, signal and image analysis, data-mining and pattern classification, and performance evaluation methods (such as goodness of fit). Analyses associated with high-throughput systems typically involve large volumes of data. Hence, it is important that the toolbox be designed to maximize efficiency with regard to time, and memory, especially if the analyses need to be
20 performed online. The algorithms in the toolbox should, as such, be optimal with respect to execution time and convergence speed.

A cell harvesting sub-system module is composed of the tools required to extract cells from the microwells of the analysis cassette, and transport them to the appropriate locations either for further analysis using molecular analysis methods, or for disposal. Example analyses
25 include DNA and mRNA analysis via single-cell PCR techniques; and protein signature analysis at the single-cell level using, for example, multi-dimensional electrophoretic techniques. The hardware components of this sub-system have many similarities in robotic manipulation functionality to the cell manipulation sub-system. The associated toolbox contains techniques to suitably extract the cells from the cassette after the multi-parameter experiment, and move them
30 to appropriate end-point analysis devices (which interface to the data acquisition sub-system), and subsequently to disposal.

Software useful for this instance of the system may include a Graphical User Interface (GUI), which serves as the interface for the end user to communicate with the system to perform the experiments. This interface contains options for data visualization, data generation, database

access, execution of standard experimental assays/protocols, specification of custom protocols, and tutorials for assistance on experiments and error handling.

An automation manager module may serve as the interface between the GUI and the sub-systems. It forms the backbone of the software architecture because it translates the high-level user commands to specific system-level commands that can be understood by the Engines, and vice-versa. This module processes the specifications given by the user via the GUI and provides the appropriate control signals to the relevant sub-system(s) to perform the required tasks. The automation manager also routes the results generated by sub-system(s) to the database for storage and back to the GUI for observation. The automation manager has the capacity to access (read and write) the database for data interpretation and analysis operations. Thus, it serves as the master control for all the operations that need to be performed on the system.

A database serves as the repository for all the data associated with the operations executed by the engines. The stored data can be accessed by all the Engines and the automation manager. The end user can access the database via the automation manager. This device stores data generated by the sub-systems, and also data input from the user. Experiments conducted for cellular analysis typically generate large amounts (up to and exceeding terabytes) of data. To handle this data load, it is important that the database has sufficient capacity and is systematically managed using well-defined data-management schemes.

Thus, the system architecture presented herein serves as a blue-print for high throughput cell analysis systems development and integration. The automation framework details the constituent aspects for high throughput analysis of single cells which is a complex engineering problem. The complexity of the problem is attributed to the sampling scale of the experimental procedures, the requisite precision in experiments and measurements, and the large volume of data (generated from the various experiments) which needs to be rapidly analyzed. A way to approach such a complex systems problem is to systematically model the system. Once this architectural model is in place, the implementation of the systems integration can be managed effectively by adhering to the architecture. This is a core problem solved by the present embodiments.

It should be noted that, in addition to particular reductions to practice, the design of the invention is novel. The specification of this instance describes in detail the various aspects of high throughput, automated single-cell analysis, and provides and uses standardized and well-defined nomenclature, and a comprehensive system model that provides specifications for hardware, software and their interactions. It incorporates the automation pipeline in addition to describing the system architecture.

Novel aspects of this invention provide several advantages including: (1) Modular design that enables easy maintenance and trouble-shooting. It also makes the system robust to sub-system failure. (2) Extensible architecture that enables enhancements to hardware and software without disturbing existing system set-up. (3) Standardized modeling methods facilitate rapid system development and easy communication between system designers and software programmers. (4) Easy integration with other automated systems. (5) User friendliness. The end user interacts via the user interface (GUI) and is abstracted from the intricacies and complexities of the system. This is especially beneficial for personnel that are not conversant in computer science. (6) Information management: The incorporation of database management into the system enables easy access and systematic storage of experimental data and analysis results. (7) The system model remains consistent at all levels of abstraction. This limits ambiguity in terminology across successive layers of abstractions.

An embodiment of the system architecture is shown in Figure 1D. The architecture includes system structure and constituent functionality: The integrated system is organized into independent sub-systems. Each sub-system has a well-defined functionality, consisting of the devices (hardware) and associated modules (software) to execute the tasks that define functionality. The devices within each sub-system are operated by methods (such as device drivers or APIs) defined in a module referred to as Engine. The tasks to be performed by a sub-system are defined in methods that are present in another module known as a Toolbox. The Engine accesses the appropriate method (per end user instructions) from the toolbox to drive relevant device of the sub-system to execute the given task. The data associated with a subsystem is stored in a database (a module). Data can be either control data (to drive a device) or result data (generated from a device). The data manipulation to and from the database is performed by the Engine. Information management and control of the various subsystems are managed by a two-tier software. This software consists of two modules: a graphical user interface (GUI) which serves as the interface for the end user to communicate with the system, and an automation manager that routes the specifications given by the user via the GUI to the relevant sub-system to perform the required tasks. The GUI is the only module that is accessible to the end user (as denoted by the user abstraction layer in Figure 1D), and the rest of the modules are abstracted.

The flow of control for input (from the user end), output (system response), and one-way access is illustrated in Figure 1D. The high-level instruction is specified by the end user at the user interface. This instruction is processed by the automation manager which routes the equivalent machine-level commands to the relevant Engine in the appropriate sub-system. Once

the task is accomplished, the appropriate results are subsequently provided to the user at the user Interface via the automation manager and the associated Engine(s).

The integration or system framework for single cell analyses can be realized by customizing the generic architecture discussed herein in order to seamlessly integrate the different hardware and software tools (Figure 1B). The integrated system consists of four sub-systems: the cell-manipulation system, the data-acquisition system, the analysis sub-system, and the cell-harvesting system.

Although the discussed automation and integration has focused on single-cell analyses, the same modeling principles can be applied to automate more complicated investigations such as multiple-cell analyses, cell-to-cell interaction analyses, tissue analyses, and microsurgery applications. The experimental methods and multiparameter analyses to be performed for these scenarios are direct extensions of the described architectural model, with the only difference being in the scale of the experiments, the generated data, the dimensionality of the analyses, and the complexity of the devices (hardware) required to implement specialized protocols. This extensibility is attributed to the usage of a standardized model and modeling tools (UML, for example) and the lack of dependence of the system model on system complexity. Thus, this novel framework can be extensible to systems requiring additional complexity.

The novel automation system is envisaged to provide significant improvements in resource utilization, personnel requirements, and throughput for cell manipulation, cell harvesting, data acquisition and analysis. 'Development time' is an objective evaluation metric, measured in units of man-hours. Development time is defined as the time spent to accomplish a particular operation using the integrated system. The operation in this context is assumed to have sufficient complexity to exploit the power of automation.

Benefits accruing from automation may be evaluated using metrics such as increased productivity and profit. Productivity improvement reflects on resource utilization, personnel requirement and system throughput, while profit relates to monetary savings. We choose evaluation metrics for their direct relation to productivity and profit increases:

Productivity improvement (η , expressed as %):

$$\eta = \left(\frac{man_hours_{manual} - man_hours_{automated}}{man_hours_{manual}} \right) \times 100$$

Profit (P, in units of currency):

$$P = (man_hours_{manual} - man_hours_{automated}) \times (unit\ man_hour\ fee)$$

High values of these metrics reflect productive, profitable automated systems. These metrics are generically applicable to the evaluation of automation systems. The current invention is intended to result in high values of these metrics.

5 A framework for automating cellular analyses was created in response to a need in the current state of the art. The objective of this framework is to formalize a systematic, well-defined specification towards the realization of an integrated, automated system for biological cell and tissue analyses. The framework discussed herein focused on single-cell analyses, but is extensible to multiple-cell analyses, cell-to-cell interaction analyses and tissue analyses. The framework design described herein as a preferred embodiment was developed using principles
10 of a universal systems modeling tool, namely UML, and can therefore be easily integrated with existing laboratory automation systems. The use of a standardized modeling tool is intended to enable systematic and rapid systems development because it is substantially freed from dependencies on platform and software language. The architecture for the framework is modular and extensible. The proposed system architecture can be tailored to suit a broad array of
15 laboratory automation requirements. An objective performance evaluation metric has been provided, which can be used to evaluate any automated system. The specification of this instance of an example embodiment also details the software hierarchy and flow-of-control, the constituent sub-system specifications and their resource requirements (if any). These guidelines enable the software design to be robust while still being user friendly. The multi-tier
20 organization of the software is envisaged to facilitate troubleshooting, and to assist end users who are not adept in programming.

The application of these objectives are reflected in another embodiment of the present invention which provides for an integration of user interface, device control, data acquisition and analysis for automated multi-spectral imaging of single biological cells. This approach also
25 provides an integrated system for single cell, multi-parameter analysis that will allow users to monitor numerous parameters pertaining to a cell and its surrounding environment simultaneously to aid in the understanding and characterization of cellular pathways, including metabolic and signaling pathways. The present automation solution differs from others by specialization to the study of selected individual biological cells, structured cell studies, and
30 cell-to-cell interaction analyses, in contrast to cell populations ("bulk cell analysis" methods), for which solutions already exist. One component of this effort is the development of approaches for the study of metabolic rates associated with controlled cell stimulus. Oxygen metabolism is an example metabolic rate of interest. Stimuli acting on a cell can cause that cell to select one of many biological pathways. Understanding the cellular pathways that link a cell's phenotype to

its genotype is an important step in the process of developing better methods of diagnosing and treating such ailments as heart disease, stroke and cancer. This embodiment emphasizes oxygen metabolism measurement to illustrate elements of the automated system development.

Prior to the automation software design developments presented herein for one example embodiment, it was required that the experimentalist operate numerous individual pieces of hardware and isolated software applications in an orchestrated sequence. In some cases the lack of a user-friendly interface required the operator to directly manipulate source code to adjust system parameters, introducing the possibility of user error. The purpose of the automation software is to integrate a plurality of components into a cohesive system controlled from a unified interface. In one embodiment, the software integrates a motorized microscope, imaging device, and peripheral devices necessary for isolation of biological cells and controlling gas compositions inside microwell arrays. These integrated, peripheral devices include a lid actuator to provide a hermetic seal, and a gas manifold which supplies the desired gas mixtures. The software obviates the need to simultaneously operate several devices either physically and/or through multiple control and data acquisition programs. In one example embodiment it incorporates the ability to run MATLAB scripts, eliminating the need for the user to learn and operate MATLAB separately. The burden on the operator in obtaining data and results is therefore reduced, and the speed and veracity of information acquisition are increased.

Regarding the hardware associated with one embodiment of the present invention, the fully automated living cell array analysis platform allows metabolic rate measurements to be conducted with higher throughput and minimal user interaction. Various modular subsystems of this platform designed such that they may mount on a standard inverted microscope base (Figures 2A, 2B, and 2C). Regarding Figure 2C thru 2K, the manipulator comprises high-resolution linear translation stages to transport and align the analysis cassette with the optical axis of a microscope base. Another set of rotation and translation stages serve to align a lid with microwell arrays containing cells. A fully-automated array scanner, such as the example embodiment shown, facilitates measurement of metabolic rates in a multi-parameter fashion. This may include a fluorescence laser scanner module for highly-sensitive, spectrally-resolved multi-parameter confocal fluorescence detection. For example, this module may be optimized for inverted microscopes and coupled through a side port. In other example embodiments, it may be adapted to suitable microscopes with infinity-corrected objective lenses by replacing the relay lens inside the scanner module.

Another approach to sensor design employs micro flow-through electrodes for the purpose of measuring media properties. These electrodes may be used to detect, for example,

pO₂, pCO₂ and pH of the liquid in a microfluidic system. An advantage of these electrodes (Lazar Research Labs., Inc., Los Angeles, CA), is their ability to connect in-line in any fluidic system, which provides the opportunity to monitor various parameters continuously. The average dead volume of these electrodes is about 80 µL. In one aspect, both pO₂ and pCO₂ electrodes are polarographic based devices. In the platform structure, peristaltic pumps can be connected both upstream and downstream to the flow of cell media/buffer through a chamber (e.g., a petri dish). The electrodes are connected downstream in series to monitor, for example, pO₂, pCO₂ and pH. The whole fluidic system can be connected by, for example, low gas permeable Tygon tubing.

One aspect of the present invention addresses a set of needs to demonstrate subsystem functionality and integrated component function for single-cell biological experiments using a novel method of isolating cells by sealing them within glass chambers and observing the subsequent response. Example hardware components used in this system are (1) microscope; (2) a miniature cell incubator, (3) glass chips with micro-arrays of lipped wells organized in arrays, (4) lid actuators which seal the wells, and (5) gas manifolds which control the content of gases that enter the wells. In all embodiments, a light emitting diode (LED) (Lumibright Light Engine, Innovations in Optics, Woburn, MA) may be used for the excitation source, coupled with a pulse generator (BNC 555, Berkeley Nucleonics Corp., San Rafael, CA) specifically for oxygen consumption measurements. Molter, *Automation of Single Cell Oxygen Consumption Experiments*, MSEE THESIS (Univ. Washington, Seattle, 2006); Molter et al., 5 IEEE Transactions Automation Sci. & Engin. (2008).

Regarding spectral imaging, a multi-spectral imaging system may include an ANDOR iStar Intensified Charge Coupled Device (ICCD) (Andor Tech. PLC, Belfast, UK). Control of this camera can be achieved using a software development kernel provided by ANDOR for the C# programming language. The iStar was selected for its high bit depth resolution, built-in digital delay generator, and other features that enable it to be used for high fidelity fluorescence intensity measurements and phosphorescence decay time constant measurements.

In this aspect, the micro-arrays consisted of 1 × 1 cm microfabricated glass devices (die) containing arrays of micro-wells. These micro-well array devices were fabricated on 3-inch borosilicate glass wafers using standard photolithography and etching techniques. Many microwell-array configurations have been developed. Each microwell-array version examined the performance achieved when varying the numbers of arrays per die and the number of wells per array. Every microwell in an array of this embodiment had a 3 µm high lip which encircles the top in order to minimize sealing contact area and allow for maximum seal pressure with

minimum applied force. For oxygen consumption experiments, sensors in the form of rings lining the circumference of the bottom of each microwell were fabricated. Each sensor ring comprising fused set of polystyrene beads, with each bead having platinum-porphyrin embedded within it. Wafer level deposition of sensors was used to enable a simple and efficient process for
5 the creation of numerous wells with sensors in parallel.

A lid actuator can be employed so that metabolic rate experiments can be conducted under conditions where the microwell-array chambers are alternately sealed and opened with respect to moieties of interest and the external macrowell environment. When closed, a fixed volume is maintained during the experimental time interval. In this case, the sensor monitors the
10 concentration of dissolved oxygen in the cell media as it is consumed by the living cell. If the microwell-array chambers are not sealed, then external oxygen in the media in the macrowell can enter the chamber and perturb the measurement.

In order to produce an isolated system whereby a single cell is trapped in a microwell, a glass "lid" is pressed down onto the top of an array of microwells. This glass-on-glass seal must
15 produce a complete oxygen barrier. To this end, it was experimentally determined that a force of 4.5 kg was adequate to insure an adequate seal. It was also found that it is very important that the force used be precisely repeatable. To achieve this objective within the automation system development, a load cell was used. To compensate for small but expected manufacturing tolerance variability, a PDMS compliance layer between the force application piston and the
20 glass seal may be used.

This lid actuator device may be automated and controlled remotely. For example, it may be manipulated via an input/output card (I/O card) (National Instruments, Austin, TX). A solenoid actuated gas control valve manifold may be used to automate sensor calibration methods. The manifold may be supported with switching system and interface for solenoid
25 driver electronics compatible with digital I/O. Tubing may connect the manifold to tanks of gas containing, for example, oxygen, carbon dioxide, nitrogen, antagonist or therapeutic gases, or combinations thereof. Using an I/O card to communicate to the system, TTL logic signals can automatically turn on and off the miniature solenoid valves that control the different gas flows.

The sensors in the sensor array of the present embodiment may be calibrated using
30 multivariate calibration techniques. These techniques or other similar methods to be used in order to take advantage of multiple sensors with selected primary- and cross- sensitivities to moieties of interest. The sensor(s) may be placed in spatial configurations depending on the optics or other considerations known to those of skill in the art.

The fundamental base/lid/sensor design may also be used to observe cell populations in 2-D formats of a suitable size. In general, the lid may be single or multiple use and is intended to be replaced on command automatically. A wide variety of base and lid configurations are possible within the scope of this invention as enabled by the automation system. The present
5 embodiment is ideally suited for the measurement of intracellular and extracellular physiological response of living cells to external stimuli using optical, mechanical, chemical, or electronic, or electrochemical sensor transduction means.

Besides a broadband light source, high-power LEDs capable of fast switching may be used for fluorescence lifetime decay measurements. The LED may possess 750 mW optical
10 power and may emit light in the violet spectrum (395 nm). Custom-built electronics may be constructed to provide the current necessary to drive the LED in addition to interfacing it with a pulse width generator to provide accurate lifetime measurements.

An automated microscope may be used to remotely control the movement of the microwell arrays across the field of view and switching of dichroics for fluorescence
15 microscopy. This microscope may have the following features to facilitate multi-spectral imaging: (1) a movable stage, (2) an adjustable objective, and (3) a dichroic turret. This hardware eliminates the need of a separate stage. In combination with the discrete filters located within the external filter wheels, a plurality of filter-dichroic combinations may be realized. An environmental chamber may provide temperature, humidity, and gas compositional control.

Regarding system software for this example embodiment, the automation application
20 may be programmed in C#. Here, objects comprise both data and methods. The software consists of three primary components: the Main GUI object, an experiment designer object, and the experiment engine object. Device driver objects exist for all hardware systems. These include the camera object, the stage object, and the digital delay generator object, among others.
25 All objects are instantiated in the Main GUI object and are then used in the definition of other objects if they are needed to accomplish their task(s). For instance, the camera object may be passed to the photographer object, which acquires and saves images.

A GUI was developed to achieve a friendly user experience and increase effectiveness in the design and deployment of user defined experiments. The user interface GUI was
30 implemented using sound graphical-based interface concepts and controls common to many Windows Applications and therefore familiar to most computer users. Importantly, the application provides immediate real-time data display.

In one contemplated embodiment, the Experiment Designer may be the conduit through which the user's experimental procedure is translated into "machine code." Within this object

and GUI, the user may select a command from a selection of steps and existing procedures. For example, the user may modify a procedure using a set of control buttons, which include Add Step and Insert Step to create new steps along with Remove Step, Move Up and Move Down to change the chronological order of the steps. Previous procedures may also be included within the current procedure thus allowing for many experiments to be conducted with minimal user input. When a step is added, the appropriate parameters required for successful execution of the step may be entered via dialog boxes by the user. As steps and procedures are added and/or removed, an extensible markup language (XML) file may be updated accordingly. The GUI reflects the state of the XML file.

The structure of XML includes the identity of the class of the step: a pause as opposed to a repeat for instance. In addition, as children to the step, the parameters are also stored. A pause will therefore store the duration of the pause in units of time and a repeat will store the numerical value of the steps to be repeated and the number of times that should be repeated. Alteration of an experiment during runtime is an enabled interface feature.

Regarding the Experiment Engine, in one embodiment, when the user elects to run a specified procedure, an instance of the Experiment Engine may be created and passed all the objects instantiated in the main GUI. These may include, but are not limited to, the photographer, the lid actuator, and the MATLAB automation server. The primary component of the Engine is a method which reads the XML information and then performs the designated instruction.

In one contemplated embodiment, extensive use of switch statements may facilitate proper execution of the user-defined procedure. The name of the step may first be acquired from the XML file, specified by the user in the Main GUI, followed by the stored parameters. The parameters may then be used to perform the task directly or passed to the appropriate object. For instance, a pause step may use the set value to cause the program thread to sleep for the allotted amount of time. An 'acquire single scan' step may call the photographer object, however, which will in turn call the camera object to perform the action with the settings defined by the user. When the step is a procedure, another Experiment Engine object may be instantiated within the first, passed the necessary objects and so on. The possibility of recursion is therefore realized and can be utilized by the user.

Regarding the file structure in one contemplated embodiment, the large quantities of data acquired using the automation program necessitate its organization for facile retrieval by the user. Image data, in the form of photon counts, may be stored in ASCII files, extension *.asc. These files may be stored as an image indexed 001 through 999 in an experiment folder

numbered 001 through 999 which may be located in another folder named as the date the experiment was executed. Given *a priori* knowledge of the experiment, any image may be accessed by any MATLAB script or function for processing. The path of the most recent image may be passed to the MATLAB automation server for use by any MATLAB scripts. The path string may be stored in the imagePath variable.

In one embodiment of the present invention MATLAB modules provide a powerful technical computing environment to enable flexible algorithm development. Much of the system data may be processed with MATLAB scripts. Before converting these algorithms into C# code, the automation program may utilize MATLAB through its automation server to perform data processing. The ability to harness the versatility of MATLAB adds to the practicality of the automation program and increases flexibility. Access to the program source code is no longer required in order to integrate new image processing and data analysis algorithms. Once developed and validated, proven algorithms may be ported into C/C++/C# code.

A long-standing goal is the acquisition of real-time oxygen consumption data through analysis of porphyrin phosphorescence lifetime decay. The benefit behind real-time measurements is that the user can see if an experiment is proceeding on track or if there are any problems - cells have died, or if the microwell-array chamber seals are not functioning properly, for instance. In the event of errors, the user can abort the experiment and rectify the experimental setup problem before proceeding and losing valuable time.

One embodiment for oxygen consumption rate estimation is called optimized rapid lifetime determination (ORLD). Oxygen levels are calculated by acquiring two images with different exposure times after the excitation pulse has passed. Each image capture integrates over a variable time window at the two different time delays with respect to the excitation interval. The output of the MATLAB algorithm is a ratio of the integrated signal of the second window over the first. This ratio can be theoretically converted to a lifetime, but for practical purposes, the ratio can be used directly for a calibration curve.

In this same embodiment, for real-time measurements, a pair of images is taken and immediately processed by the MATLAB script. The script exploits the image path variable, passed from the automation program to the MATLAB server. Based on this information, the second to last image is located and processed. The data points are then plotted in a MATLAB figure and displayed for the user to examine. The process is repeated for however many pairs of images the user wishes. Typically, a pause is also placed between pair acquisitions. As data points are processed, they are added to the plots.

Automated cell counting is an aspect of this embodiment. The process of placement of cells into individual microwells is called "cell seeding". The objective of cell seeding is to attain as closely as possible the goal having one cell per microwell, thereby enabling dense data accumulation of single-cell statistics. In practice, using a process called random seeding, 5 microwells in general contain zero, one, or more cells. Classification of wells as containing cells and the number of cells present may be performed as an automated control in all such example embodiments.

To do this, an algorithm implemented in MATLAB was used to process the images via a number of image processing techniques. Using area, circularity, and other features, cells can be 10 identified and assigned to wells. McVittie et al., *Automated Classification of Macrophage Membrane Integrity Using a Fluorescent Live/Dead Stain*, IEEE Conf. Automation Sci. & Engin. (2007). The number of cells per well is then returned. Given this information, data analysis scripts can filter out erroneous information with minimal user feedback.

Furthermore, live/dead dyes can be injected into the cell media. Given the appropriate 15 excitation, dead cells will emit one wavelength of light and live cells another, or ratiometric spectral mixing combinations thereof. If the filters and dichroics are adjusted accordingly, the number of live and/or dead cells can be found in each well. This allows for the potential study of the effects of live cells on each other and the effect of dead cells on live ones.

Autofocus is an important aspect when analyzing single cells. In one embodiment, the lid 20 actuator exerts force on the lips of the wells in an array. If chamber substrate deformation occurs, then this substrate deformation needs to be compensated for by adjusting the objective in the z-plane to restore image focus. To perform the autofocus, a series of single scan images is taken at equal z increments. The objective must therefore be moved between images. Each image is then processed. The algorithm examines selected columns of the image matrix and 25 finds the variance of the photon counts. Bueno-Ibarra et al., *Fast autofocus algorithm for automated microscopes*, Optical Engin. (2005). The larger the variance, the more in-focus the image is. Upon finding the peak, or most in-focus image among the series, the automation program then adjusts the objective to the z-coordinate at which that image was taken.

This embodiment, as with the others described herein, provides versatility. The 30 integration of a MATLAB automation server greatly improves the versatility of the automation program. Access to the source code is no longer required to add measurement modules to C#. The measurement modules are readily available to the user and are no longer hidden in the background of the source code. The resulting flexibility allows full utilization of the flexibility of MATLAB, which provides various functions and algorithms

A particular aspect of the invention employs the principles of a commonly used cell transfer technique with many novel incorporations and entirely new adaptations. These example embodiments, share as a commonality the use of glass capillary micropipettes to aspirate and dispense cells. Using a closed-loop vision-based feedback control process, two individual three-axis robotic stages may be used to position the micropipette tip in proximity to the cell of interest. The cell is aspirated and the tip is moved to a target location, where the cell is dispensed. The target location for living cells of interest may be a microwell containing sensors that measure metabolic parameters. The system offers a robust and flexible technology for cell selection and manipulation. Applications for this technology include precise tools for multi-parameter analysis of single cells, cell patterning, tissue engineering, and cell surgery.

Another example embodiment of the invention provides for an automation platform for the manipulation and interrogation of biological organisms. This platform comprises a fully robotic system that allows for the optical, electrochemical or temperature sensing of single, or small groups of, prokaryotic or eukaryotic cells. This platform further comprises in its realization motorized stages, gear driven motorized assemblies, limit sensors, proximity sensors and other components that all contribute in part to the whole system. In one embodiment stages and motors are used to manipulate a disposable cassette that holds cells (such as human cells) in individually segregated microwells (a cassette). The cassette is moved from one measurement position to the next across a stationary optical detection train axis to perform multiple assays in a sequential manner using the same cassette. During an assay the cassette is engaged by a secondary subsystem of the platform which, using motorized stages and gear driven assemblies, applies a seal to the microwells, isolating and sealing the chambers where cells have previously been placed. An aspect of this embodiment relates to a fluid engagement unit. Using a single motor a dual rack and pinion moves two identical tapered teeth that simultaneously align, engage secure the Cassette. When secured, in one example embodiment, the Cassette is secured to a fluidic manifold for integral management of reagent delivery to macrowells of the analysis cassette and waste removal from the same.

Other embodiments include, but are not limited to: the use of piezo driven movement of the stages or other moving components, different detection techniques outlined below, different assay parameters (outlined below) and/or a reduction or addition of components that still allow the system to maintain its full functionality. Different detection techniques could include, but are not limited to: moving or scanning optics, electrochemical (in-microwell) sensors that transmit to external detectors, and thermal detectors to monitor the effects of minor environmental changes and thermal actuators to affect local environment temperature changes. Different assays

could expand from a single cell detection to include prokaryotic cell division where one could test what environmental conditions effect their multiplication. The configuration can also include a reagent delivery system that allows for exchange of various buffers, catalysts, stimuli or insults over the biological samples. Control of environmental conditions such as temperature, atmospheric gas concentrations and humidity can also be provided in the automation Platform. These controls simulate physiological conditions, reduce the variability between experiments and allow for a more realistic and well-characterized biological assay.

An embodiment of the invention provides a device comprising an analysis cassette, a cell loading module, a multi-parameter analysis module, and an end-point analysis module. The cell loading module selects and loads cells into the analysis cassettes; selection may be based on any number of parameters of interest for the purpose of study design. Generally, the loaded cassettes are then incubated to rest the cells before analysis to remove any residual loading effects from the subsequent study. The cassettes are then placed in the multi-parameter stimulus/response analysis system module for automated analysis. Full fluidic stimulus control is automated, as are all scan and data acquisition events and all data storage routines. After the multi-parameter analysis is complete, the cassettes are transferred to the end-point analysis module. Interfaces for two end-point analyses are automated in this module: (a) quantitative PCR, for example LATE-PCR, and (b) capillary based 2D electrophoresis. The analysis cassettes may then be recycled or disposed of according to good laboratory practices.

A particular aspect of the present invention provides the capability to automatically pickup a single cell from a culture dish, manipulate and move the cell to a specific microwell in a microwell-array, and finally release the cell into the selected microwell. Figures 4A-4C present a schematic showing an example of a microwell array, which includes nine microwells created on a borosilicate glass substrate. The loading process must be repeated successfully to include one cell in each microwell. A microwell-array, loaded with an single cells of analytic interest, can then be used for single cell analysis.

One embodiment of the present invention provides for a six-axis robotic system constructed to perform the cell manipulation process. The process is monitored using vision feedback, provided through a microscope and a charge-coupled device (CCD) camera. A glass capillary micropipette tip is used as the robot end effector to aspirate a cell suspended in a culture dish solution, and dispense the cell into the target microwell. The robotic system consists of two sets of three-degree-of-freedom (DOF) translation stages, an $X-Y-Z_t$ stage, and an $X-Y-Z$ stage, attached to an inverted microscope. The culture dish (cell source) and the microwell-array (cell target) are fixed to the $X-Y-Z$ stage, while the micropipette end effector is attached to the

X_r - Y_r - Z_r stage. The system controls the motion of both the X_r - Y_r - Z_r and X - Y - Z stages. Positive and negative pressures are applied to the micropipette, filled with fluid medium, through the use of a syringe pump and fluid tubing. A schematic showing the various components of the cell placement system is presented schematically in Figure 2.

5 The translation stages position the micropipette tip to address the cell or microwell, while the pump controls the aspiration and release. The system is constructed of three subsystems, a vision system, a motion control system, and fluid control system. The three subsystems are integrated together to enable manual or automated cell manipulation through the use of software.

10 In one embodiment, the vision subsystem consists of an inverted microscope (TE-2000U, Nikon, Tokyo, Japan) equipped with a $10\times$ objective (CFI Plan Achromat, Nikon) that has a numerical aperture of 0.25, and a working distance of 10.5 mm. Illumination may be provided through a 100 W Halogen light source (LHS-H100P-1, Nikon) driven by a 12 V power supply (TE2-PS100W, Nikon). Images may be captured by a high resolution FireWire digital CCD
15 color camera (Micropublisher 5.0, QImaging, Surrey, BC, Canada).

 Another aspect of the present embodiments is the motion control subsystem consisting of the X_r - Y_r - Z_r micropipette tip positioning stage (T-LS28-I, Zaber, Richmond, BC, Canada) and the X - Y - Z microscope positioning stage (MS-2000, ASI, Eugene, OR). The X_r - Y_r - Z_r stage may be controlled using a computer through serial connection and is used to align the tip of the
20 micropipette with the microscope objective in order to keep it in the microscope field of view and in focus. The vertical stage Z_r also controls the vertical displacement of the micropipette tip to and from both the culture dish and the microplate. The X - Y - Z stage may be either controlled manually using a joystick or through a serial connection. The X - Y stage positions the mounted culture dish and microplate in the horizontal plane, and the Z -stage is used to vertically move the
25 objective lens upwards and downwards, to bring objects to focus.

 Another aspect of the present embodiments is the fluid control subsystem consisting of a syringe pump (Versa 6, Kloehn, Las Vegas, NV) with a 10 μ L glass syringe (Kloehn). Using the 10 μ L glass syringe, the flow rate can be controlled between 0.01 μ L/s and 2 μ L/s, achieving a volume resolution of 0.2 nL. The pump is connected to the micropipette through
30 polyetheretherketone (PEEKTM) tubing of 1 mm inner diameter (ID), fittings, and connectors (Upchurch Scientific, Oak Harbor, WA). The pump is configured with a four-port rotary distribution valve, of which two distribution ports are used. One port is connected to the micropipette tip tubing (V_t) and the other is connected to a reservoir (V_R). Commercially available borosilicate glass micropipette tips may be used (MBB-FP-L-45, Humagen,

Charlottesville, VA) with 40 μm inner diameter (ID), an outer diameter (OD) of 50 μm , and with its tip angled at 45° , as shown in Figure 7. In order to have a clear optical view of the cell, before and during aspiration, the tip may be inclined at an angle between 0° and 5° with the culture dish bottom. As a practical matter, it may be optimal to use a positive inclination angle ($>0^\circ$), with a point contact with the dish bottom, rather than a (0°) angle with a line contact, because at larger angles ($>0^\circ$) the tip is more likely to bend than break.

Another aspect of the present embodiments provides for computer software useful in controlling the various components of the system. Computer software was developed, using LabVIEW v8.0 (National Instruments, Austin, TX), to control the various hardware components. A personal computer powered by an Intel Core 2 Duo processor was used providing 2.13 GHz of speed and 3.0 GB of memory. The graphical user interface (GUI), shown in Figure 6A, enables manual or automated control of the different stages of the cell manipulation process. The software consists of four modules working in parallel, operating the capillary tip positioning stage (X_t - Y_t - Z_t), the microscope positioning stage (X - Y - Z), the syringe pump, and the vision system. Operation of the two positioning stage modules includes the control of the absolute position and velocity of the stage motors. The position and speed of each stage motor is used as feedback information for the closed-loop control of the system.

The pump module controls the absolute position of the syringe piston, the velocity of the piston and thus the output flow rate, the piston acceleration, and finally the change of pump valve position settings between distribution valve ports (V_L), and (V_R).

The vision module controls the CCD camera settings and the acquisition of images. Images, once collected, are further processed to determine and correct for image focus, and object detection and identification. Camera initial setting controls are included for adjusting binning, exposure, and image type, whether colored (RGB) or grayscale. Image processing controls include brightness, contrast, gamma correction, and settings of upper and lower thresholds. Object recognition controls include the specification of maximum and minimum object sizes, aspect ratio, and search area. The vision module collects feedback information on the recognized objects. This includes the area, and the centroid position in the image frame used in the cell selection process.

When operated in full automatic mode the system coordinates the control of all software modules, collects available feedback data, and uses both closed- and open-loop control using the LabVIEW-based software. The objective of automatic operation is to achieve accurate cell manipulation with minimum human operator intervention.

The workstation provides a system to aspirate, manipulate, and dispense a single cell. For example, the cell may be dispensed into a microwell, where a microarray with microwells arranged in a 3×3 array is used. The microwell array has a pitch distance of 300 μm , well diameter of 100 μm , and well depth of 10 μm . A microwell may have a diameter as small as 20 μm .

Further regarding the microwells and analysis cassette, the analysis cassette, in addition to containing the cell containing substrate, also has several features that facilitate the automation of the sub-system. Different stimuli are delivered into the cassette via the manifold. A gasket, bonded to the topside of the cassette, interfaces with the fluid delivery manifold and prevents leakage. Channels in the cassette, seen in Figures 3B and 3C, pass fluid to the Macrowells (four large squares shown in figure). Design of the macrowells, Figure 3C, prevents bubble build-up in the wells, assuring complete wet-out of the macrowell. A constant height of fluid in the macrowell is maintained using a thin-slit construct that applies suction to the macrowell at a precisely defined macrowell chamber height. The thinness of the slit is critical to the function of the construct in maintaining fluid height with control to as small as approximately 0.2 mm height variance. *See* Figure 3B at the interface of fluidic channels with macrowells. Constant fluid height is maintained by application of vacuum to the thin-slit feature whereby fluid is precisely drawn from the fluid meniscus in a continuous manner during perfused operation. During static, un-perfused, operation the fluid level inside the macrowell is depressed in relation to the dynamic flow configuration. The thinness of the aspiration feature minimizes this effect to as little as approximately 0.2 mm. The aspirated fluid passes through the channels in the cassette, past the seal gasket, into the fluid interface manifold, and subsequently to waste.

Knowledge of the cassette position relative to the rest of the automation platform is critical. Registry features built into the cassette and corresponding features in the fluid interface manifold make this possible. Two rectangular notches cut into the lower portion of the cassette are picked up by tangs on the fluid interface manifold, Figures 2E and 2F. The horizontal tapers on the tangs position the cassette in one axis, the vertical tapers engage the cassette after horizontal alignment is assured and during engagement draw the cassette in and press the gasket against the fluid manifold. Upon completion of grip closure, the cassette is fully secured and prepared for automated motion on the analysis platform.

As the cassette and manifold are moved into a position where multi-parameter experiments can be performed, planarity and flatness of the cell constraining substrate are critical. Raised features on the underside of the cassette, Figure 3C, ensure that the substrate is planar with the surface on which it is set.

Concerning the process of cell aspiration, Figure 6E shows a flow chart that describes the sequence of operations through which a cell is aspirated and dispensed to a microwell. This process is repeated to place additional cells in microwells. The process begins with the initialization of the system. In this process the micropipette tip is translated to one of three

5 Z_r -positions, namely the culture dish bottom position (Z_{dish}), the microwell bottom position (Z_{well}), or its home position (Z_{home}). The system includes three inner loops for: (1) automated cell selection and positioning, (2) cell aspiration, and (3) cell dispensing. The process is repeated continuously until only one cell exists in each desired microwell.

In the initial set-up, a culture dish and microplate are mounted onto the microscope

10 X - Y - Z stage, and the micropipette tip is fixed on the X_r - Y_r - Z_t stage. The planes of focus of the culture dish bottom and the microplate are recorded, i.e., the Z -stage is positioned such that it brings both to focus. It is also necessary to determine the vertical distance between the planes of focus of both the culture dish bottom and the microplate, and the micropipette tip. This is performed through displacing the Z_r -stage, which carries the micropipette tip downwards until

15 the tip comes into focus or a contact is confirmed between the tip and the culture dish bottom, or the microwell bottom. The positions are recorded as (Z_{dish}) and (Z_{well}), respectively. It is important to completely flush out any fluids present in the fluid pump, tubing, and micropipette tip, in order to remove contaminated medium and air bubbles. During this process, the micropipette valve port (V_t) and the reservoir valve port (V_R) are controlled. With the valve port

20 (V_t) closed and (V_R) open, the pump withdraws fresh medium from the reservoir. When (V_t) is open and (V_R) is closed, the pump dispenses old medium and air bubbles out of the fluid circuit through the micropipette tip.

When suspended cells-in-medium solution is added to the culture dish, the cells sink to the dish bottom and tend to adhere to its surface. The aspiration of the cell starts by lowering the

25 micropipette tip to the vertical position Z_{dish} . At this position, the tip, dish bottom, and the cells to be aspirated are all in the same horizontal plane. The 3-D cell-tip positioning problem is reduced to a 2-D problem. To capture a single cell, the cell must be positioned with the micropipette end-effector tip in the horizontal plane. This is performed through the displacement of the X - Y stage, carrying the culture dish, in the X -, Y -directions, using images captured through

30 the camera as visual feedback.

Image processing and object recognition techniques are implemented in order to determine the positions of both the micropipette tip and all available cells in the image plane region of interest. This enables the determination of the relative positions between the micropipette tip and available cells. A single cell is selected based on some selection criteria,

which may include the cell size, its position in the field of view, and relative cell-to-cell positions. The selected cell, whose coordinates are calculated, is positioned in direct proximity to the micropipette tip using a closed-loop targeting algorithm. The block diagram of this vision-based feedback control system is presented by Figure 6F. The outer loop of the controller
5 utilizes an internal built-in closed-loop trajectory-driven algorithm. The *X-Y-Z* built-in controller accepts parameters as maximum velocity, and acceleration, while controlling the stage velocity. The output of the automated cell-micropipette positioning controller is an *X*-displacement, followed by a *Y*-displacement. This control loop is repeated until the distance between the micropipette tip and cell is less than a specified threshold distance.

10 Regarding fluid control, once the cell is aligned with the micropipette tip in the *X*, *Y*, and *Z* directions, aspiration can be performed. A negative pressure is applied to the micropipette capillary thereby generating a hydrodynamic force on the cell that pulls it inside. Strong adherence between the cell and the culture dish bottom surface may generate an opposing force, however, and may cause difficulties in the cell aspiration. To overcome these adhesion forces,
15 we proposed and implemented a method comprising the application of a pulse of positive pressure strong enough to displace the cell from an adhered state to a suspended state. The now non-adherent (suspended) cell is identified and an attempt to aspirate this cell into the capillary tip using negative pressure pulses is performed. This process is repeated a certain number of times (N_S) until the cell is successfully aspirated into the micropipette. If not, a new cell is to be
20 selected, as seen in the aspiration loop of Figure 6E.

Once the cell is aspirated, the *X*-, *Y*-, *Z*-, and *Z_r*-stages are translated using open-loop control, to position the micropipette tip with direct address to the desired microwell. Applying a series of small pulses of positive pressures dispenses the cell from the micropipette. Machine vision is used to detect the dispense of the cell at the end of each pressure pulse. This dispensing
25 process is repeated a number of times (N_D) until the cell is verified to have been dispensed and is in the target microwell (Figure 6E). All fluid flowing into and out of the micropipette is controlled to be gentle so as to not cause damage to the cell.

Central to the novel attributes of the cell manipulation system is the provision for ultraprecision control of fluid velocity profiles through the operation of drawing the cell into a conveyance chamber (or chambers), and, similarly, the ultra-precise control of fluidic velocity
30 profiles during the process of cell placement. These attributes enable heretofore unachievable fidelity in control of mechanical stimulus in cell manipulation. Terms otherwise used such as 'aspiration' and 'dispense' are by comparison inherently ill-defined and blunt. The same high

fidelity attributes for aspiration and dispense are central extensible attributes that are crucial to embodiments of the end-point-analysis module.

Monitoring metabolic rates at a single-cell level with simultaneous acquisition of multiple parameters enables the collection of unprecedented volumes of highly correlated data that is currently not possible with commercially-available systems. The present embodiment minimizes cell exposure to excitation light and permits, but does not require, internal cell labeling. High detection sensitivity and actively-controlled excitation intensity options reduce significantly potential sensor photobleaching rates and phototoxicity artifacts. System measurement accuracy is potentially increased by active excitation intensity monitoring and compensation. Multi-parameter data acquisition, designed specifically for single cell experiments requires integrated excitation and detection calibration procedures that can be used in non-imaging (cellular) and imaging (subcellular) modes; as well as in steady-state or time-resolved detection modalities. The invention also provides through these and other modalities for quantitative, multiple parameter, single cell monitoring for drug screening, disease pathways, metabolomics, genomics research purposes.

Detailed descriptions of data acquisition and sensor calibration procedures have been reported previously. Molter et al., 2008; Dragavon et al., 5 J. R. Soc. S151-59 (2008). For example, when using a Pt-porphyrin sensor to determine the oxygen concentration within a microwell, a phase modulation technique with a diode laser coupled the rear port of the microscope may be used to excite the oxygen sensor. An ICCD camera connected to the base port of the microscope can collect the emission signal. In another example embodiment, a digital light modulation microscope (DLMM) that utilizes a digital micromirror device (DMD) on an epifluorescence microscope configuration has also been developed and demonstrated to modulate excitation light in spatial and temporal domains for phosphorescence lifetime detection. Local O₂ concentration can be inferred through the detected lifetime around an O₂-quenching phosphorescent porphyrin microsensor. Combined with microsensor arrays, the DLMM can sequentially address light to each microsensor element to construct a discrete lifetime image or O₂ distribution. Chao et al., 15 Opt. Express. 10681-89 (2007).

In particular embodiments, the experimental procedures for single cell analysis may be performed using a microarray of microwells. In particular examples discussed herein, procedure were performed using a custom microarray (Figure 4A thru 4E). *See also, e.g.,* McQuaide et al., *Living Cell Array (LCA) for Multiparameter Cell Metabolism Studies*, PROC. IEEE-BIO ROB 971-76 (2006). Metabolic rate measurements are achieved by sealing each microwell using an impermeable lid (Figure 4B). Having demonstrated device principle of operation and

initial subsystem controllability, the need for a top-down approach to full integrated system design was recognized, inclusive of user interface, workflow, and dataflow design for the entire sample handling and analysis pipeline.

As shown in Figure 1A, the appropriate experimental parameters may be specified at the user interface, this information is used in the control and coordination of relevant hardware to accomplish the tasks that implement the automation pipeline. First, the target cells are moved from a reservoir onto the cassette. Cells are placed at precise locations on the analysis cassette and the appropriate reagents are introduced. The required excitation signals are then provided and the required data is collected from the cassette. Once the required data has been collected, the cells are transferred from the cassette to other locations. The collected data is subsequently analyzed. Results from each of these operations are stored in a database for purposes of analysis or verification of task completion. The contents of the database (such as experimental data, and results from analysis) are made available to the user via the user-interface.

Some of the various experimental stages listed above have been automated as reported in Anis et al., *Automated vision-based selection and placement of single-cells in microwell array formats*, presented at 4th IEEE Int'l Conf. Automation Sci. & Engin. (Washington, DC, 2008). The benefits with regard to time, accuracy and resources can be realized when all these packages are fully integrated into a single system with complete automation. The present invention achieves the goal of an automated, integrated system by providing a framework that incorporates all the necessary hardware components, associates them with their respective control software, and provides a layout for systematic integration of the various sub-systems. This can be then be used as a reference to develop the consolidated experimental platform that integrates all the components to provide the required automated workflow.

EXAMPLES

Example 1. Manipulation of human Barrett's esophagus cell line

Human Barrett's esophagus (BE) cell line was selected for initial cell manipulation experiments. The BE cells are adherent cells, cultured in cell culture flasks. In order to place single cells at desired locations they must first be released from the cell culture flask and brought into a suspended state by trypsinization. Lieber et al., 17 Int'l J. Cancer 62-70 (1976). The average diameter of several BE cells were measured, while in a suspended state, and found to be approximately 15 μm . Manipulation of live cells requires special operating precautions and conditions, such as a contamination free (sterile) environment for cell culture preparation, in addition to operating at specific temperatures and media compositions and pH. Therefore,

preliminary experiments were performed using rigid polystyrene spherical (PS) beads (Duke Scientific, Fremont, CA), instead of live cells. The PS beads, packaged as aqueous suspensions, have a diameter of $20\text{ }\mu\text{m} \pm 0.10\text{ }\mu\text{m}$ and a specific gravity (SG) of 1.05. This density is slightly larger than that of water (SG 1.0), making PS beads a suitable cell substitute for conducting automated cell manipulation runs. The PS beads were introduced to the phosphate-buffered saline (PBS) culture dish solution. The beads slowly sedimented under gravitational influence towards the dish bottom. Once they reached the bottom, they began to adhere to the surface as a result of surface tension, which is analogous to cell surface protein interaction with the culture dish surface, when using live cells.

Regarding cell selection and aspiration, in the field of view, there could be more than one cell. Cell selection is necessary to determine which of the available cells should be selected. Cell selection, image processing, and object recognition were all performed using the previously discussed vision module. Here, PS beads were used instead of live cells.

The CCD camera was used to capture grayscale 8-bit monochrome images of size 640×480 pixels, Figure 6B(a). The images represent the culture dish bottom with PS beads in solution. The size of each image pixel is $1.29\text{ }\mu\text{m} \times 1.29\text{ }\mu\text{m}$. Each grayscale image was segmented by applying a threshold to the captured image, resulting in a binary image.

Morphological image dilation processing was performed afterwards to remove minor particles that are not beads. The resulting binary image showed the micropipette tip, available PS beads, and other particles or defects that are identified as lesser objects, Figure 6B(b). The final processing step was the classification of beads from other objects, debris, and defects. This was performed in two steps: Only objects of areas close to that of the cell area were selected. This cell acceptance area was thus defined to be within defined maximum and minimum bounds; and the object height to width (aspect) ratio was also found to be in the range between 0.8 and 1.3.

Therefore it was found for this example embodiment that only substantially circular objects simultaneously satisfied cell selection criterion.

Figure 6B(c) shows six beads that were correctly classified in the image frame based on these conditions. For each PS bead, the centroid of the bead area is determined in image coordinates in units of pixels. The micropipette tip position, in the image frame, was determined during the initial system setup. With the micropipette tip and the cell positions known in the image frame, the relative cell-tip positions (in pixels) are determined in the x - and the y -directions, which therefore can be converted to the global coordinates using common coordinate transformation operations. Two conditions must be satisfied to select the cells that can be aspirated: The relative distance between a cell and a neighboring cell must be larger than a

chosen value ($\sim 60\ \mu\text{m}$ was used). If not, then both are excluded; and the cell must be located within the area facing the micropipette tip opening, represented by the dashed rectangle in Figure 6B(c). For cells satisfying these conditions, the cell at the shortest relative distance to the micropipette tip is selected. Therefore, from the six beads in Figure 6B(c), bead number (5) is
5 selected by the automated selection system. The X - Y horizontal stage is then automatically displaced in the X - and then the Y -direction, to position the cell with respect to the micropipette tip. The method is described by the block diagram and the cell positioning loop in Figures 6E and 6F. Figure 6B(d) shows bead (5) positioned with the micropipette tip. Once the automated positioning is performed, the cell aspiration, described by the loop in Figure 6F, is activated,
10 followed by an open-loop control of the X -, Y -, Z -, and Z_r -stages, previously described herein, to position the micropipette tip with respect to a microwell in the array shown in Figure 6E.

Further regarding cell dispensing, the cells or beads aspirated from the culture dish were manipulated in space and dispensed using the cell dispensing algorithm (*see* Figure 6C). The feasibility and the performance of the proposed system to manipulate both PS beads and single
15 live cells was assessed. In this Example, live Barrett's esophagus (BE) cells were stained with Calcein acetoxymethyl (AM) cell-permeant dye that is used to determine cell viability. Exciting the stained cells with a light source at 496 nm wavelength caused live cells to glow green (517 nm). A Xenon-arc illuminator (Sutter, Novato, CA) that produces light output from 340 nm to a cutoff of 700 nm, was used. Figure 6D shows PS beads that were individually placed in
20 a 3×3 microwell array. Figure 6C shows a 3×3 microwell array, loaded with cells. The bottom center well was intentionally left empty for purposes of comparison. In this Example, a 100% loading success rate achieved. The average time to load a cell or bead, between selection and dispensing, was approximately 60 sec.

This work demonstrates full function of the engineering systems and associated software
25 and biology protocols for a fully automated workstation for single cell manipulation. Hardware components, software, control and automation methodology, preliminary experimental results have been presented. These results indicate that a high success rate is feasible using the proposed cell transfer method. The time consumed to transfer a single cell can be significantly reduced to fractions of the preliminary experiments time, perhaps well below 20 sec per transfer. The
30 extension of cell aspiration and targeted cell placement to live cells of different types is provided for, as is the direct placement of living cells in arrays of microfabricated wells for subsequent metabolic rate measurement experiments.

Example 2. Comparison of automated and manual versions

To compare the effectiveness of the automated software for oxygen drawdown experimentation to the manual version of the software, an experiment was conducted. During the experiment, the time required for a user to acquire the ambient oxygen concentration in an array of microwells using both methods was measured. This involved the following steps: (1) focusing on a microwell-array; (2) darkening the room; (3) selecting a filter set; (4) centering a microwell-array over the objective; (5) centering the piston tip over the microwell-array; (6) collecting sets of drawdown (ORLD) images; and (7) processing the image data in MATLAB. In this experiment, as is typical of a cell oxygen drawdown experiment, each set of ORLD images consisted of lowering the lid actuator to seal the microwell array, acquiring ten oxygen concentration data points spaced six seconds apart, and raising the lid actuator to let the wells reoxygenate for ten minutes before taking the next data set.

In both the manual and automated experiments, steps (1)-(5) took an equal amount of time (about 7 min) because these were setup tasks that were automated. Once the system was ready for data collection, the advantages of the automated system became apparent.

In order to perform steps (6) and (7) with the manual system, the user had to perform the following steps: (1) Create a new directory for data storage; (2) Open the ANDOR Visual Basic program and input the data save path to the new directory; (3) Take sample images while altering gain and binning of the camera to obtain optimum settings; (4) Open the MATLAB image processing program and input the new save directory path; (5) Open the Lid Actuator GUI; (6) Lower the piston to seal the microwell-array; (7) Run an LSM image scan to verify a seal has been made between the glass piston lid and the microwells; (8) Run the ANDOR Visual Basic program; (9) Continually reprocess data with the image processing program to plot each consecutive oxygen concentration data point; (10) Raise piston and let wells reoxygenate for 10 min; (11) Change the data save directory path to a new folder; and (12) Repeat steps (6)-(11) twice.

The total time the user had to be present in order to manually run steps (1)-(12) was about 30 min. This was typical of many experiment run-times, however for other cases the total experiment time could be much longer depending on the total number of data points taken. Furthermore, experiment run-time would be much longer if the user was inexperienced because of the overall complexity of the data acquisition methods. In contrast, to perform steps (6) and (7) with the automated system, the user had to perform the following steps: (1) Open the automation program; (2) Create a new experiment with the experiment designer GUI (not

needed if this step was completed previously and saved); (3) Load the new experiment; and (4) Run the new experiment.

5 The total time the user had to be present in order to run steps (6) and (7) with the automated software was 3 min. This number would remain the same regardless of the number or time spacing of the data points. With the automated method, the user could set up and run the experiment and come back later to a complete set of data. When working with unfamiliar cells, a user could monitor the first set of data points as they were automatically presented on-screen, making sure oxygen drawdown rates were at levels that would not stress the cells during the experiment timeframe. This automated feature offered the further advantage over the manual
10 data acquisition method of not having to reprocess oxygen data in MATLAB after every data point was collected.

Example 4. Automated selection and placement of single cells using vision-based feedback control

15 Briefly, the embodiment of the invention presented in this Example is a platform that provides for a robotic manipulation system for automated selection and transfer of individual living cells to analysis locations. A commonly used cell transfer technique, adapted and substantially enhanced with new function and form, using glass capillary micropipettes was used to aspirate and dispense living cells suspended in liquid growth medium. Using vision-based
20 feedback and closed-loop process control, two individual three-axis robotic stages position the micropipette tip in proximity to the cell of interest. The cell was aspirated and the tip moved to a target location where the cell was dispensed. Computer vision was used to monitor and inspect the success of the dispensing process. The target cell destination was a microwell etched in a fused silica substrate. The system offers a robust and flexible technology for cell selection and
25 manipulation. Applications for this technology include embryonic stem cells transfer, blastomere biopsy, cell patterning, and cell surgery.

By way of introduction to define distinctive contrast, a well-known approach for single-cell manipulation uses glass capillary micropipettes. Sanford et al., 9 J. Nat'l Cancer Inst. 229-46, (1948). A negative pressure was applied to a growth media filled capillary that was
30 immersed in a cell culture dish to affect control of the aspiration of a desired cell. A positive pressure was used to dispenses the cell. In several studies, micropipette aspiration of cells was used to quantify the mechanical properties of cells, and the forces between cells and surfaces. Hochmuth, 33 J. Biomechanics 15-22 (2000); Shao & Hochmuth, 71 Biophysical J. 2892-2901 (1996). Motion stages with multiple degrees-of-freedom were used to manually manipulate the

micropipette and accurately control its tip position to perform either micromanipulation or microinjection. Further examples include commercially available manual cell manipulation systems include the Quixell (Stoelting, Wood Dale, IL) and TransferMan NK 2 (Eppendorf, Hamburg, Germany) systems. The Quixell system provides some degree of automation through the ability to have programmed destination locations within wells on a microplate. Its cell selection and collection processes are performed manually using a keypad and a joystick. Wewetzer & Seilheimer, 179 J. Immunological Methods 71-76 (1995). Such single-cell manipulations using a micropipette have been demonstrated to be reliable, minimally traumatic, and widely accepted. In the absence of cell selection and placement automation, however, it is time consuming, labor intensive, and unsuitable for processing large numbers of single cells.

Other approaches for single-cell manipulation have been advanced and many are suitable for application within the context of the present invention. For example, the use of electromagnetic field forces, exerted by a strongly focused laser, has been proposed and demonstrate for the capture and subsequent movement of cells of interest. Ashkin et al., 330 Nature 769-71 (1987); Ashkin & Dziedzic, 86 P.N.A.S. 7914-18, (1989). The development of these "optical tweezers" led to clinical applications in such areas as *in vitro* fertilization, and manipulation of suspensions of red blood cells. Svoboda & Block, 23 Ann. Rev. Biophys. Biomol. Str. 247-85 (1994); Grier, 424 Nature 810-16 (2003). Trapping configurations have been demonstrated with high-energy infrared (IR) light. Infrared light is capable of producing large forces, innocuous to cells, but collateral thermal stress may ensue. Ashkin et al., 1987. Electrical forces have also been used for microscale cell manipulations either by electrophoresis (EP) or dielectrophoresis (DEP). Classification as EP or DEP depends on whether the forces act upon the fixed or induced charge of a particle. Both have been successfully used for cell sorting, a utility process to the current invention. Voldman, 8 Annu. Rev. Biomed. Eng. 425-54 (2006).

Despite the sophistication of these alternate and auxiliary methods, capillary-based cell manipulation using aspiration and dispensing remains the most widely accepted and used technique. This Example addresses a fundamental need in the area of biological laboratory automation: fully automated cell manipulation using capillary micropipettes and associated robotics. This system implements full automation of cell selection, micropipette positioning, cell placement, and dispense. This comparatively inexpensive, robust, and flexible technology can be deployed in biology laboratories with creative adaptations, enabling new experimental protocols. Other than the manipulation of suspension cells, the system can be used for applications such as the transfer of embryonic stem cells, or blastomere biopsies during preimplantation genetic diagnosis.

In order to realize the promise of genomics in curing major diseases, it is necessary to develop precise tools for multi-parameter analysis of single cells and apply these tools to the understanding of biological questions involving the heterogeneity of cell populations. The present invention provides for a high-throughput, multi-parameter integrated system to monitor in parallel cellular parameters such as respiration rates and gene expression. Lidstrom & Meldrum, 1 Nature Rev. Microbiol. 158-64 (2003); Molter et al., 5 IEEE Trans. Automation Sci. & Engin. 32-42 (2008); Molter et al., 135 Sensors & Actuators: B Chemical 678-86 (2009). As stated previously, this Example embodies the capability to automatically select and pick up a single cell from a culture dish, manipulate and move the cell to a specified target location, and dispense the cell. Target locations could be microwell-array chambers or PCR tube caps, by way of limited example. In this Example, target locations were microwells etched in a fused silica substrate (Zhu et al., 19 J. Micromech. & Microengin. (2009)), affixed to the bottom of a petri dish, as shown in Figure 4E. The microwells were arranged in 3×3 arrays of nine microwells. The loading process involved a repeated selection and placement of one live cell into each microwell. When completely loaded with single cells, the microwell-arrays were incubated and then used for single-cell analyses. In principle, the system can manipulate any type of cell suspended in solution, including mammalian cells (including macrophages), and bacterial cells. Anis et al., Proc. Int'l Conf. Automation Sci. & Engin. 315-20 (2008).

A six-axis cell manipulation robotic system was built, shown schematically in Figures 2A and 2B. The system was constructed of three subsystems: a motion control system, a vision system, and a fluid control system. The three subsystems were integrated to enable both manual and automated cell manipulation through the use of software. The motion control system consists of two sets of three-degree-of-freedom (DOF) translation stages, an X_t - Y_t - Z_t stage, and an X - Y - Z stage, assembled on an inverted microscope. The cell selection and placement are monitored using vision-based feedback, captured using a microscope and a charge-coupled device (CCD) camera. A glass capillary micropipette was used as the robot end effector. Single cells suspended in cell growth medium in a culture dish were aspirated, moved, and dispensed into target microwells. Applying negative or positive pressures to the medium-filled micropipette controlled the cell aspiration and dispensing.

The micropipette tip positioning stage X_t - Y_t - Z_t (T-LS28-I, Zaber, Richmond, BC, Canada) and the microscope positioning stage X - Y - Z (MS-2000, ASI, Eugene, OR) comprise the motion control system stages. The X_t - Y_t - Z_t stage manipulates the micropipette in space for single-cell pick and place operations. The X_t - Y_t stage uses closed-loop DC servomotors to displace the micropipette in the x_t - and y_t - directions to vertically align the micropipette tip with

the center of the microscope field of view. The Z_t stage controls the micropipette vertical displacement (in the z_t -direction). The X_t - Y_t - Z_t stage is controlled through serial connection to a computer. The petri culture dish is mounted to a 2-axis X - Y microscope motorized stage that also carries a microwell array substrate, bonded to the bottom of another petri dish. The X - Y stage
 5 displaces the culture dish and the microwell array substrate in the x - and y -directions. The position of the X - Y stage depends on whether a cell is being aspirated from the culture dish or dispensed into a microwell. The Z stage vertically moves the microscope objective in the z -direction, to bring monitored objects into focus. The X - Y - Z stage is controlled either manually using a joystick or algorithmically through a serial connection.

10 The vision system includes an inverted microscope (TE-2000U, Nikon, Tokyo, Japan) with a 10 \times objective (CFI Plan Achromat, Nikon) having a numerical aperture of 0.25, and a working distance of 10.5 mm. Brightfield illumination is supplied by a 100 W halogen light source (LHS-H100P-1, Nikon) with a 12 V power supply (TE2-PS100W, Nikon). A 5 megapixel (2560 \times 1920 pixels) FireWireTM CCD color camera (Micropublisher 5.0, QImaging,
 15 Surrey, BC, Canada) was used to capture images.

The fluid control subsystem consists of a syringe pump, a micropipette, and tubing and fittings. The syringe pump (Versa 6, Kloeohn, Las Vegas, NV) incorporates a 10 μ L glass syringe. The flow rate can be controlled between 0.01 μ L/s and 2 μ L/s, achieving a volume resolution of 200 pL. The piston displacement and velocity are directly proportional to the
 20 volume and rate of flow. The pump is connected to a micropipette through poly-etheretherketone (PEEK) tubing, fittings, and connectors (Upchurch Scientific, Oak Harbor, WA). The pump has a single four-port rotary distribution valve, of which two distribution ports are used. One port (V_p) is connected to the micropipette tubing and the other (V_r) is connected to a reservoir. Commercially-available borosilicate glass micropipettes were used (MBB-FP-L-45, Humagen,
 25 Charlottesville, VA) with 40 μ m inner diameter (ID), and 50 μ m outer diameter (OD), where the tip (0.5 mm long) is angled at 45 $^\circ$, as shown in Figure 7. The 40 μ m ID micropipettes are suitable to manipulate suspended cells of 5 to 35 μ m diameters. The micropipette tip was chosen to have an inclination angle of 45 $^\circ$ to the horizontal to provide an unobstructed view of the cell before and during aspiration. The micropipette is connected to the X_t - Y_t - Z_t through a holding
 30 fitting. The micropipette, assembled with the holding fitting is called the micropipette assembly, shown in Figure 2A.

Control software was developed using LabVIEW (v8.5, National Instruments, Austin, TX). An Intel Core 2 Duo processor personal computer was used, running at 2.13 GHz with 3.0 GB memory. The graphical user interface (GUI), shown in Figure 23, enables manual, semi-

automated, or automated control of the different stages of the cell manipulation process. The software consists of four modules working in parallel, controlling the positioning of the micropipette stages, the positioning of the microscope stages, the syringe pump, and the vision system. Operation of the two positioning stage modules includes control of the absolute position and velocity of the stage motors. The position of each stage motor is used as feedback for the closed-loop control of the system. The pump software module controls the displacement, velocity and acceleration of the syringe piston in addition to the valve position settings between distribution valve ports V_p , and V_r . The vision module controls the camera settings, image acquisition, image processing, and object recognition. Camera settings include binning, exposure, and image type, whether colored (RGB) or grayscale. Image processing controls include brightness, contrast, gamma correction, and settings of upper and lower thresholds. Object recognition controls include the specification of maximum and minimum object sizes, aspect ratio, and search area. The vision module collects feedback information regarding recognized objects for use in the cell selection process. This includes the cell projected area, and cell centroid position in the image frame. When operated in full automatic mode the system coordinates the control of all software modules, collects available feedback data, and uses both closed-and open-loop control to achieve accurate cell manipulation with minimum operator intervention.

The workstation is used to automate the selection, aspiration, manipulation and dispense of single cells. Each cell is dispensed into a microwell; one of the 3×3 microwells forming an array, shown in Figure 4C. The microwells are wet-etched on a fused silica glass wafer using standard photolithography and etching techniques. Zhu et al., 2009. The microwell array has a pitch of $300 \mu\text{m}$, well diameter of $100 \mu\text{m}$, and well depth of $10 \mu\text{m}$. A flow chart describing the sequence of operations through which cells are aspirated and dispensed, in general, is presented in Figure 6E. The system includes two subsystems for: (1) automated single-cell aspiration, and (2) automated single-cell dispense. Open-loop control of the X - Y stage vertically aligns the micropipette tip with the center of the petri dish, followed by an "automated single-cell aspiration" process. Once the cell is aspirated, the X - Y stage is translated to vertically align the micropipette tip with the desired microwell (N), followed by the execution of the "automated single-cell dispense" process. In this Example, the number of wells in an array (N_{max}) was chosen to be nine. Cells were picked up and dispensed one-by-one until each well contained one, single cell. If a failure to dispense a cell was experienced, the pickup and placement process was repeated.

Preparatory to automated cell manipulations, system setup for cell manipulation involves multiple manual steps: (1) fluidic circuit cleaning and removal of contaminated media and air bubbles; (2) the vertical alignment of the micropipette orifice with respect to the microscope objective; (3) defining the micropipette tip working plane (p_t) and microscope objective working plane (p_o); and (4) recording the dish center and the well positions.

Regarding the fluidic circuit cleaning, before installing the micropipette assembly to the system, the fluidic circuit was primed. Priming included the removal of contaminated medium and air bubbles present in the fluid tubing, and filling the fluidic circuit with fresh medium. This flushing process was performed by manually controlling the syringe pump, the micropipette valve port (V_p), and the reservoir valve port (V_r). With the valve ports V_p closed and V_r open, the syringe pump was controlled to aspirate filtered fresh media from the reservoir. The valves were then reversed with V_p open and V_r closed and the syringe pump was controlled to push the freshly aspirated medium through the circuit, which flushed spent media and air bubbles out of the fluid tubing. This process was repeated until clean media filled all the circuit lines and only then the micropipette assembly was installed. After installing the micropipette, the flushing process was repeated to ensure that the micropipette was air-free. Flushing, while the micropipette was connected, must be done at small flow rates ($\leq 0.1 \mu\text{L}/\text{sec}$) to avoid clogging the micropipette.

Regarding micropipette tip alignment, the micropipette tip was lowered until it intercepted the focal plane. The X_t and Y_t stages were controlled manually to bring the micropipette orifice to the center of the field of view and thusly aligned with the microscope objective. This procedure was only performed when the pipette was changed or moved.

Referring to the working plane setup, both the culture dish (petri dish) and the microwell array substrate were mounted onto the microscope X - Y stage. An inclination between the working substrate plane p_s and the horizontal plane is possible, as shown in Figure 25. As the stage moves, if the petri dish bottom plane p_{sd} is inclined with respect to the horizontal, the following will occur: (a) a change in the vertical distance between the micropipette orifice and the dish bottom, δ_d , and (b) a change in the vertical distance between the microscope objective and the dish bottom, f_d . An increase in δ_d may cause the failure to aspirate cells. A decrease in δ_d may cause contact or collision between the micropipette and the dish bottom, damaging the micropipette or contaminating its tip with other cells. In the case of microwell substrate plane (p_{sw}) inclination, the following will be experienced: (a) a change in the vertical distance between the micropipette tip and the microwell substrate surface, δ_w ; and (b) a change in the vertical distance between the microscope objective and the microwell substrate, f_w . An increase in δ_w

may cause failure to properly dispense cells to the desired microwells. A decrease in δw may cause a collision between the micropipette tip and the substrate, causing damage to the micropipette. A change in the distance f_d or f_w causes poor image focus. It is therefore necessary to control the Z and Z_t stages to ensure that the distances δ_d , δ_w , f_d , and f_w remain constant. In this

5 Example, the value of δ_d is set to 40 μm , and the value of δ_w is -15 μm (i.e., 15 μm deep into the well). The values of f_d and f_w must equal the microscope objective working distance (10.5 mm).

To determine the absolute positions of the stages Z and Z_t for each any X - Y stage position, equations of the planes p_t and p_o are required, *see* Figure 25. The micropipette tip and the microscope objective working planes p_t and p_o are parallel to the substrate (petri dish or

10 microwell substrate). For every X - Y microscope stage position, plane p_t includes the micropipette tip position Z_{ti} , while plane p_o includes the microscope objective position Z_t . The equation of the planes p_t and p_o , in the case of the petri dish bottom, are determined with the use of surface features that are easy to focus on. Three surface indentations, inscribed on the petri dish bottom surface, are used. The three indentations, I_1 , I_2 , and I_3 are located at the microscope

15 stage positions (X_1, Y_1) , (X_2, Y_2) , and (X_3, Y_3) . The X - Y stage is translated such that I_1 in the center of the field of view. The objective Z stage is manually displaced until the indentation I_1 is in focus. This Z stage position is recorded as Z_1 . The Z_t stage is slowly displaced to lower the micropipette tip until it touches and is seen to slightly deflect off the surface. This micropipette stage position Z_t is recorded as Z_{t1} . Similarly, (Z_2, Z_{t2}) , (Z_3, Z_{t3}) are recorded for indentations “2”

20 and “3”. The plane equations are determined using the three X - Y stage positions (X_1, Y_1) , (X_2, Y_2) , (X_3, Y_3) , and the recorded (Z_1, Z_2, Z_3) and (Z_{t1}, Z_{t2}, Z_{t3}) . The stage positions Z and Z_t are therefore determined at any X - Y stage position using the plane equations (1) and (2), (Gellert & Van Nostrand Reinhold, VNR CONCISE ENCYCLP. MATHEMATICS (Van Nostrand Reinhold, New York, 1989)):

$$Z = \frac{1}{c} (d - aX - bY) \quad (1)$$

$$Z_t = \frac{1}{c} (d_t - aX - bY) \quad (2)$$

$$\text{where } a = \frac{\begin{vmatrix} 1 & Y_1 & Z_1 \\ 1 & Y_2 & Z_2 \\ 1 & Y_3 & Z_3 \end{vmatrix}}{\begin{vmatrix} X_1 & 1 & Z_1 \\ X_2 & 1 & Z_2 \\ X_3 & 1 & Z_3 \end{vmatrix}}, \quad b = \frac{\begin{vmatrix} X_1 & 1 & Z_1 \\ X_2 & 1 & Z_2 \\ X_3 & 1 & Z_3 \end{vmatrix}}{\begin{vmatrix} X_1 & Y_1 & 1 \\ X_2 & Y_2 & 1 \\ X_3 & Y_3 & 1 \end{vmatrix}}, \quad c = \frac{\begin{vmatrix} X_1 & Y_1 & 1 \\ X_2 & Y_2 & 1 \\ X_3 & Y_3 & 1 \end{vmatrix}}{\begin{vmatrix} X_1 & Y_1 & Z_1 \\ X_2 & Y_2 & Z_2 \\ X_3 & Y_3 & Z_3 \end{vmatrix}}, \quad d = \frac{\begin{vmatrix} X_1 & Y_1 & Z_1 \\ X_2 & Y_2 & Z_2 \\ X_3 & Y_3 & Z_3 \end{vmatrix}}{\begin{vmatrix} X_1 & 1 & Z_1 \\ X_2 & 1 & Z_2 \\ X_3 & 1 & Z_3 \end{vmatrix}}, \quad d_t = \frac{\begin{vmatrix} X_1 & Y_1 & Z_{t1} \\ X_2 & Y_2 & Z_{t2} \\ X_3 & Y_3 & Z_{t3} \end{vmatrix}}{\begin{vmatrix} X_1 & 1 & Z_{t1} \\ X_2 & 1 & Z_{t2} \\ X_3 & 1 & Z_{t3} \end{vmatrix}}.$$

An analogous process is carried out for the microwell array; however, the well edges at three of the four microwell array corner wells are used instead of inscribed indentations.

Regarding microwells and dish position recording, the X - Y stage position (X_{wj}, Y_{wj}) for a

30 microwell “ j ” is defined when the micropipette tip position coincides with the center of a

microwell. To calibrate the X - Y positions for all wells in the microwell array, first, the substrate is manually orientated such that the sides of the square bounding the microwell array are orthogonal to the image frame. This is the case when the X -stage position for top-right well (Well-1) is equal to that of the top-left well (Well-3), i.e., $X_{w1} = X_{w3}$. Second, the position for (Well-1) is recorded, (X_{w1}, Y_{w1}) . Knowing the relative well-to-well distance " l ", the positions of all the microwells are determined using equation (3):

$$\begin{bmatrix} X_{w1}, Y_{w1} & X_{w2}, Y_{w2} & X_{w3}, Y_{w3} \\ X_{w4}, Y_{w4} & X_{w5}, Y_{w5} & X_{w6}, Y_{w6} \\ X_{w7}, Y_{w7} & X_{w8}, Y_{w8} & X_{w9}, Y_{w9} \end{bmatrix} = \begin{bmatrix} X_{w1}, Y_{w1} & X_{w1} + l, Y_{w1} + l & X_{w1}, Y_{w1} + 2l \\ X_{w1} + l, Y_{w1} & X_{w1} + l, Y_{w1} + l & X_{w1} + l, Y_{w1} + 2l \\ X_{w1} + 2l, Y_{w1} & X_{w1} + 2l, Y_{w1} + l & X_{w1} + 2l, Y_{w1} + 2l \end{bmatrix}. \quad (3)$$

The centroid of the triangle formed by the three petri dish surface indentation (I_1, I_2, I_3) is defined as the petri dish position (X_{d1}, Y_{d2}) .

The automated single-cell aspiration subsystem performs: (1) cell selection, (2) cell positioning with respect to the micropipette tip, and (3) cell aspiration. The aspiration of the cell starts by automatically displacing the micropipette stage to a position Z_{ti} until the micropipette tip-to-dish distance is δ_d . The microscope objective is then automatically displaced to a position Z_i until the microscope objective-to-substrate distance is f . A cell was selected and vertically aligned with the micropipette orifice using vision-based feedback. A flow chart describing the sequence of operations in this subsystem is presented in Figure 26. The flow chart includes two loops, a cell selection and positioning loop, and a cell aspiration loop. In the cell selection and positioning loop, image processing and object recognition techniques are implemented in order to determine the positions of all cells available in the image plane region of interest. This enables determining the relative positions between the micropipette orifice and available cells.

Regarding cell selection and positioning, a common image processing technique called blob analysis was used to detect and analyze distinct two-dimensional shapes within the image field of view. This provides information about the presence or absence, number, location, shape, area, perimeter, and orientation of cells within an image. A set of selection criteria, including cell size, cell position in the field of view, and relative cell-to-cell positions, are used to rank cells of interest. A cell is selected and positioned with the micropipette tip using a closed-loop vision-based feedback controller. The block diagram of this control system is presented in Figure 27. The X - Y stage hardware has a built-in PID controller that accepts velocity,

acceleration, and maximum velocity as parameters. The input to the automated cell-micropipette positioning controller is the micropipette orifice position. The input to the X - Y stage controller is the relative micropipette-cell distance while the controller output is the actual cell position.

The X - Y stage controller aligns the cell with respect to the micropipette orifice by performing an X -displacement, followed by a Y -displacement. This control loop is repeated until the distance between the micropipette orifice and the cell is less than a specified threshold distance.

Regarding cell aspiration, when the selected cell is aligned with the micropipette orifice, aspiration can be performed by applying a negative pressure to the micropipette capillary, which generates a hydrodynamic force on the cell and pulls it inside. Strong adhesion forces between cells and the culture dish bottom, due to surface protein interaction with the dish surface, generate an opposing force, however, and may cause some difficulties in the aspiration. To overcome these adhesion forces, a positive pressure pulse, just strong enough to displace the cell from an adhered state to a suspended state, was applied. The now non-adherent (suspended) cell was identified and an attempt made to aspirate this cell into the capillary tip using negative pressure pulses, each aspirates a volume of medium V_{pulse} . A negative pressure pulse causes the cell to move towards the micropipette orifice. This process, visually monitored, was repeated as required until the cell is successfully aspirated and disappears into the micropipette. The maximum number of attempts is set at (T). If the desired cell was not successfully aspirated, a new cell may be selected, as seen in the cell aspiration loop of Figure 26. The location of the cell inside the micropipette depends upon the magnitude of the volume V_{pulse} .

The automated single-cell dispense subsystem is responsible for the placement of an aspirated cell into the desired microwell. The microscope stage (X - Y) is first open-loop controlled to vertically align the desired microwell with the micropipette orifice. Knowing the stage position of the microwell (X_{wi} , Y_{wi}), the objective stage (Z) is automatically displaced to the position Z_{wi} , calculated using equation [1], where the objective-to-substrate distance is f . A flow chart of the sequence of operations in the automated cell dispense subsystem is presented in Figure 28. Cell dispense is then performed through the following fully automated steps: (1) the micropipette is vertically lowered to the position Z_{twi} , calculated using equation [2], where the tip-to-substrate distance is δ_w , (2) a positive pressure was applied to the micropipette capillary, generating a hydrodynamic ejection force on the cell, (3) the micropipette assembly is displaced upwards, and (4) vision-based feedback, resulting from image processing and blob analysis, indicated the presence or the absence of a cell in the microwell. These four steps were repeated until either the cell is successfully dispensed or the maximum number of dispense attempts (S) is

reached. The fluidic dispense of the cells should be slow and gentle to minimize damage to the cell.

Three immortalized human cell lines were used in this Example: A549 human alveolar basal epithelial cell carcinoma; K562 myelogenous leukaemia; and Barrett's esophagus (BE).

5 The cell lines were grown in cell culture flasks until no less than 90% confluent. Single cells were released from the cell culture flask and brought into a suspended state by standard trypsinization. Traces of tripsin were removed by the addition of 10% serum DMEM medium. The suspension was transferred to a 15 mL tube where centrifugation, and supernatant removal are performed. Cell preparation was completed by the addition of Ham's F-12 medium
10 with 10% serum. The target density of cells in the petri dish was approximately 20 cells/ μ L. A higher cell concentration may lead to the aspiration of multiple cells, which was undesirable in this Example. BE cells were selected for several cell manipulation experiments. The diameters of these suspended cells were measured and the average suspended cell diameter was found to be 15 μ m. Manipulation of live cells requires special precautions and conditions,
15 including a contamination free environment, regulated operating temperature, media composition, 5% CO₂ and pH. Experiments were performed at ambient conditions.

The CCD camera captures 5 megapixel color (RGB) images (2560×1920 pixels) of the petri dish bottom with cells suspended in medium, as presented in Figure 29A. The images are processed to recognize all cells available in the image frame. Background subtraction is the first
20 in a series of image processing steps applied to each image. Thresholds are applied to the image resulting in a binary image showing available cells and other particles or defects that are identified as lesser objects (*see* Figure 29B). The final processing step is the classification of live cells to differentiate them from other objects, debris and defects. Cell classification includes two steps: only objects having areas close to that of cells are selected, falling within defined
25 maximum and minimum values, and the object height-to-width (aspect) ratio must fall in the range of 0.8 and 1.3 to eliminate elongated objects. Figure 29C shows three cells that were correctly classified in the image frame based on these criteria. Each cell centroid is determined in image coordinates, in units of pixels. The micropipette orifice is positioned in the center of the image frame during initial system setup. With the micropipette orifice and cell positions known,
30 the x and y relative positions (in pixels) between the cells and the micropipette orifice are determined. Measurements in pixels are converted to the global coordinates using coordinate transformation operations. An additional constraint that must be satisfied for cell selection is that the relative distance between any two cells must be larger than a chosen value, for example ~ 60 μ m, or both cells are excluded. This reduces the chance of multiple cell aspiration. For cells

satisfying all conditions, the cell closest to the micropipette tip is selected. Therefore, cell-1 in Figure 29C was selected by the automated system. To align the cell with the micropipette orifice, closed-loop control was used to displace the X - Y horizontal stage in the x - and then the y -directions, as indicated in the block diagram of Figure 27. Figure 29D shows the cell-1 positioned at the orifice of the micropipette. Once automated positioning was performed, the cell aspiration loop in Figure 26 was activated. The applied flow pulses have a volume $V_{pulse} = 2$ nL at a flow rate of 200 nL/s. This was followed by an open-loop control of the X -, Y -, Z -, and Z_r -stages to position the micropipette orifice with respect to an array microwell of known coordinates.

Single cells were automatically dispensed in the desired microwells in the manner described in the flow chart in Figure 28. Difficulties may be faced when identifying the nearly-transparent cells in their background and surroundings, and in differentiating between cells and artifacts such as debris on the substrate surface. A computer vision object recognition method was implemented to solve these problems: An image of the empty microwell was captured before lowering the micropipette (Figure 30A). Once the empty well image was captured, the tip was lowered (Figure 30B), a cell dispense attempt was performed (Figure 30C), and the micropipette was withdrawn upwards. The presence of a dispensed cell in the microwell was verified by subtracting the recorded image of the empty microwell (Figure 30A) from the post-dispense images of the object well (Figure 30D). The difference image was segmented by applying a threshold, resulting in a binary image (Figure 30E). Morphological closing was performed to remove minor particles, followed by the blob analysis process to detect the presence of a cell in the well. The blob analysis was performed using the IMAQ Vision software (National Instruments). Figure 30D shows a successful single-cell dispense. The microwell image was processed and a single cell was recognized, indicating the dispense of the cell, *see* Figure 30F. In this Example, positioning the cell at any location inside the well fully satisfied the performance specifications.

Several experiments evaluated the performance of the cell dispense system. The system was optimized for cell selection and placement accuracy. Optimization for speed was not addressed, where all motorized stages operations were performed at intermediate speeds. Cells available in the field of view were visually inspected and manually selected based on their size, state (adherent or suspended), and viability. A cell was selected by placing a crosshair at its center using the software GUI. Closed loop positioning presents the cell to the orifice of the micropipette. This is followed by the aspiration of the positioned cell.

Iterations were run to load single cells into 163 wells. Of the 163 loading attempts, 151 cells (92.60 %) were successfully loaded into microwells, while 12 failed. For the 12 failures, 11 cells were successfully loaded on the second attempt, while one was loaded on the third attempt. In summary, the total number of loading attempts was 176, of which 163 were successful.

5 Therefore, the probability of successfully loading a single cell was 93.1%. Using the closed-loop control algorithm, all 163 wells were loaded with a 100% loading rate. The average time needed to successfully load one cell, between cell selection and dispense, was 40 sec. Figure 31 shows a 3×3 microwell array, loaded with cells. Cell loading failures were attributed to one of the following: escape of the cell from the micropipette orifice when vertically withdrawing the tip
10 out of the culture dish solution, or when vertically immersing the tip into the microwell array solution; or a cell is dispensed in well, but when the micropipette tip retracts, the generated fluid disturbance pulls the cell out of the well.

To investigate the viability of loaded cells, Barrett's esophagus (BE) cells loaded to wells were incubated over a period of 2 hr and inspected every 30 min. Loaded cells were found
15 to adhere to the substrate, tending to stretch, and crawling towards the wall of the well. These are signs of cell viability (Gumbiner, 84Cell 345-58 (1996)), indicating the gentleness of the process. Figure 32 presents a example of a cell, loaded into a 50 μm well (A) before incubation; (B) after 30 min of incubation; and (C) after 2 hr of incubation, respectively.

The current Example presents an embodiment of an automated workstation for single-
20 cell manipulation. Hardware components, software, control and automation methodology and experimental results are presented. The system incorporated numerous novel innovations substantially improving in new ways upon the commonly used approach of aspirating cells using glass capillary micropipettes, enabling full automation of the process. The uniqueness of this proposed system, compared to other systems, is in its ability to automatically transfer individual
25 cells from a culture dish to their target locations at a 100% success rate. Vision-based feedback was used to control the cell selection and capture, in addition to check the cell dispense. Experimental results indicate that a high success rate is feasible using the proposed cell transfer method. The time required to transfer a single cell can be significantly reduced by operating the microscope and the micropipette stages at their maximum speeds.

30

Example 5. Respiratory response measurement:

The improved cell loading and incubation procedures have led to higher cell survival rates after loading and therefore increased the overall system throughput. The respiration rates of two types of cells: CP-C (a Barrett's esophagus cell line) and HeLa (human cervical cancer cell

line) were measured. Cell survival experiments have shown increased survival rates when a thin layer of the cell adhesion agent laminin is applied to the bottom of the microwells prior to cell loading. Laminin induces faster adhesion of cells to the bottom of the microwells, thus stabilizing the cells mechanically and preventing them from moving outside the microwell when transferred to an incubator, and laminin increases the survival rate of cells by providing an interface between the fused silica surface and the cell membrane. Laminin likely creates a physiologically more favorable milieu for the cells to be placed on compared to bare glass. These two advantages were more pronounced in the case of CP-C cells, whereas HeLa cells appeared to be less influenced by the presence of laminin.

Drawdown experiments were performed on an embodiment based on an inverted optical microscope that includes a manually controlled lid actuator assembly and an optical excitation and detection train. Software for excitation and detection synchronization and control and for data acquisition was implemented. Oxygen consumption rates in single cells was measured for several cell types. Oxygen consumption measurement in single cells. Nine CP-C cells were loaded in a 3 x 3 array of microwells and incubated for 16 hr under physiological conditions prior to and during the experiment. Differing slopes of oxygen consumption curves indicated a probable strong heterogeneity in cell metabolic activity. The calculated oxygen consumption rates were 0.17 and 1.32 fmol/min/cell, as shown in Figure 33A and 33B. Figures 34A and 34B also shows oxygen consumption measurement in single cells. Multiple draw-downs were conducted on the same CP-C cell set: The lid array was lifted and oxygen concentration allowed to equilibrate with the surrounding medium prior to resealing. One cell stopped consuming oxygen, perhaps due to prolonged anoxia. Cells showed strongly increased respiration rates in the second drawdown. Further optical sensors for other metabolites and multi-sensor base/lid arrays are consistent with the present approach to platform architecture.

After real-time measurements of oxygen consumption, each adhered cell is fixed, lysed, extracted and delivered from the microwells for "end-point analysis." For example, single cells are aspirated and loaded into PCR tubes.

Example 6. Single cell genomic analysis

The cells, once loaded into a PCR tube using the technology presented above, are analyzed by RT-PCR and qRT-PCR. Single-cell RT-PCR and qRT-CPR assays as well as cell freezing for RNA expression profile are valuable analyses following after live-cell experiments.

Reverse transcription (RT)-PCR is a sensitive technique for the analysis of gene expression, particularly for rare, low-abundance mRNA transcripts. The RNA template used for

RT-PCR is purified from the source of interest to avoid inhibition of PCR by lysis buffer. This process is time-consuming and costly. Developing the cell lysis method is a crucial step for performing RT-PCR on whole cell lysates without prior RNA isolation. A cell lysis method combining chemical and physical processes with RNaST lysis buffer and quick freezing and thawing of cells on dry ice was used. p53 gene expression was analyzed in Barrett's esophagus CP-C cells and GAPDH transcript in A549 cells, respectively, at the single-cell level. Expression of p53 gene was detected three out of four times in single-cell-tubes. The detectable C_t values appear to be slightly low (Figure 38A). However, the band of correct size was identified upon agarose gel imaging (Figure 38B). Gene expression in single-cell samples showed detectable signal using PCR techniques thereby suggesting strong evidence for demonstrable single cell heterogeneity. As further supporting evidence, Figures 39A-39B show the buffer inhibition of RT-PCR of A549 cells at 25 μ L volume. The result showed no inhibition of RT-PCR with 3 μ L or less of RNaST buffer.

15

CLAIMS

We claim:

- 5 1. A robotic manipulation system designed to perform high-throughput analysis of biological cells, wherein the system comprises:
- at least one analysis cassette, which holds at least one cell during analysis;
- 10 a cell loading module, which selects and loads at least one cell into the analysis cassette;
- a multi-parameter analysis module, which carries out an automated analysis which produces data on at least one cell in the analysis cassette;
- 15 and an end-point analysis module, wherein at least one automated end-point analysis is carried out on at least one cell of the analysis cassette, producing additional data on at least one cell; and
- 20 a database, which stores the data produced by the multi-parameter analysis module and the end-point analysis module.
- 25 2. The system of claim 1, wherein cell selection and cell release are carried out using at least one of: an optical trap and robotics.
3. The system of claim 1, wherein the end-point analysis includes quantitative PCR.
4. The system of claim 1, wherein the end-point analysis includes capillary-based 2-D electrophoresis.
- 30 5. The system of claim 1, wherein cell selection, cell-micropipette positioning, and release are carried out using at least one of: capillary micropipettes and robotics.

6. The system of claim 1, wherein the analysis cassette comprises at least one chamber that can alternately be opened or closed.

7. The system of claim 6, wherein the chamber of the analysis cassette, when opened,
5 may be perfused with a media or stimulus.

8. The system of claim 6, wherein the chamber encloses a single cell.

9. The system of claim 6, wherein said analysis cassette further comprises at least one of:
10 sensors or sensor chemistries, which may be used when the chamber of the analysis cassette is closed to detect the depletion or accumulation of moieties of interest.

10. The system of claim 6, wherein the chamber surface that opens and closes is a single use, robotically exchangeable component.

15

11. The system of claim 6, wherein the chamber that opens and closes is a multiuse, robotically controlled exchangeable component.

12. The system of claim 6, wherein intracellular and/or extracellular physiological
20 response of at least one living cell to at least one stimulus is tested using optical, mechanical, chemical, electronic, or electrochemical sensor transduction means.

13. The system of claim 6, wherein the multi-parameter analysis is designed to monitor metabolic rates at a single-cell level with simultaneous acquisition of multiple parameters.

25

14. The system of claim 6, wherein the multi-parameter analysis monitors one or more of respiration rates, protein expression, cytokine expression, membrane integrity, cell movement, and ion gradients.

15. The system of claim 9, wherein the sensors or sensor chemistries are present on or
30 incorporated into the chamber surface materials.

16. The system of claim 9, where the sensors or sensor chemistries are present on or incorporated in the chamber lid.

17. The system of claim 9, where the chamber is comprised of at least one zone, each zone comprised of zone-specific materials, said materials conveying structural, mass transport, and detection sensor properties.

5

18. The system of claim 6, wherein the chamber materials are selectively permeable to gases and impermeable to molecules of interest and the system further comprises sensors designed to detect the molecules of interest.

10

19. The system of claim 6, where the interior base of a chamber is treated with a cell attachment-promoting substance.

15

20. The system of claim 16, wherein the chamber is comprised of at least one zone, each zone comprised of zone-specific materials, said materials conveying structural, mass transport, and detection sensor properties.

20

21. The system of claim 18, wherein the chamber is comprised of at least one zone, each zone comprised of zone-specific materials, said materials conveying structural, mass transport, and detection sensor properties

22. The system of claim 1, further comprising a graphical user interface which allows the user to give high-level instructions to an automation manager, which controls one or more subsystems that control the functioning of the other components of the system.

25

23. The system of claim 22, where the automation manager controls the one or more subsystems by routing an instruction to an engine.

30

24. The system of claim 22, where the engine operates one or more devices in the subsystem as directed by the automation manager by using a toolbox, which contains algorithms for acquiring data.

25. The system of claim 22, where an XML file is used to store the high-level instructions.

26. The system of claim 22, wherein the user interface has the capability to graphically display the data obtained by the multi-parameter analysis module and the end-point analysis module.

5 27. The system of claim 1, where the multi-parameter analysis module uses a platinum-porphyrin sensor to detect oxygen.

28. The system of claim 1, where the multi-parameter analysis module uses an optical beam path.

10

29. The system of claim 1, where the cell loading module uses image processing and object recognition software for microparticle selection, targeting, or positioning.

30. The system of claim 29, where the cell loading module uses vision feedback techniques to aid in the microparticle selection, targeting, or positioning.

15

31. The system of claim 1, further comprising an experiment designer module which creates objects to aid the user in outlining experimental procedures.

20 32. The system of claim 1, where the cells are manipulated using one or more of: pumps, valves, mixers, motion stages, optics, and glass micropipettes.

33. The system of claim 1, further comprising at least one analysis sub-system which performs analyses on the data from at least one of the multi-parameter analysis module or the end-point analysis module which executes analysis functions on the data, which includes one or more of: mathematical operations, regression, curve-fitting, optimization, statistical computations, algorithms for signal and image processing, signal and image analysis, data-mining, pattern classification, performance evaluation methods, and goodness of fit.

25 34. The system of claim 1, wherein the system architecture is implemented in accordance with a UML model which standardizes the features and operation of the system.

30

35. The system of claim 1, further comprising the use of a photon excitation microscope for imaging in the multi-parameter analysis module.

36. The system of claim 1, further comprising the use of micro flow-through electrodes in the multi-parameter analysis module as a sensor technology.

5 37. The system of claim 1, where the intracellular and extracellular physiological response of living cells to a stimulus is tested using optical, mechanical, chemical, electronic, or electrochemical sensor transduction means.

10 38. The system of claim 1, further including an environmental chamber to provide temperature and humidity control.

39. The system of claim 1, where the multi-parameter analysis is designed to monitor metabolic rates at a single-cell level with simultaneous acquisition of multiple parameters.

15 40. The system of claim 1, where the multi-parameter analysis monitors one or more of: respiration rates, gene expression, protein expression, cytokine expression, membrane integrity, cell movement, and ion gradients.

20 41. A robotic cassette management system designed to provide kinematic registry, fluidic interface to cassette, and close-coupled management of reagent delivery and return from the cassette, wherein the system comprises:

 a robotic gripper that first aligns the cassette with the fluidic interface and then engages and seals to the fluidics;

25 a fluidic interface that engages an elastomeric seal on the analysis cassette; and

 an interface to a fluidic management module which may comprising tubing, pumps, and valves for reagent metering and switching.

42. An automated fluid management module system designed to provide close-coupled fluidic interface to an analysis cassette, wherein the system comprises:

5 pumps for the metered delivery of reagents;
valves for the switching, multiplexing, and/or fluidic routing for mixing
of reagents;
interface to reagent storage; and
interface to analysis cassette, wherein said interface is direct or via a
cassette interface.

10 43. The system of claim 42, wherein the fluid management module is comprised of a multi-layer laminate structure.

44. The system of claim 42 wherein the laminate structure comprises a:
15 pneumatic control layer;
thermal set bonding layer;
valve chamber layer;
thermal set bonding layer;
valve membrane;
thermal set bonding layer;
20 valve chamber;
thermal set bonding layer; and
fluidic routing layer.

45. The system of claim 43, wherein the laminate structure comprises a stacked plurality
25 of structures as defined in claim 44 thereby enabling by design high density packing of complex
fluidic routing topologies.

46. The system of claim 44 wherein the layers ordering is adjusted within the
context of the manufacturing methodology to accommodate alternate pneumatic and fluidic
30 routing topologies.

47. A analysis cassette system designed to interface with an analytical system, seal to fluid management fluidics, enable close-coupled reagent management to independent analysis chambers, and provide for access and analysis of a plurality of regions of interest via various
5 field force and optical interrogation means.

48. The analysis cassette of claim 47 wherein the analysis cassette comprises:
a fluidic seal;
a seal to top cassette half bonding means;
10 a top cassette half containing fluidic management features;
a bonding means between top and bottom cassette halves;
a bottom cassette half containing fluidic management features, automation
registry features, and manufacturing alignment features to the analysis substrate;
a bonding means between the bottom cassette half and the analysis
15 substrate; and
an analysis substrate.

49. The system of claim 48, wherein the analysis substrate contains chambers.

20 50. The system of claim 48, wherein the analysis substrate contains microwell-arrays.

Sheet 1/54

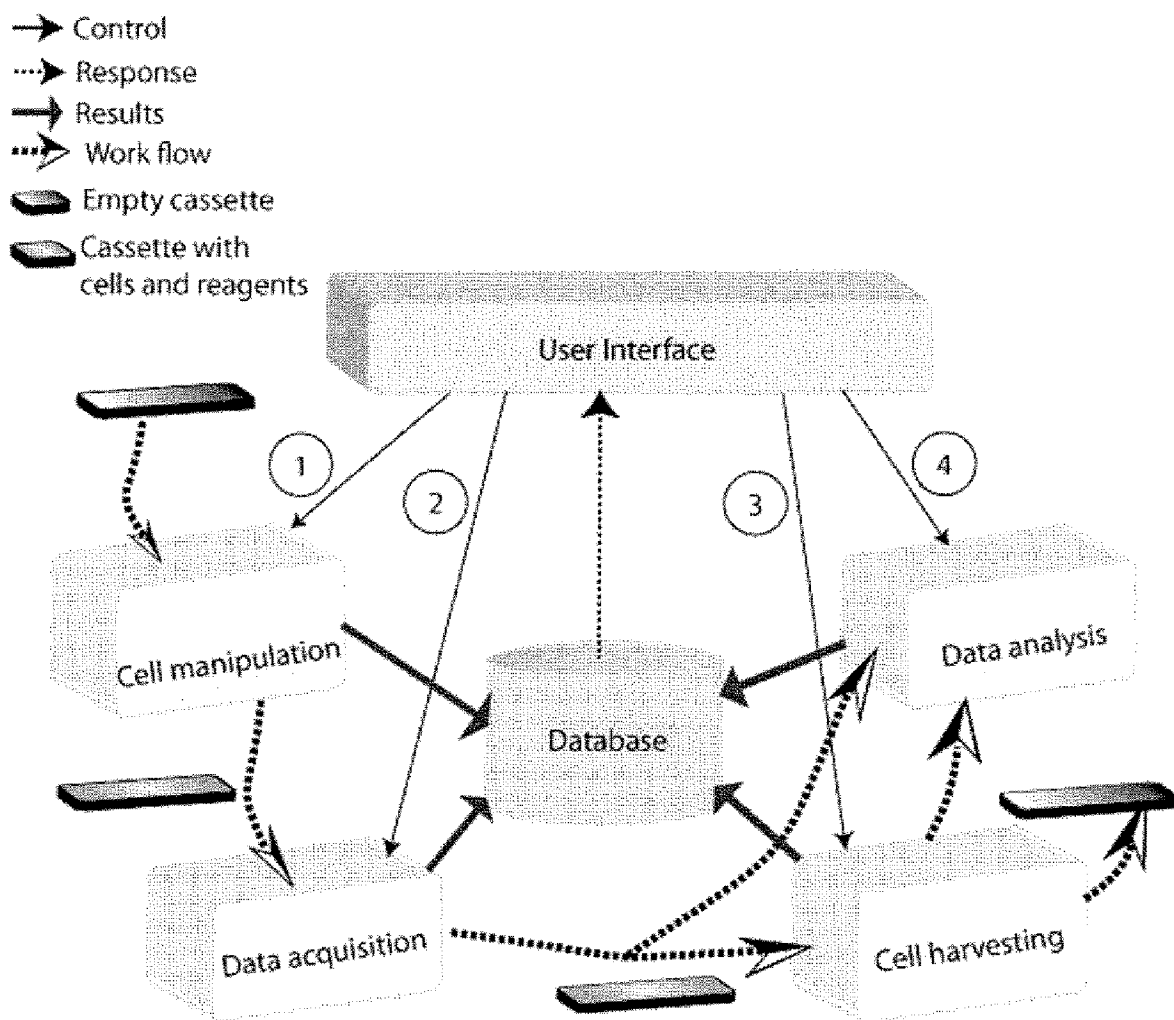


Figure 1A

Sheet 2/54

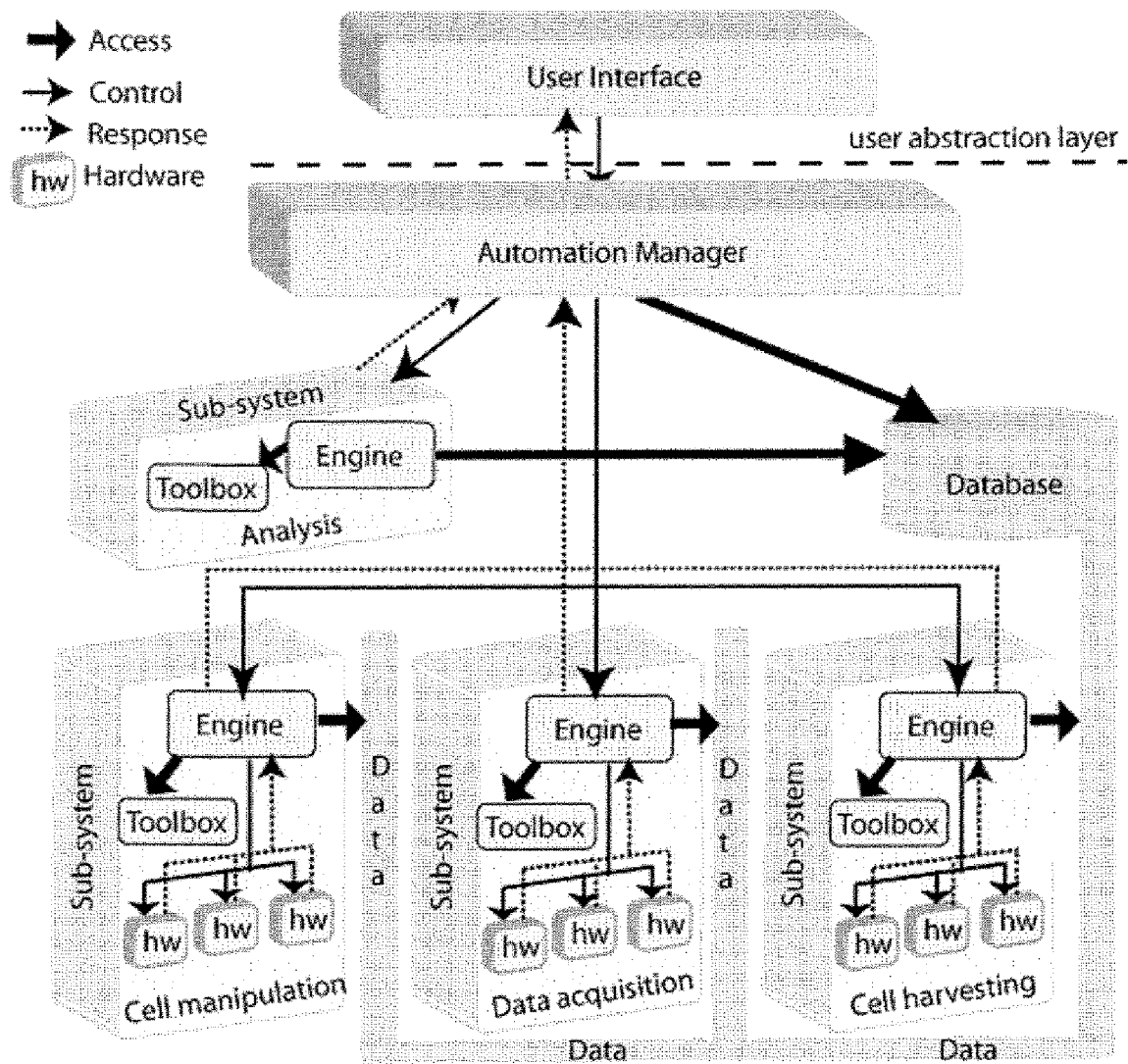


Figure 1B

Sheet 3/54

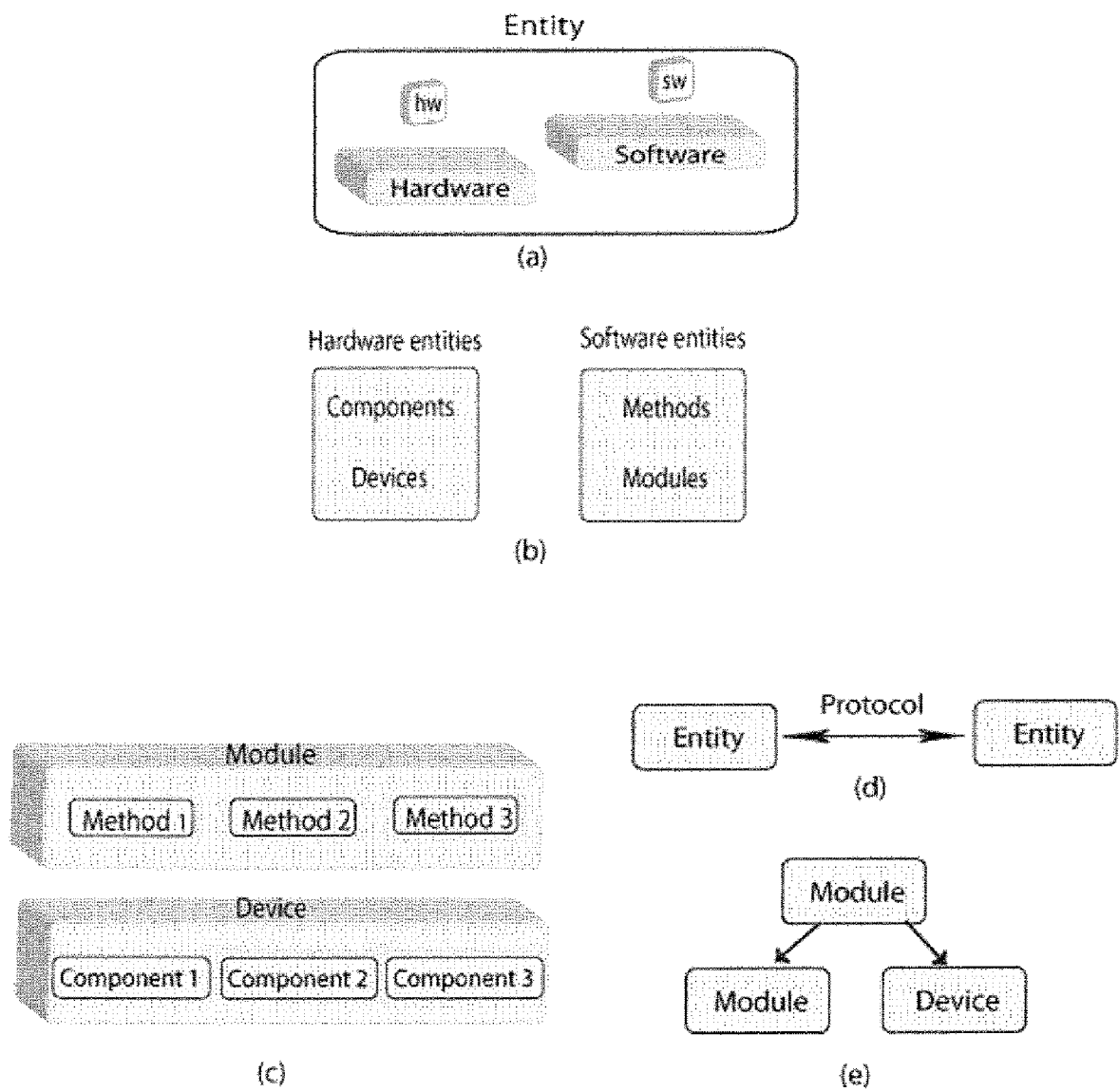


Figure 1C

Sheet 4/54

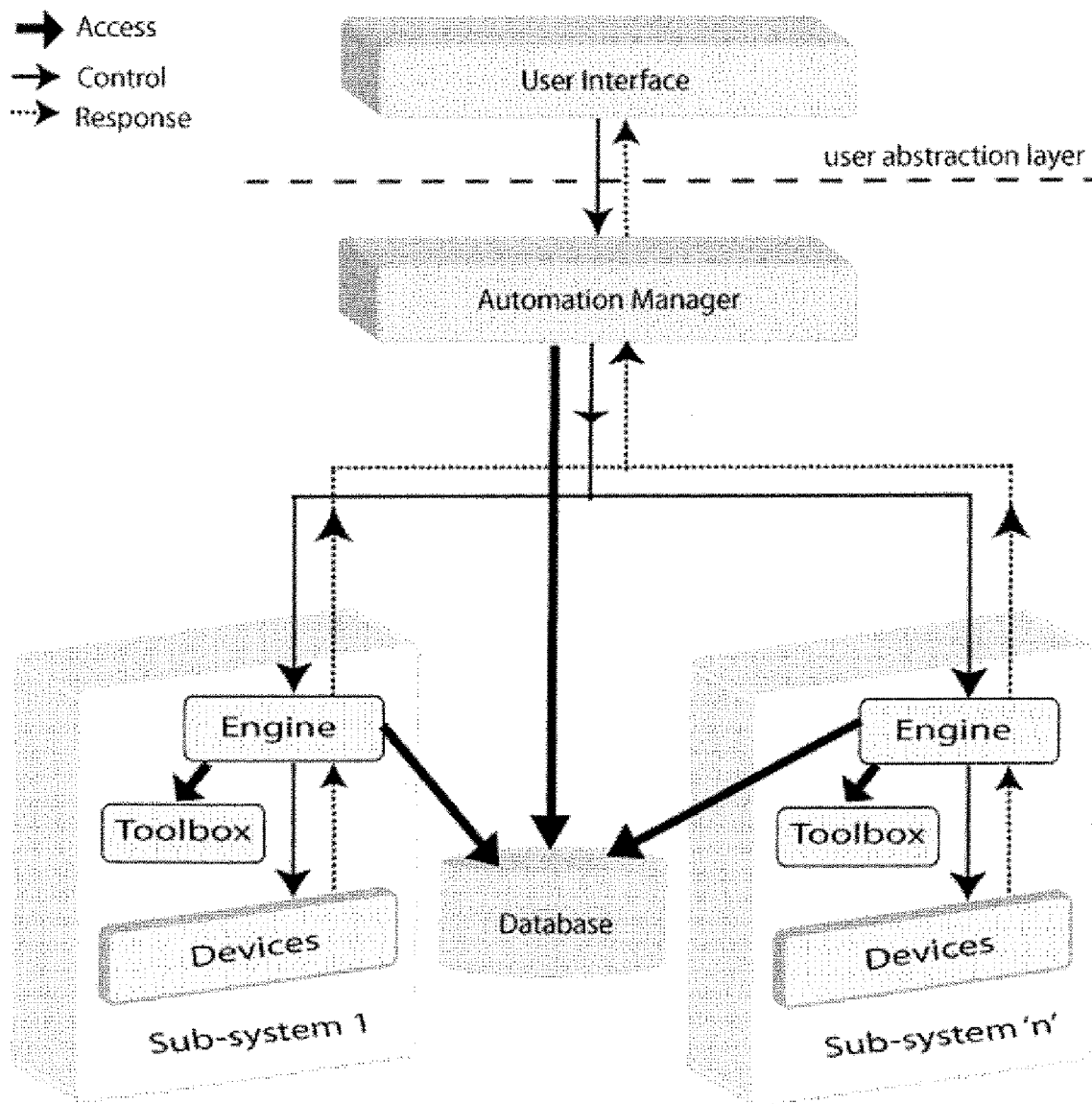


Figure 1D

Sheet 5/54

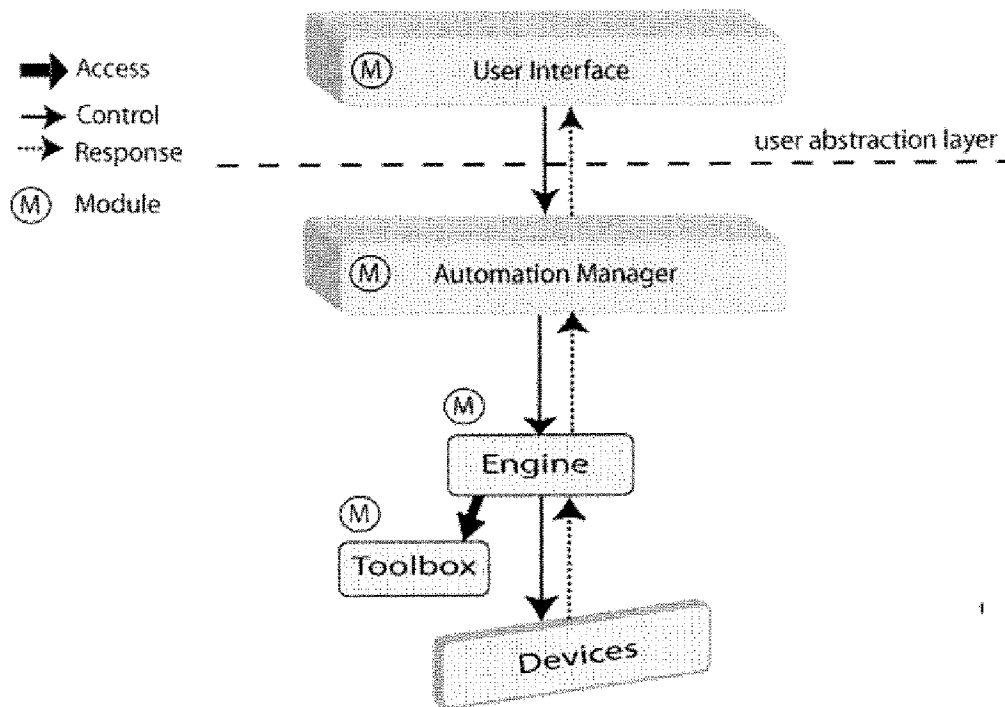
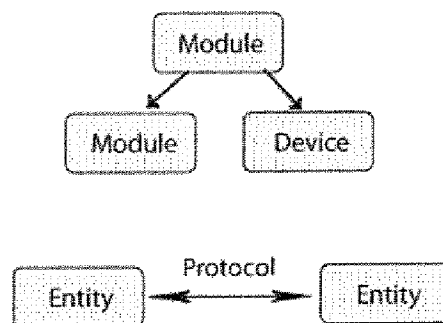
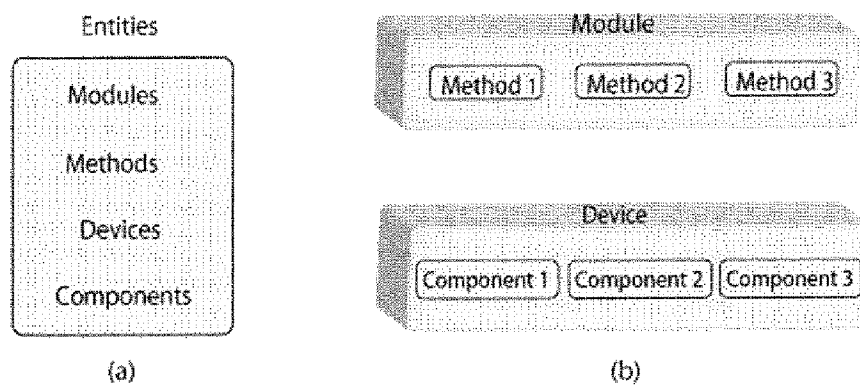


Figure 1E



Sheet 6/54

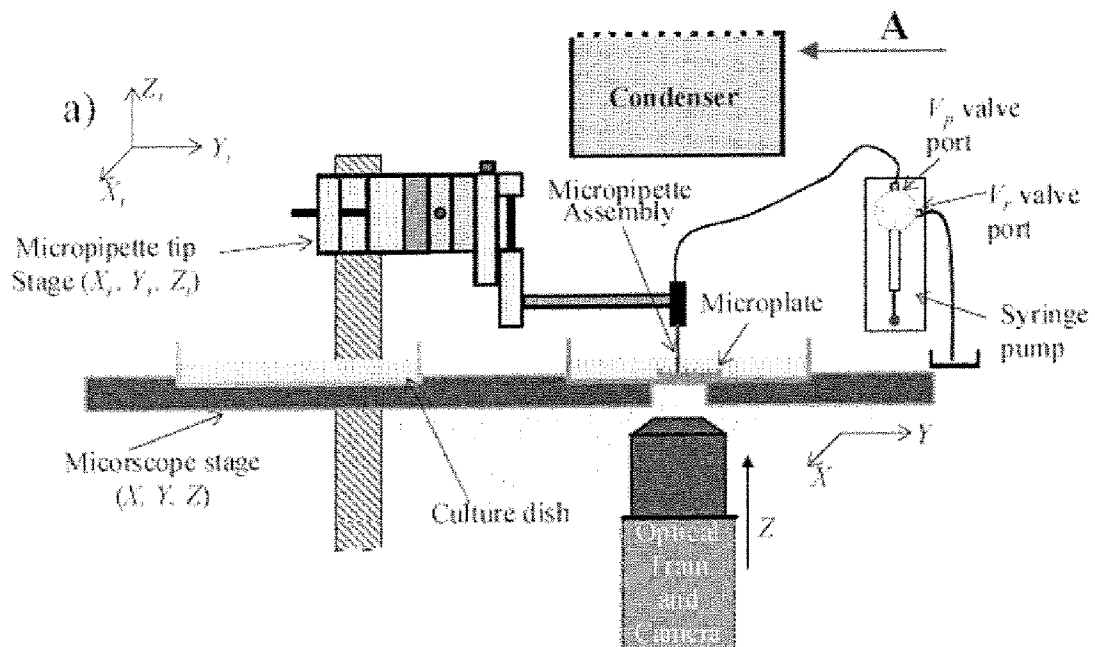
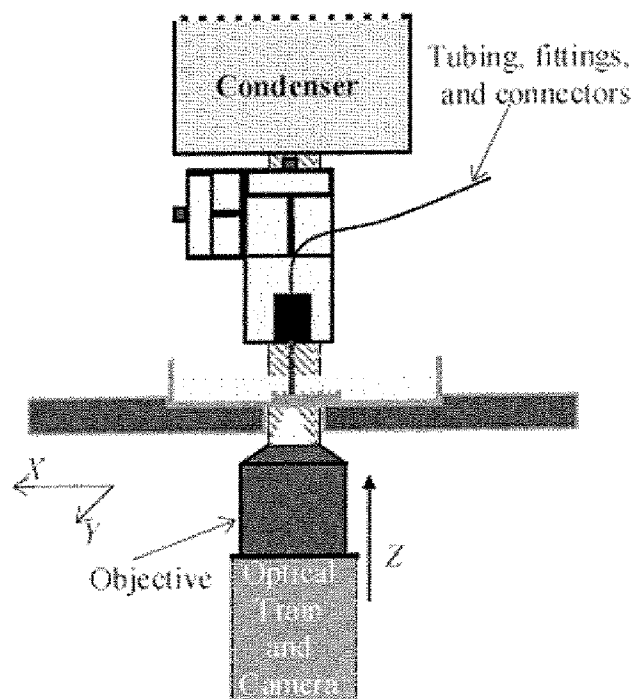


Figure 2A



Sheet 7/54

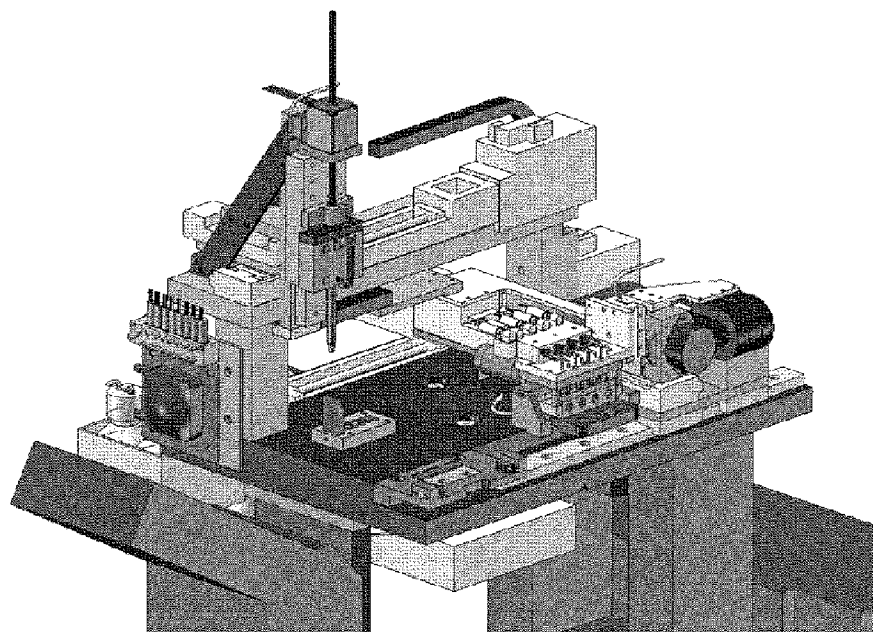


Figure 2C

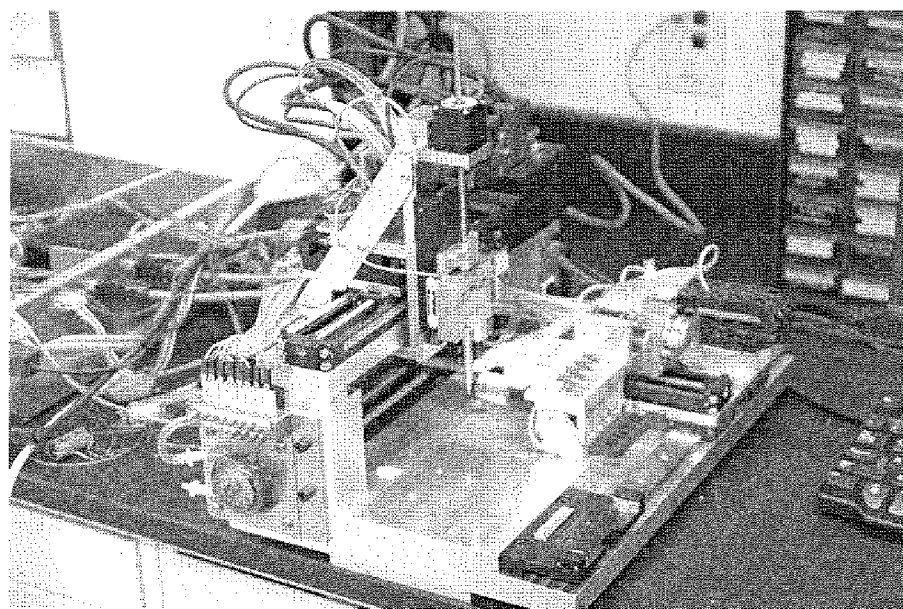


Figure 2D

Sheet 8/54

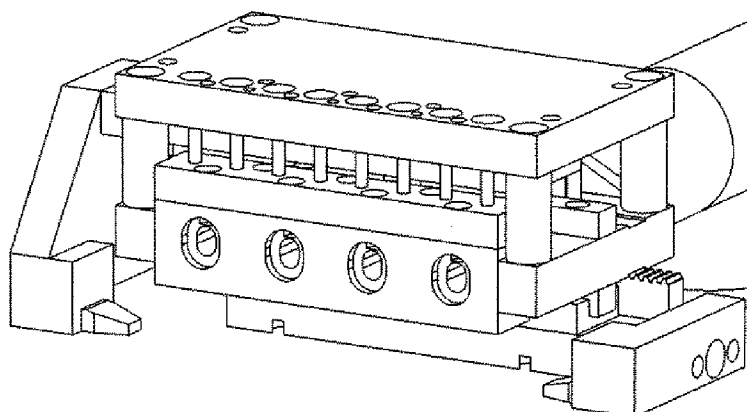


Figure 2E

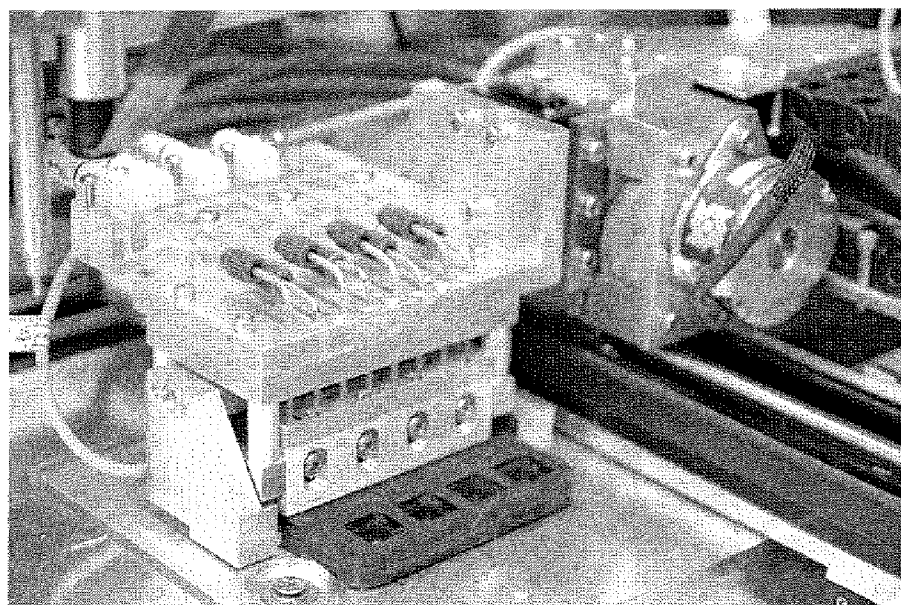


Figure 2F

Sheet 9/54

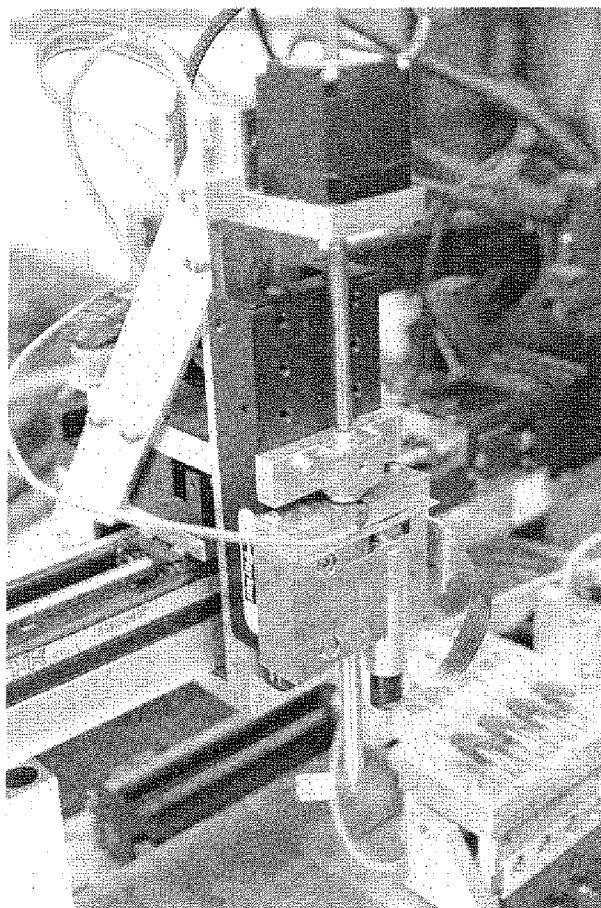


Figure 2G

Sheet 10/54

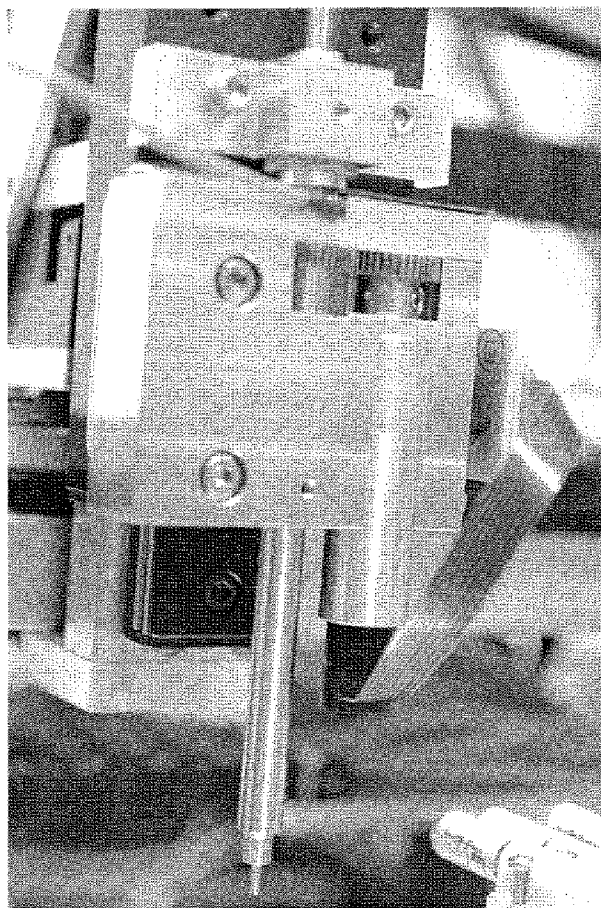
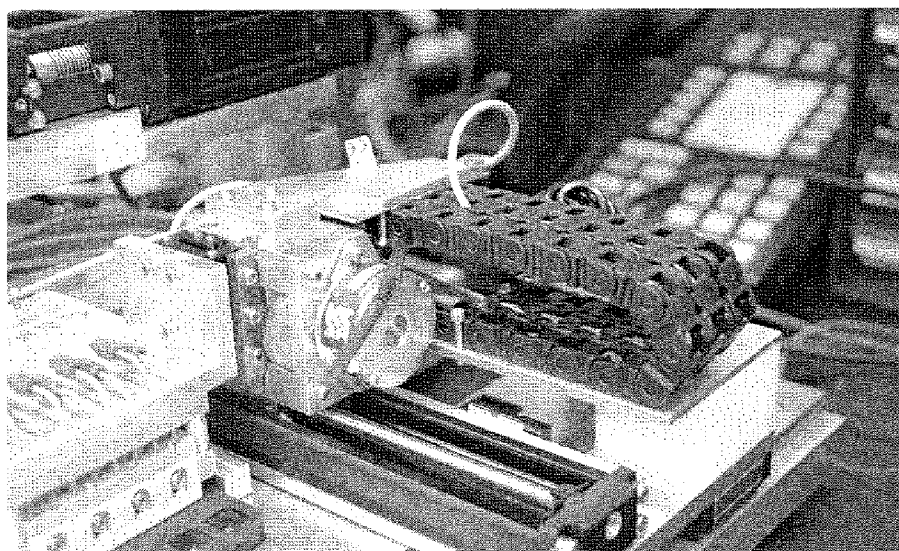


Figure 2H



Sheet 11/54

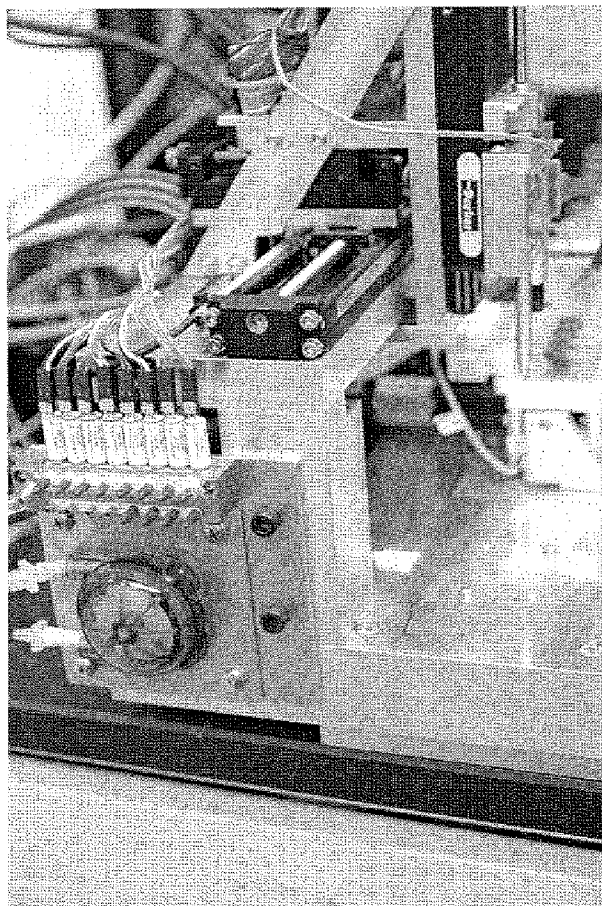
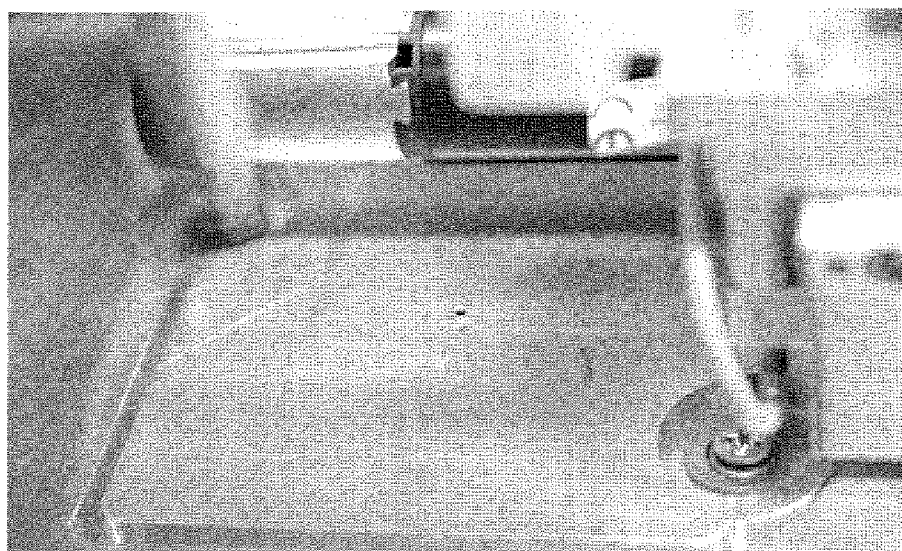


Figure 2.J



Sheet 12/54

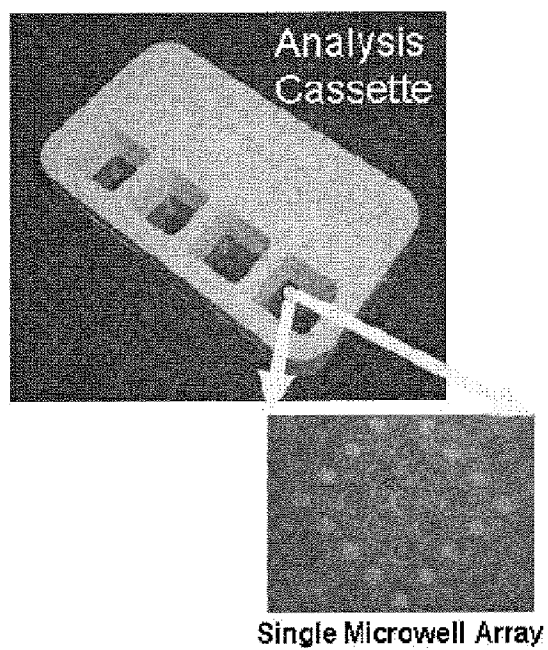


Figure 3A

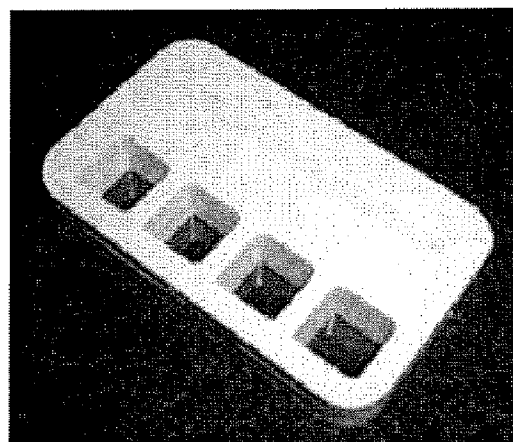
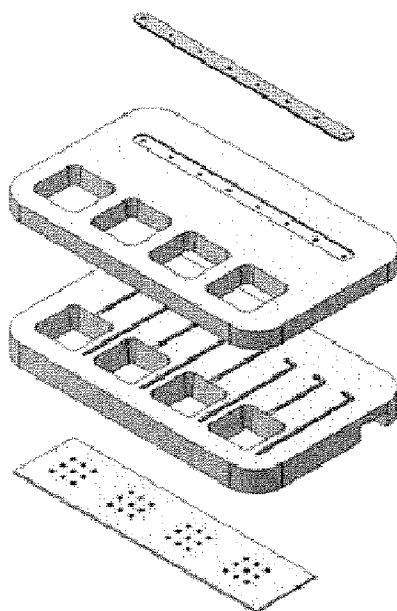


Figure 3B

Sheet 13/54

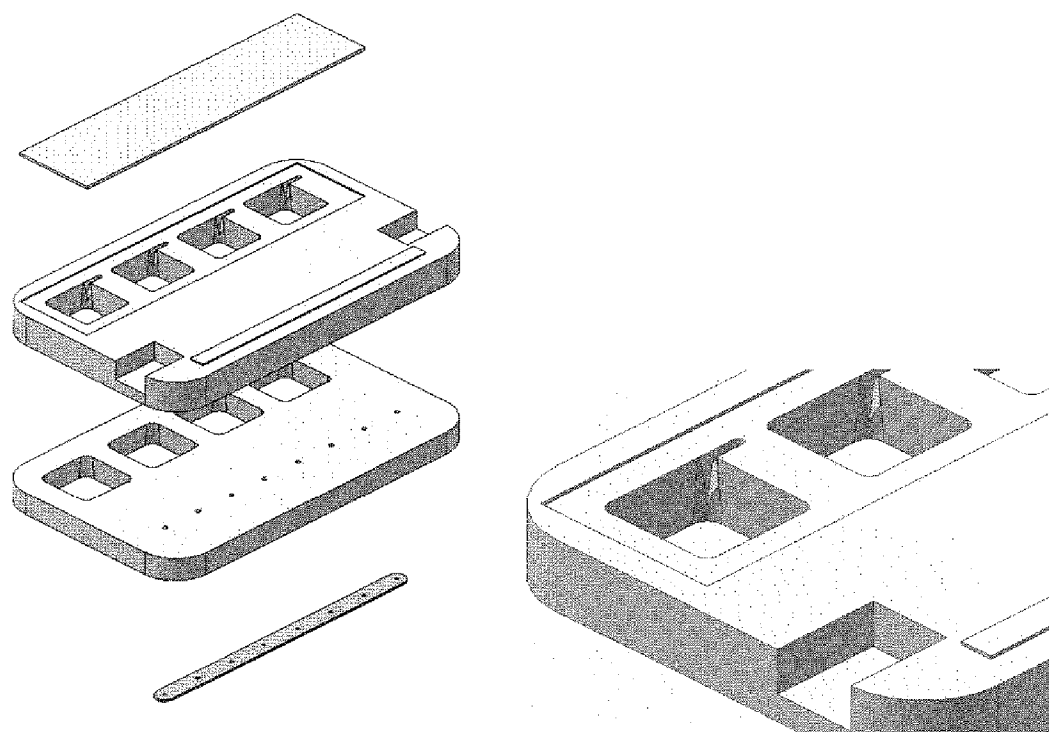


Figure 3C

Sheet 14/54

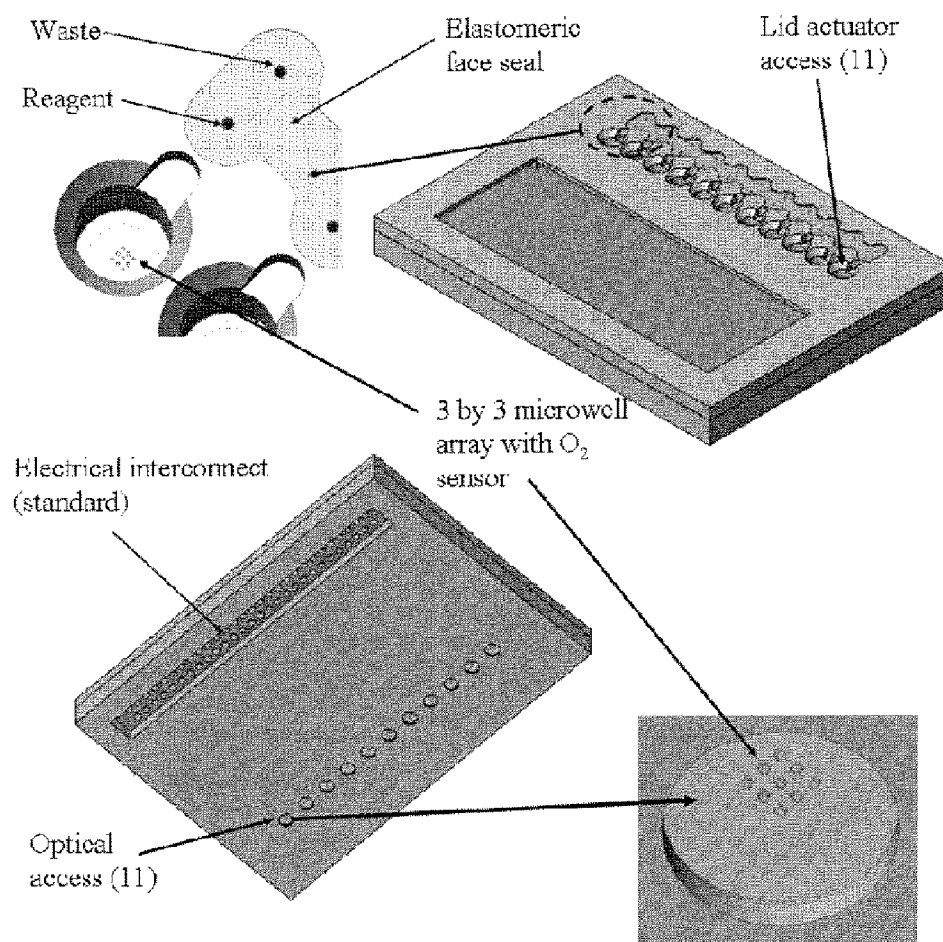


Figure 3D

Sheet 15/54

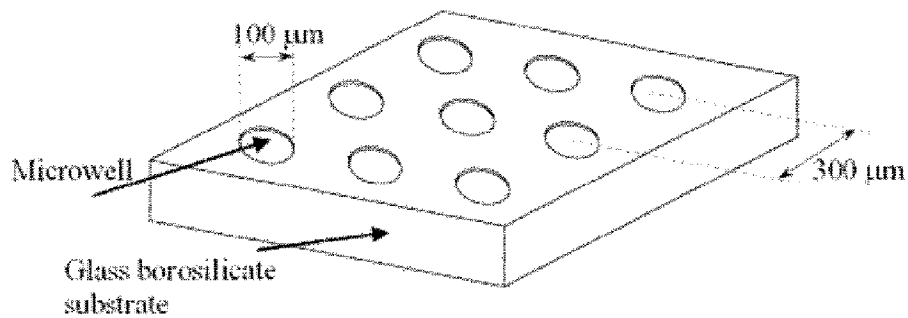


Figure 4A

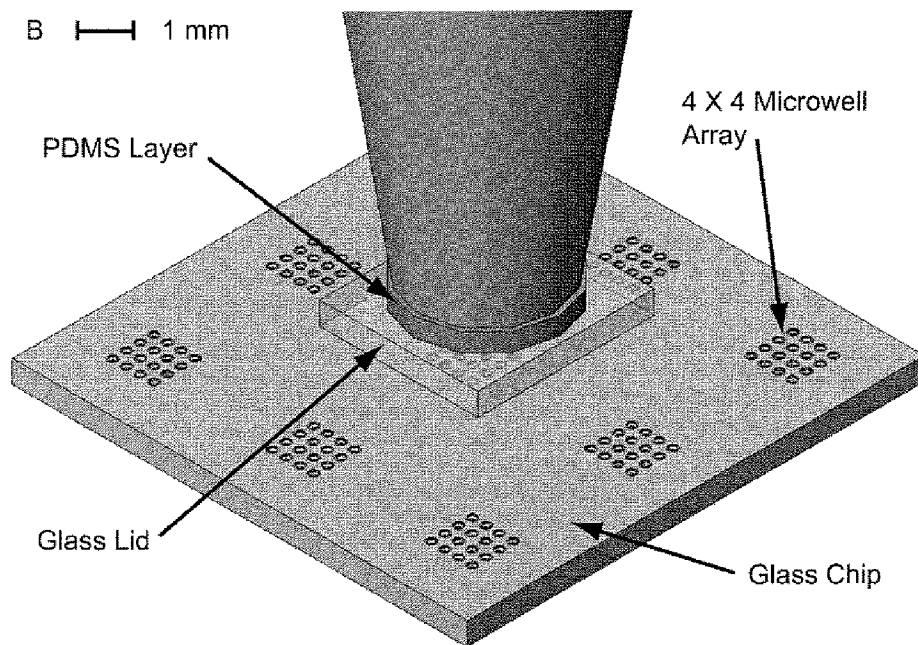


Figure 4B

Sheet 16/54

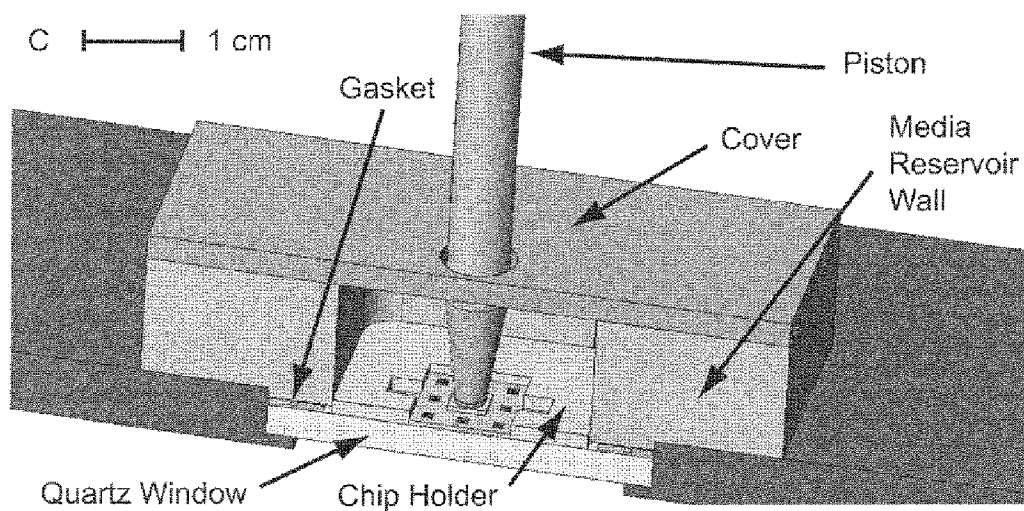


Figure 4C

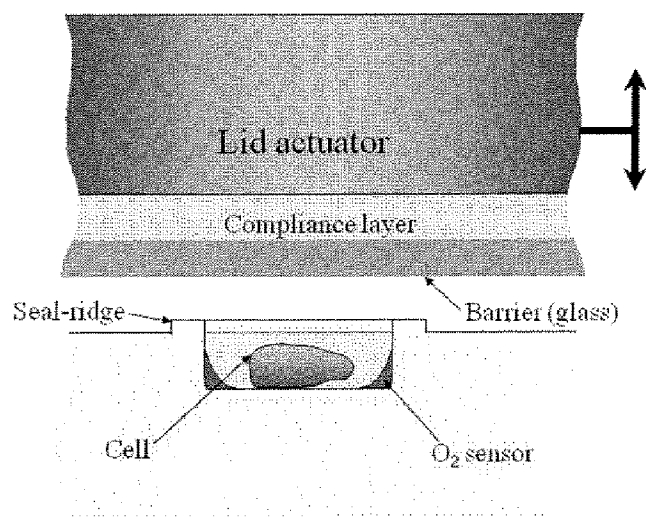


Figure 4D

Sheet 17/54

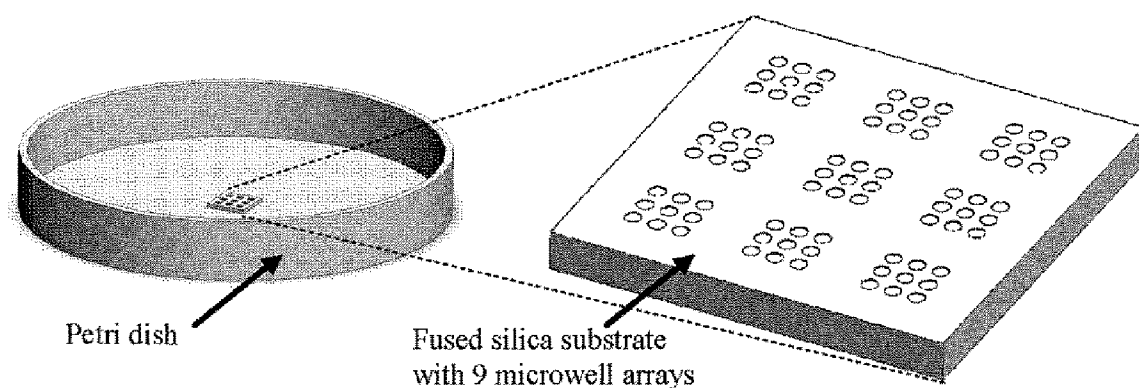


Figure 4E

Sheet 18/54

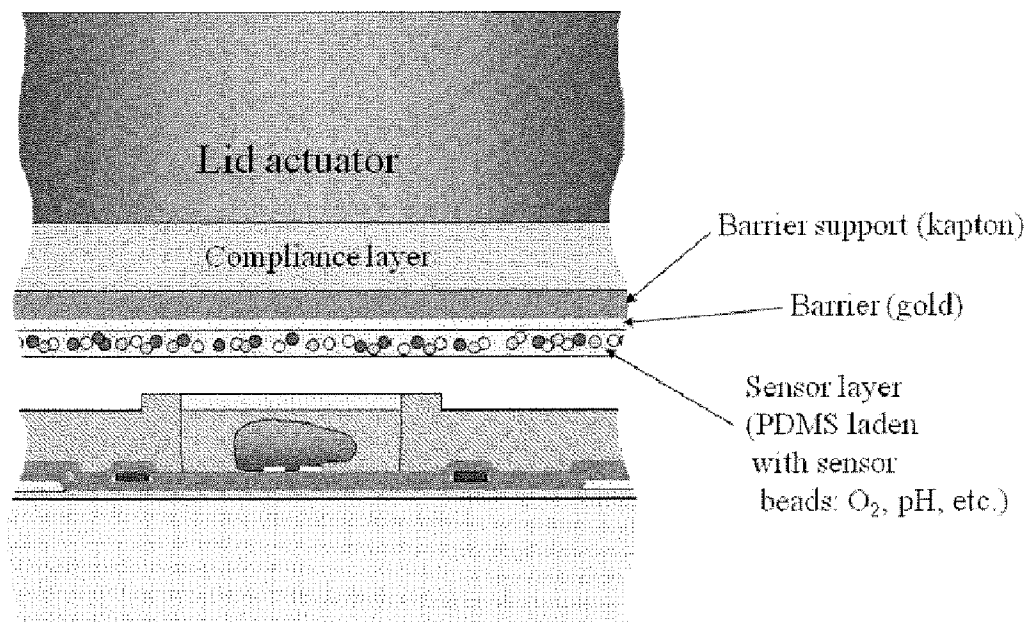


Figure 5A

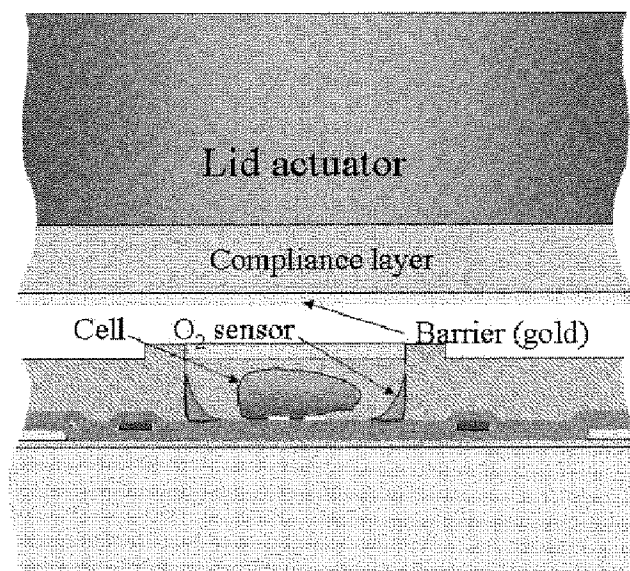


Figure 5B

Sheet 19/54

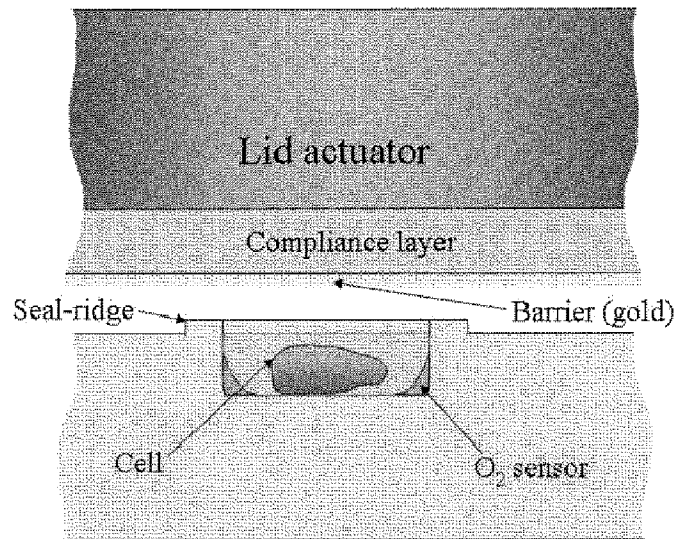


Figure 5C

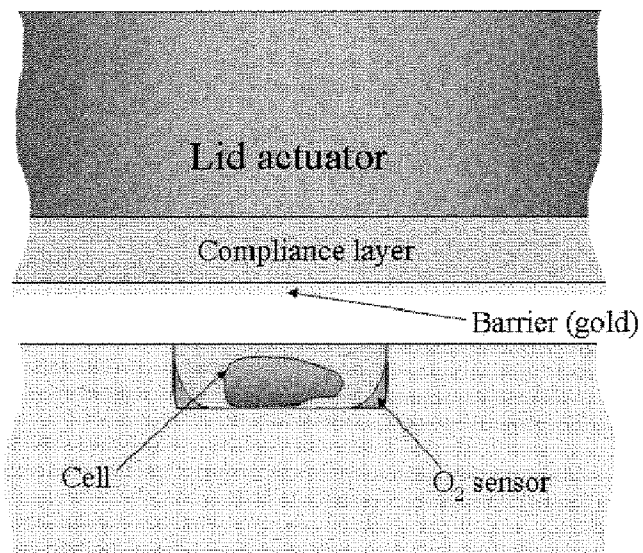


Figure 5D

Sheet 20/54

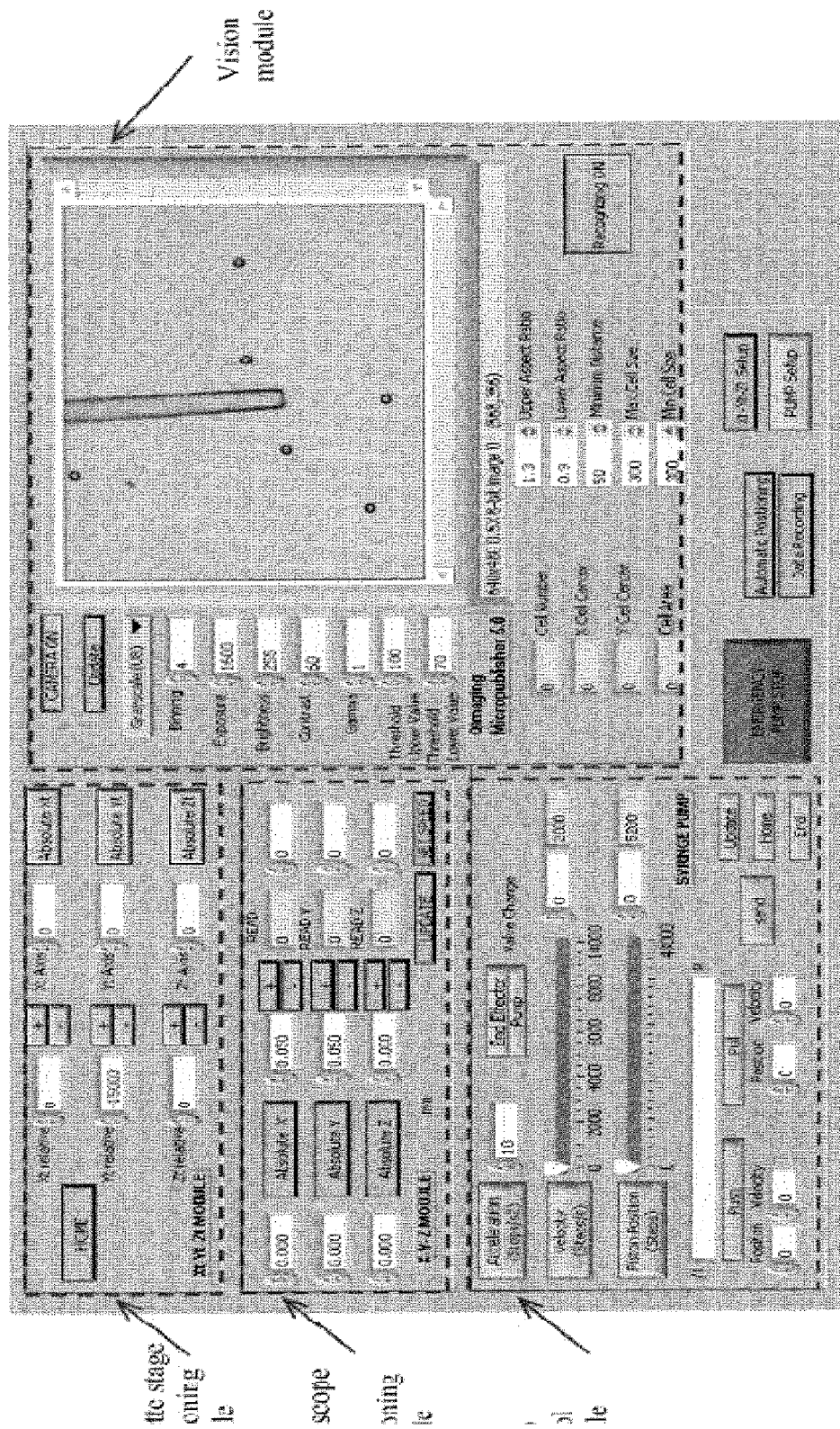


Figure 6A

Sheet 21/54

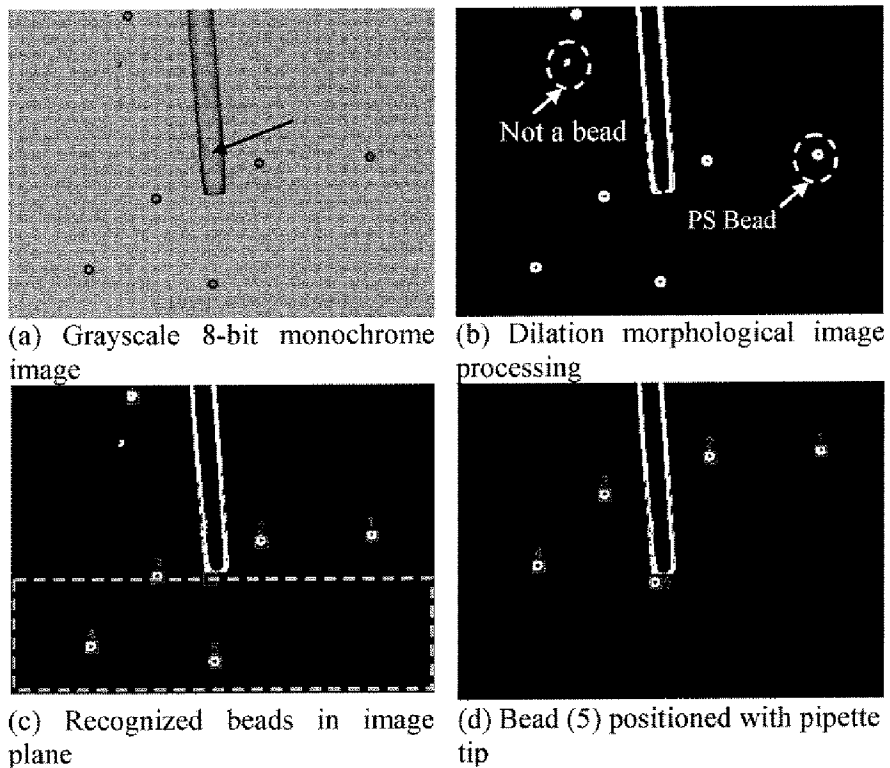


Figure 6B

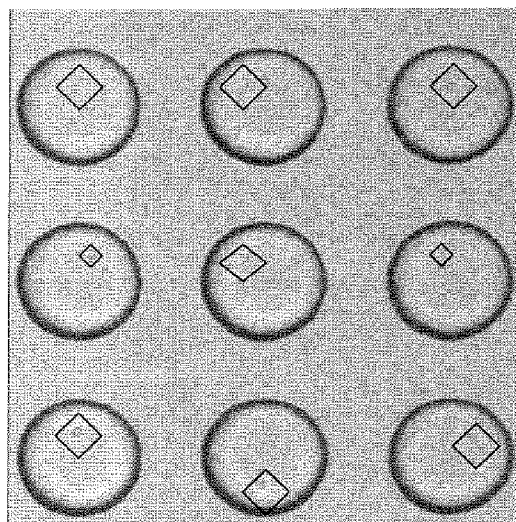


Figure 6C

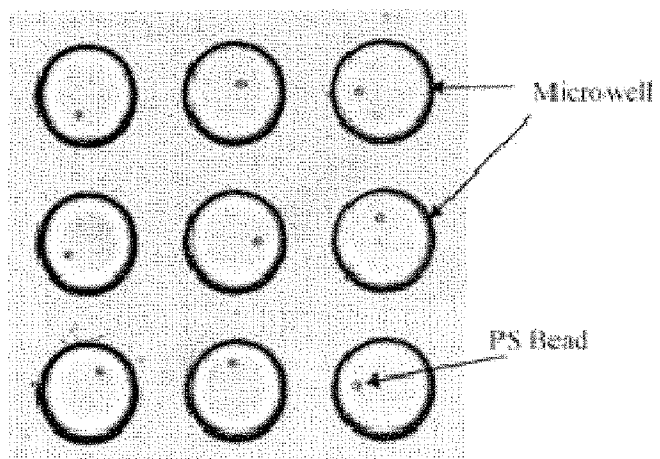


Figure 6D

Sheet 22/54

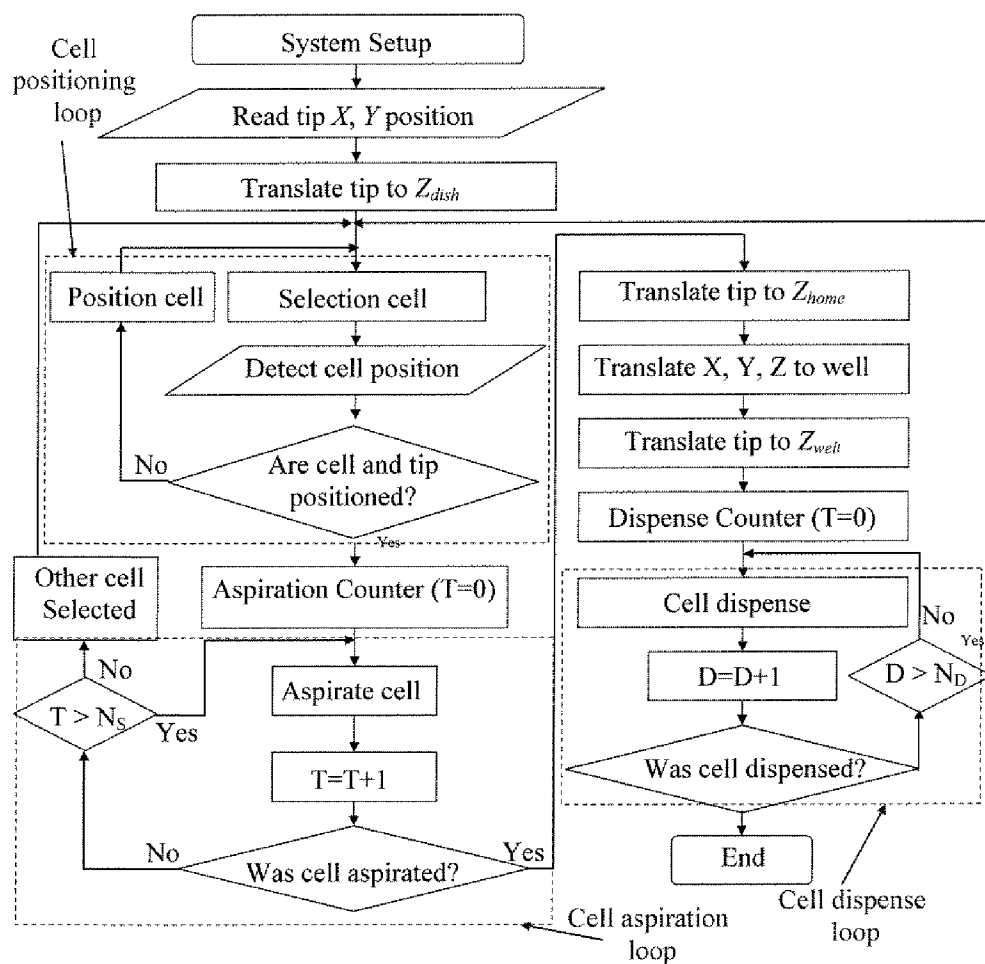


Figure 6E

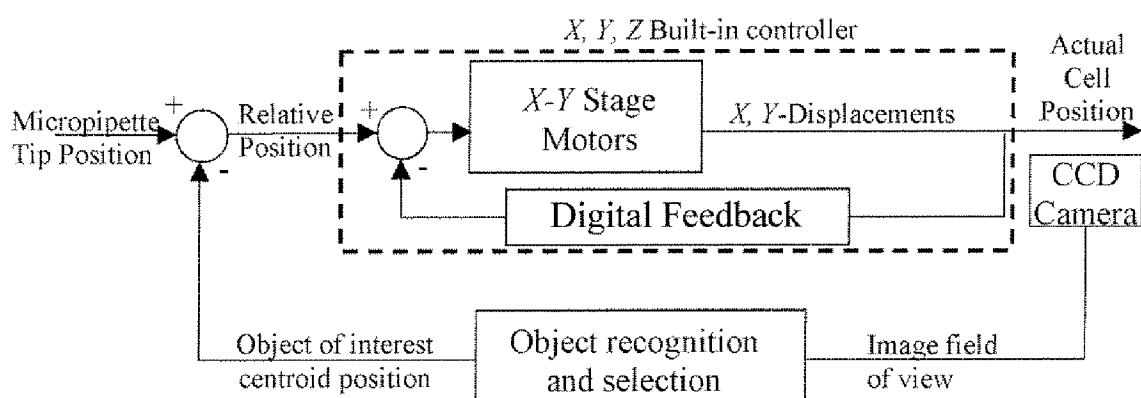


Figure 6F

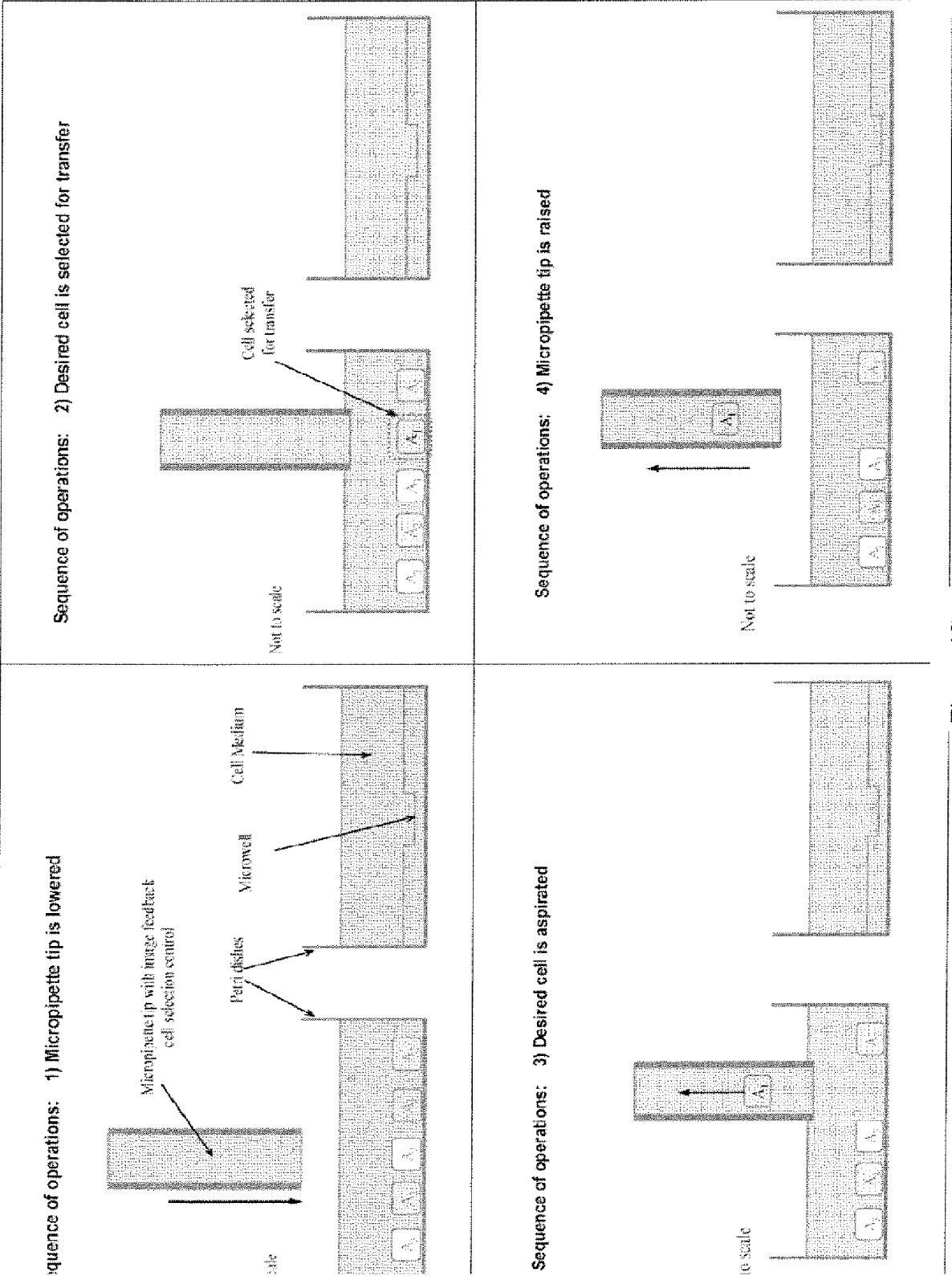


Figure 6C

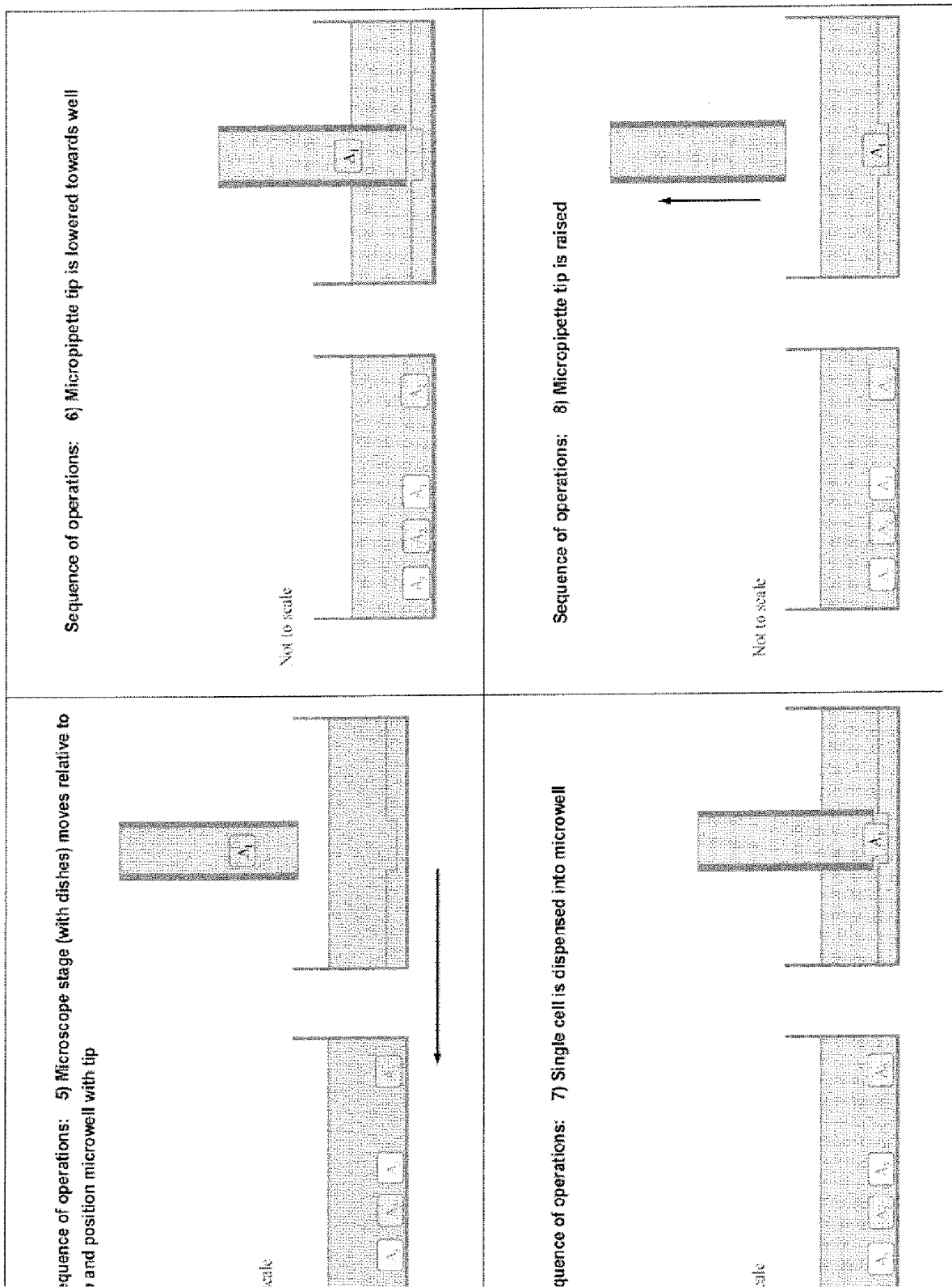


Figure 6G (con't)

Sheet 25/54

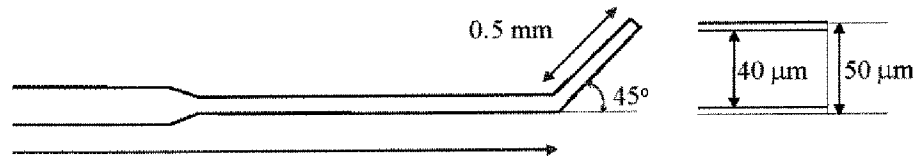


Figure 7

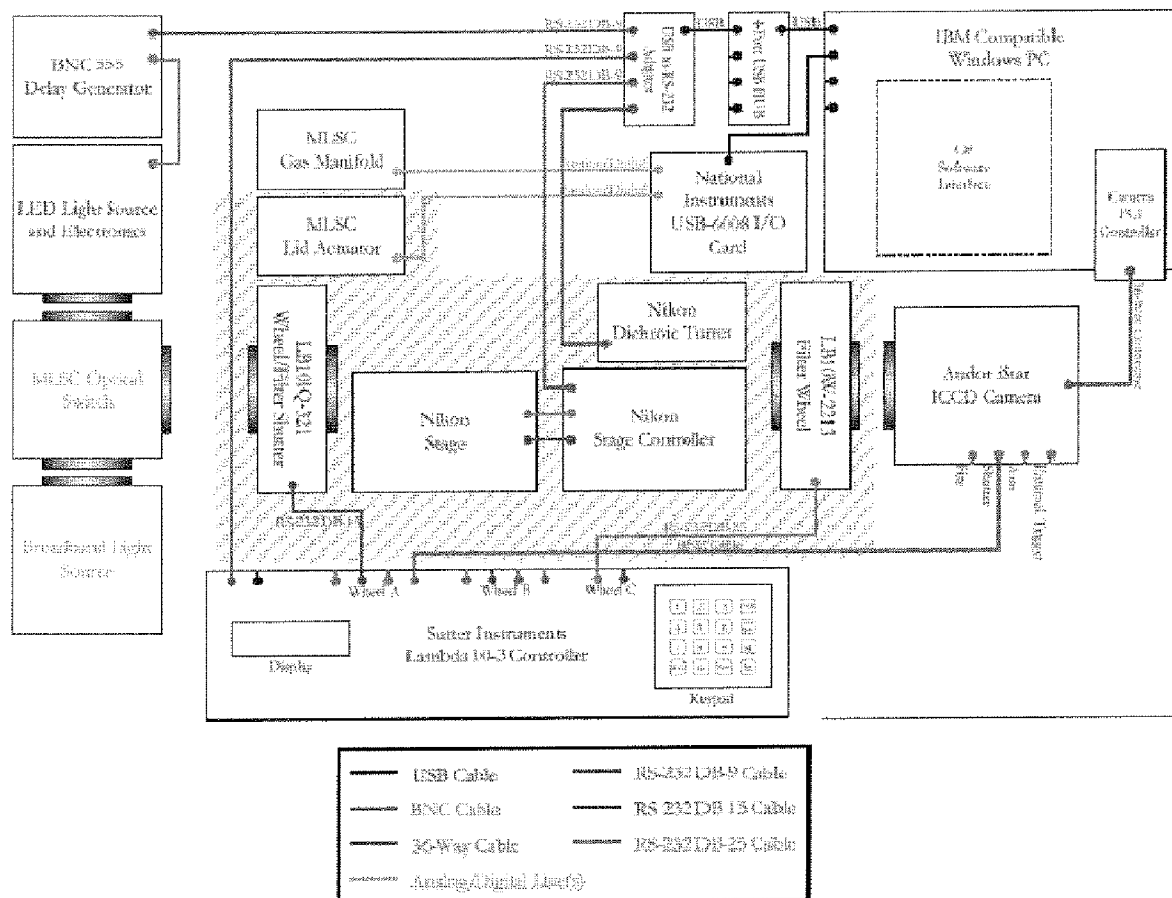


Figure 8

Sheet 26/54

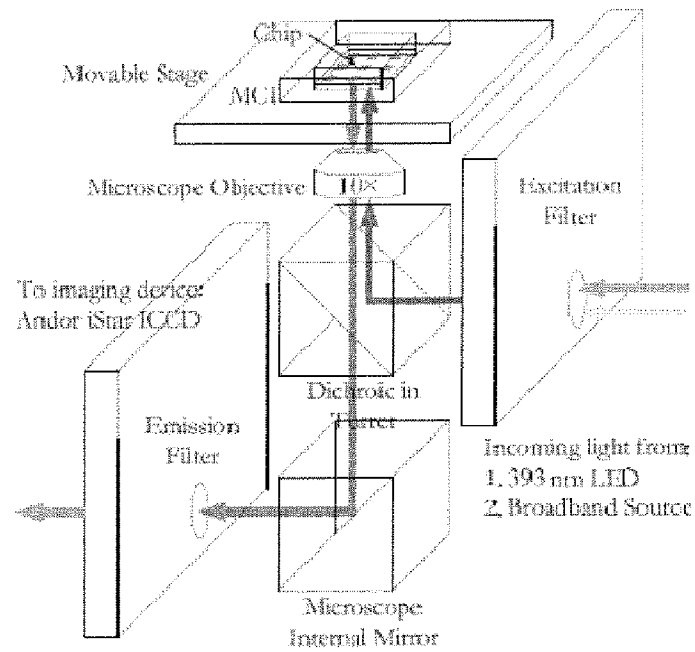


Figure 9

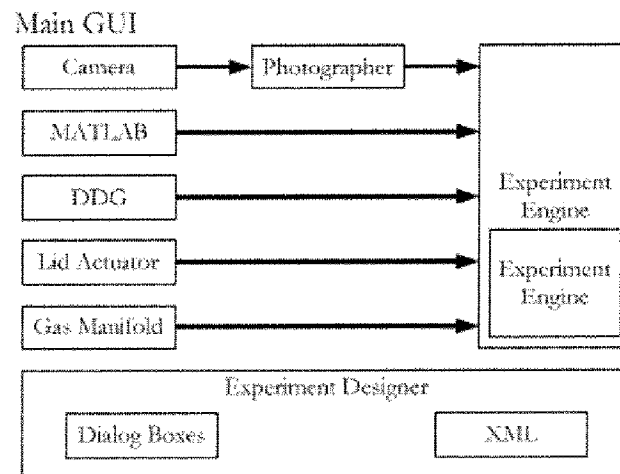


Figure 10

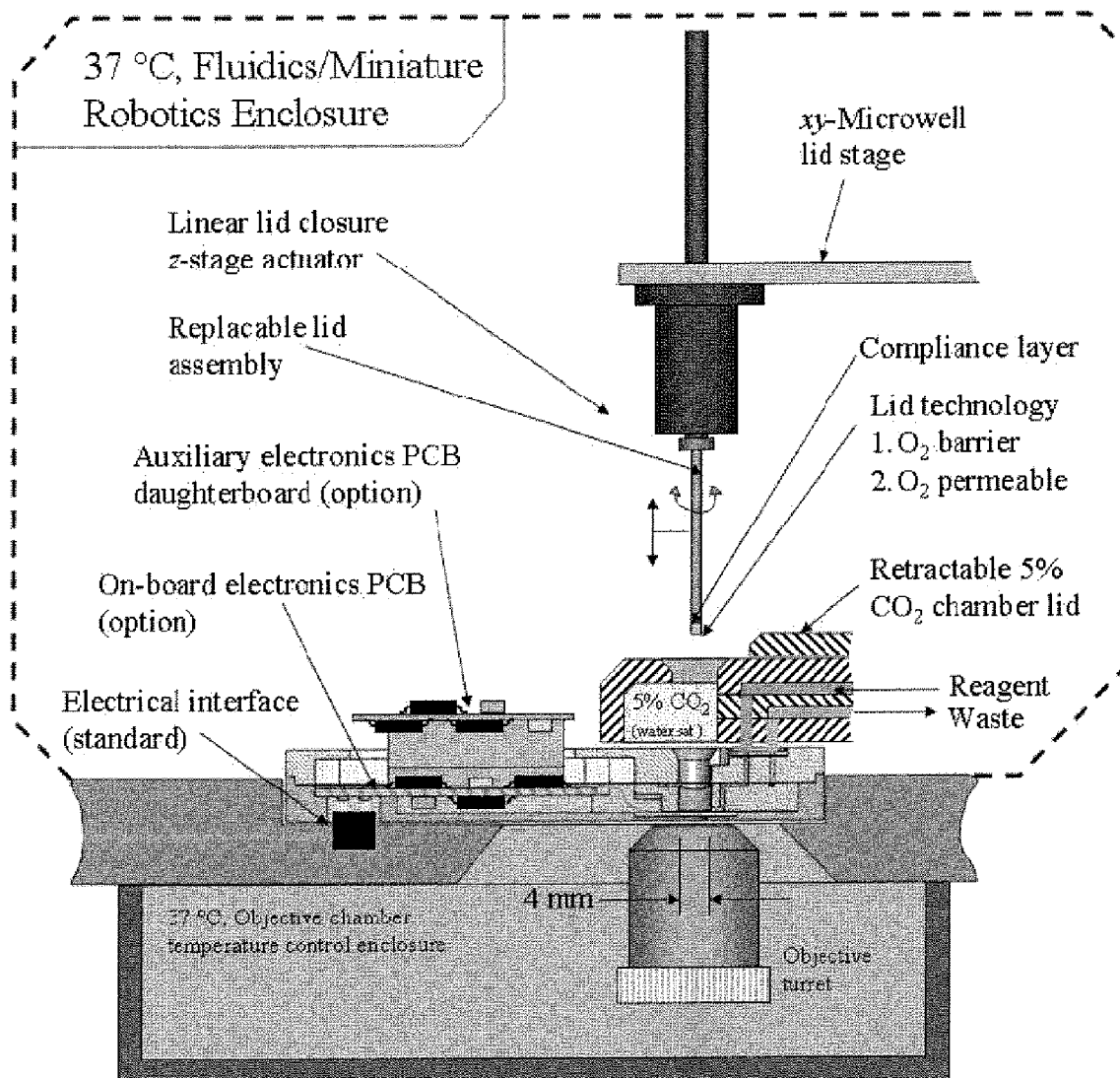


Figure 11

Sheet 28/54

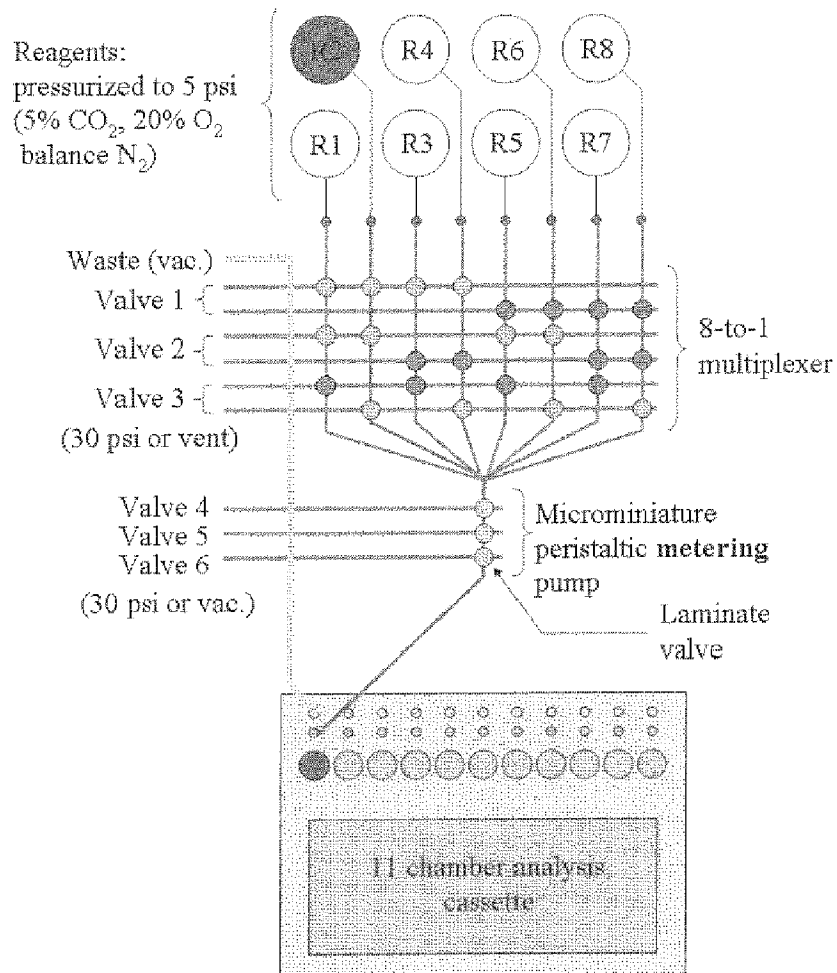


Figure 12

Sheet 29/54

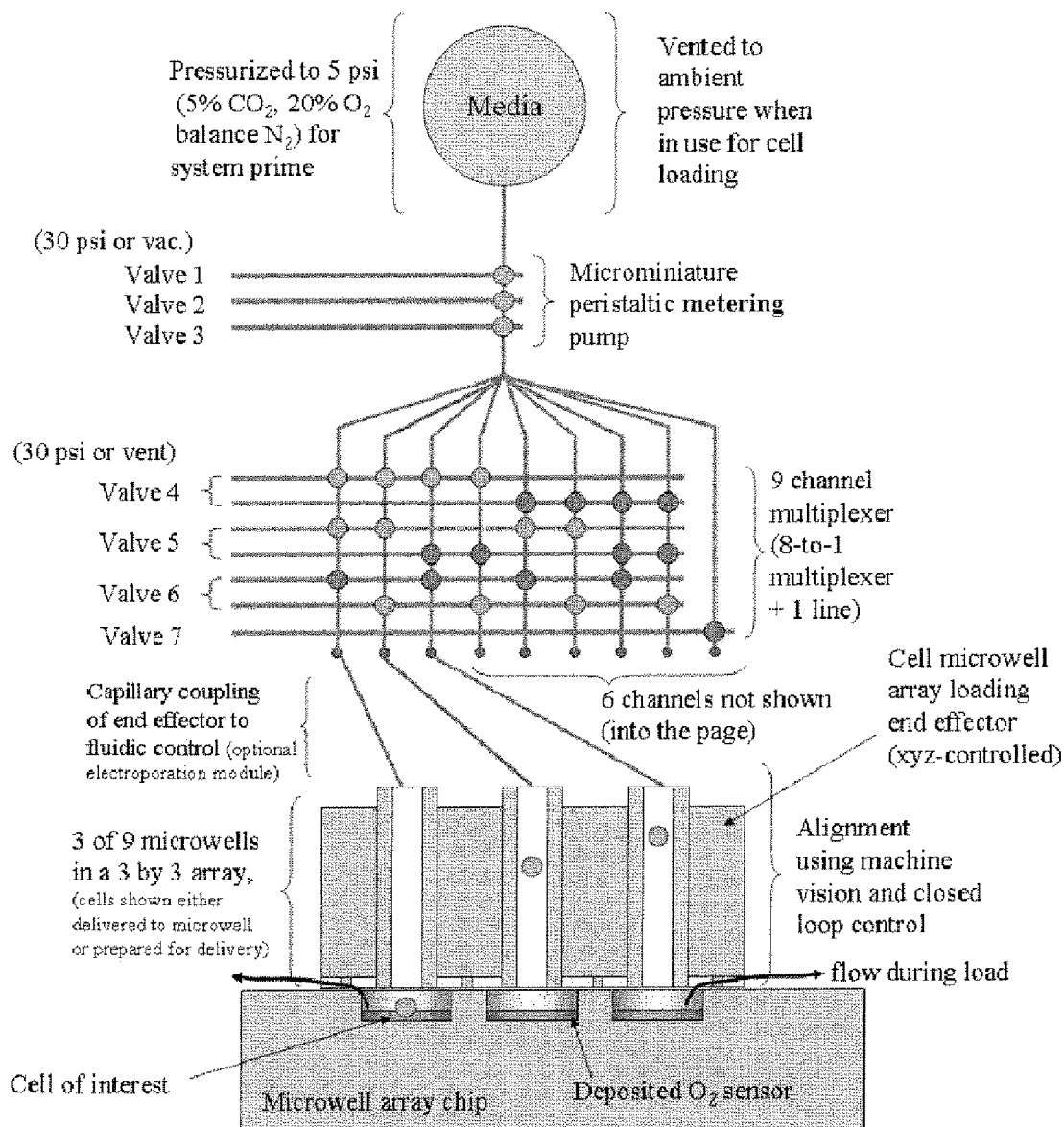


Figure 13

Sheet 30/54

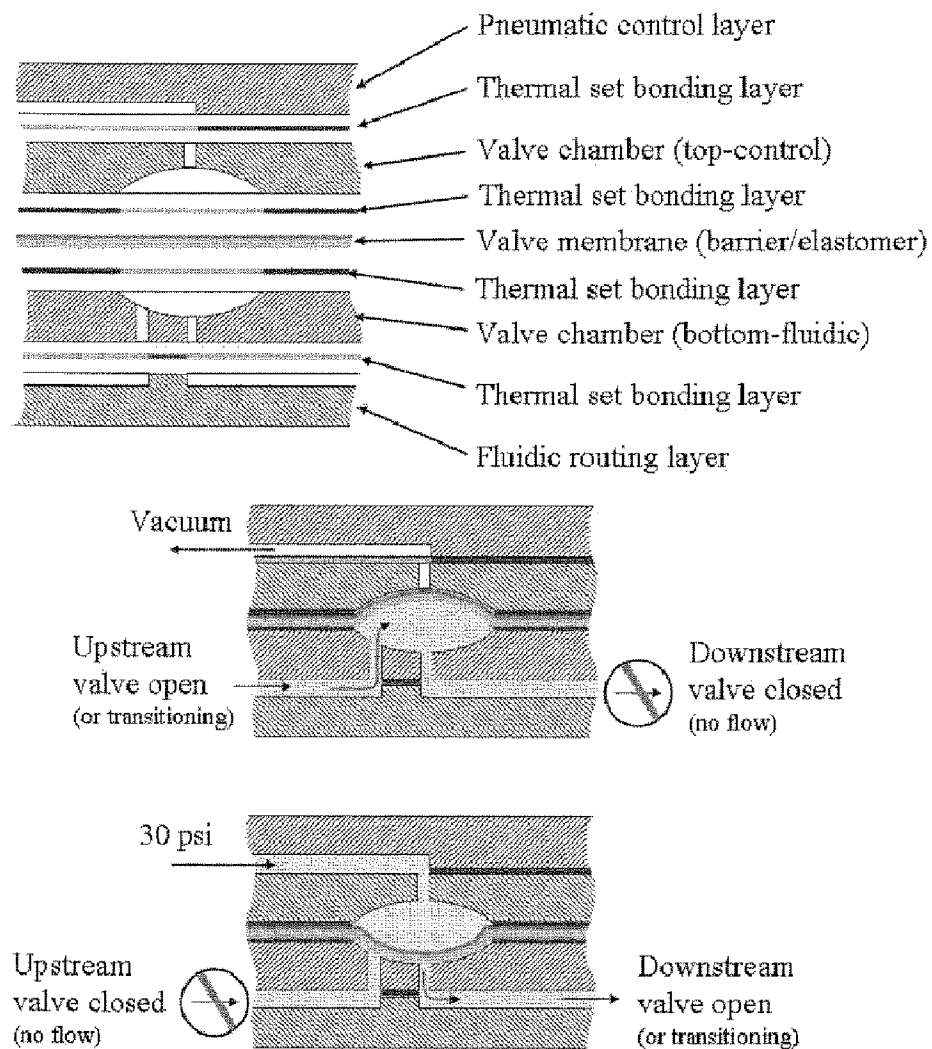
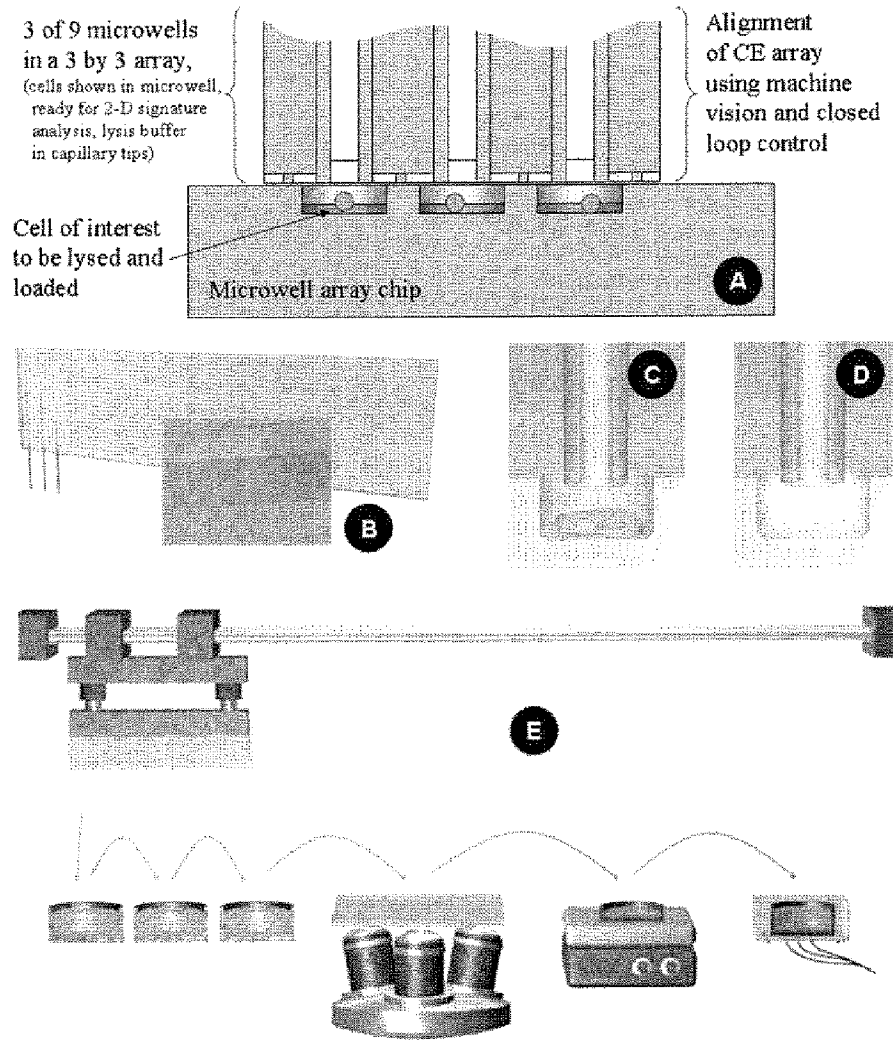
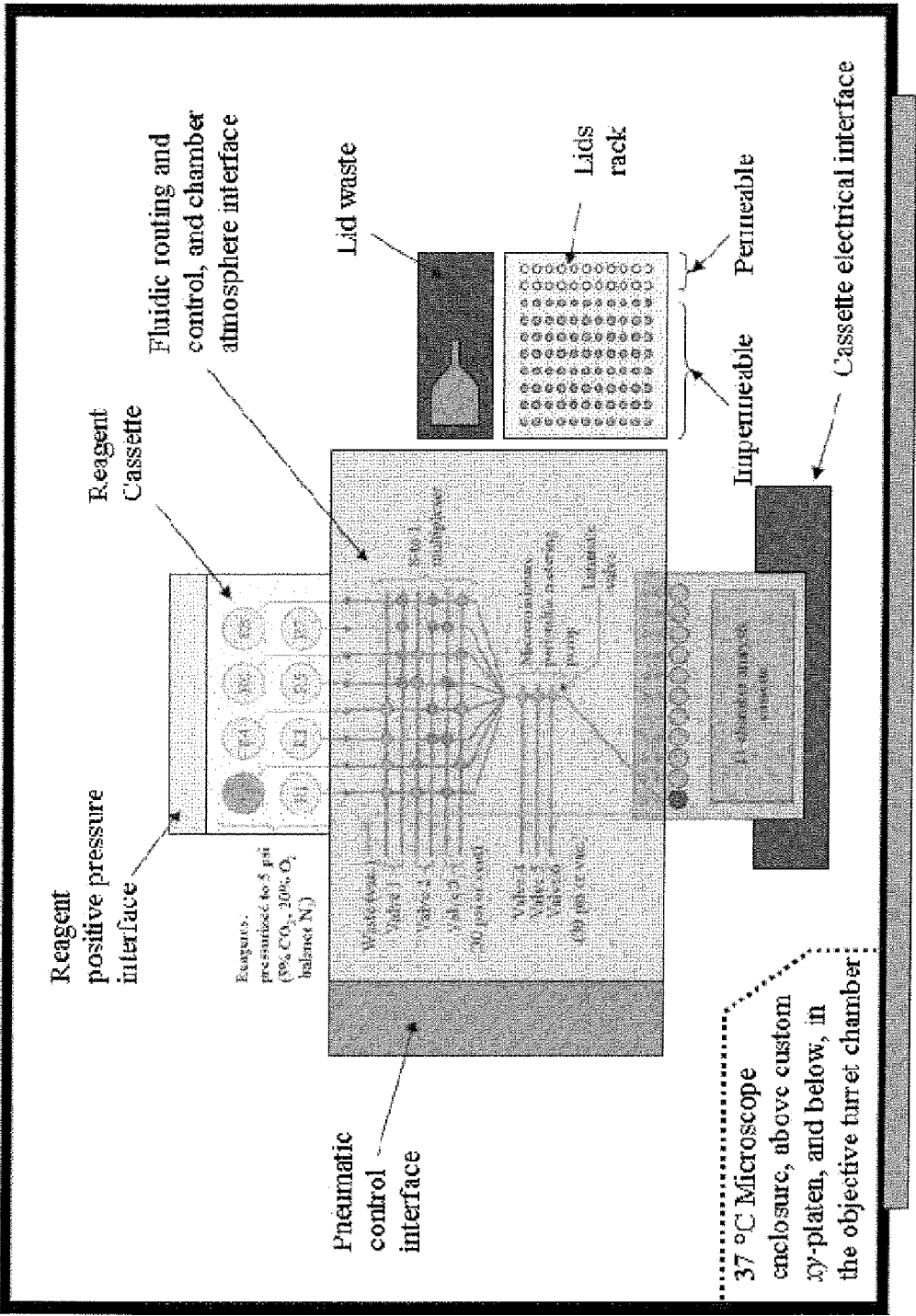


Figure 14

Sheet 31/54





Front panel access for reagent cassette, analysis cassette, and lid rack insertion.

Figure 16

Sheet 33/54

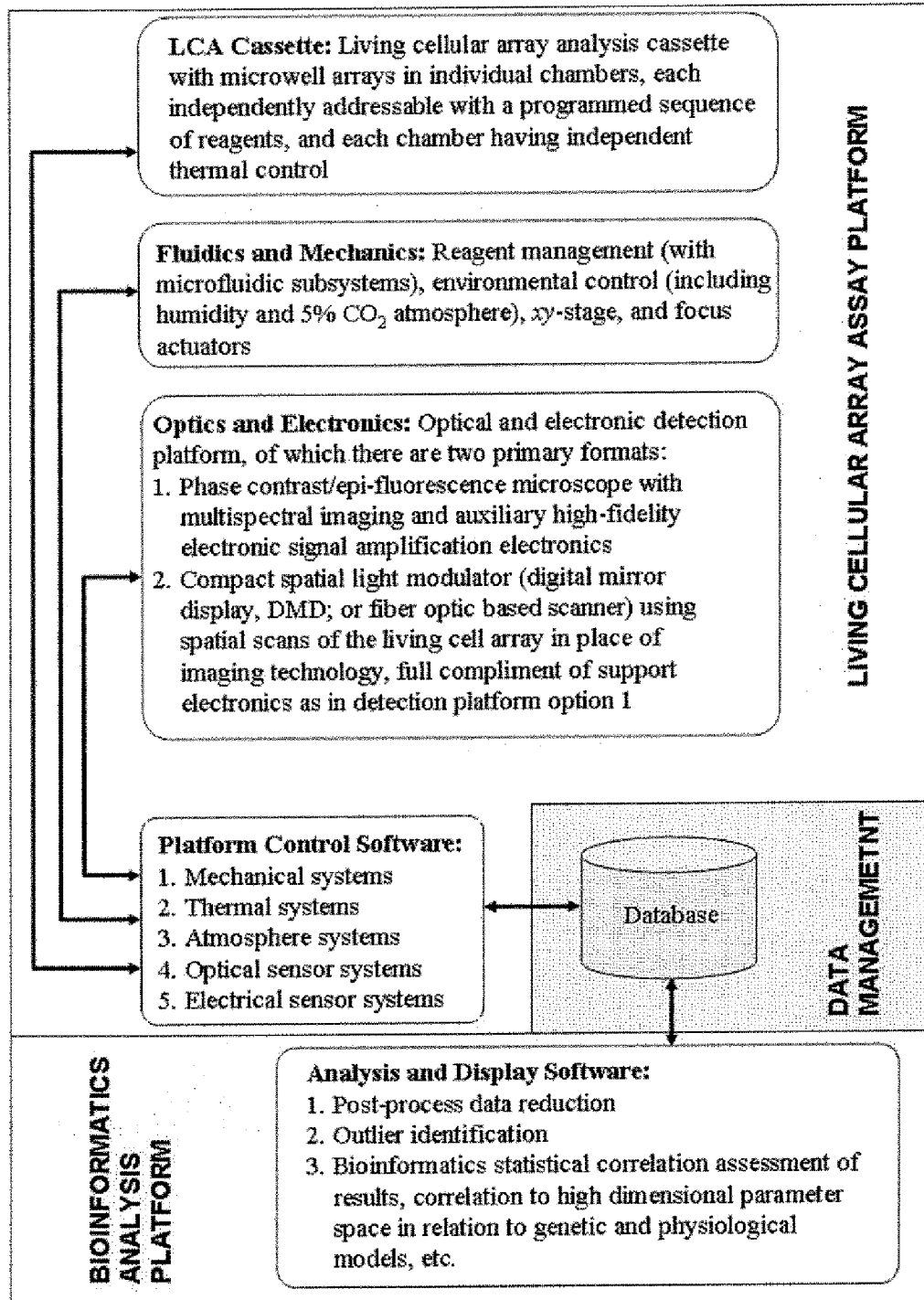


Figure 17

Sheet 34/54

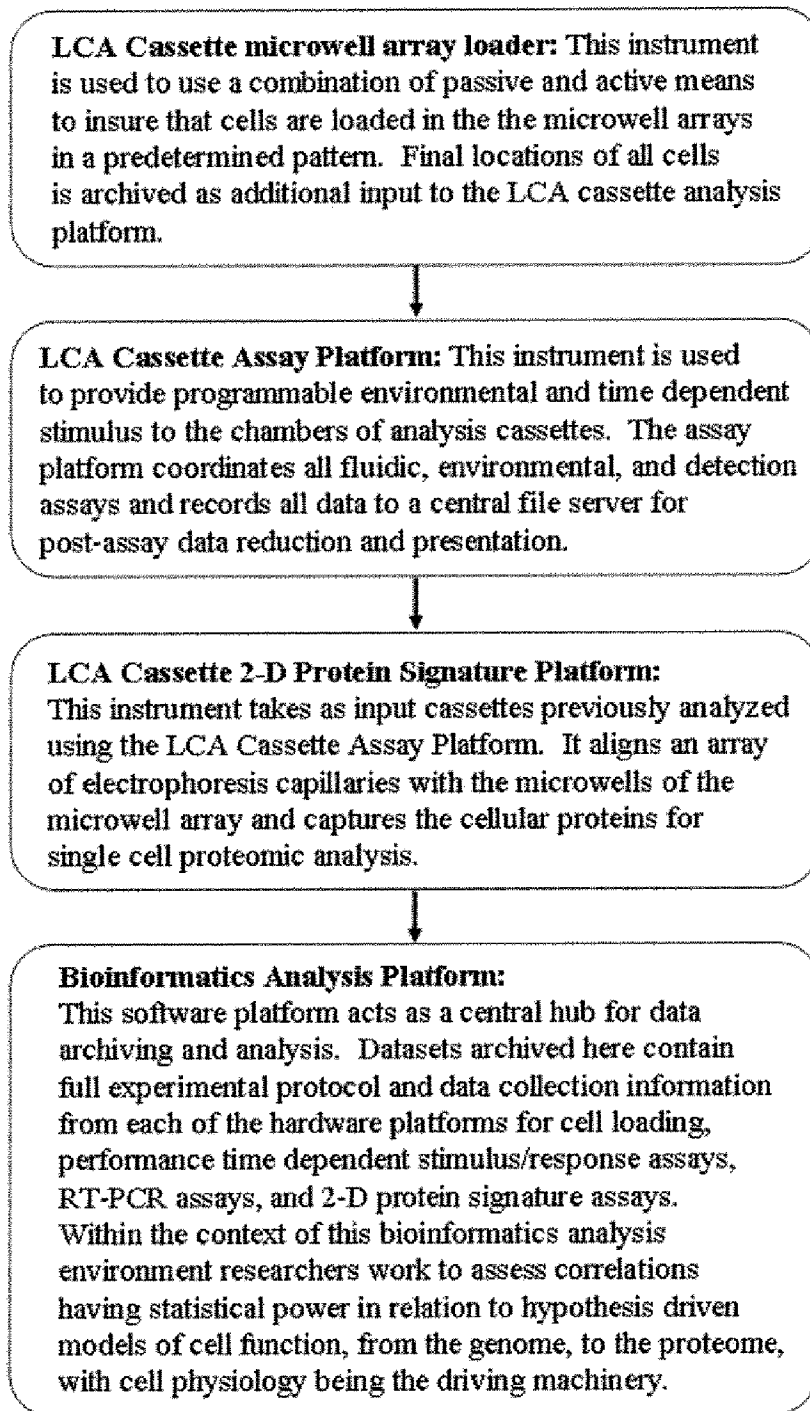


Figure 18

Sheet 35/54

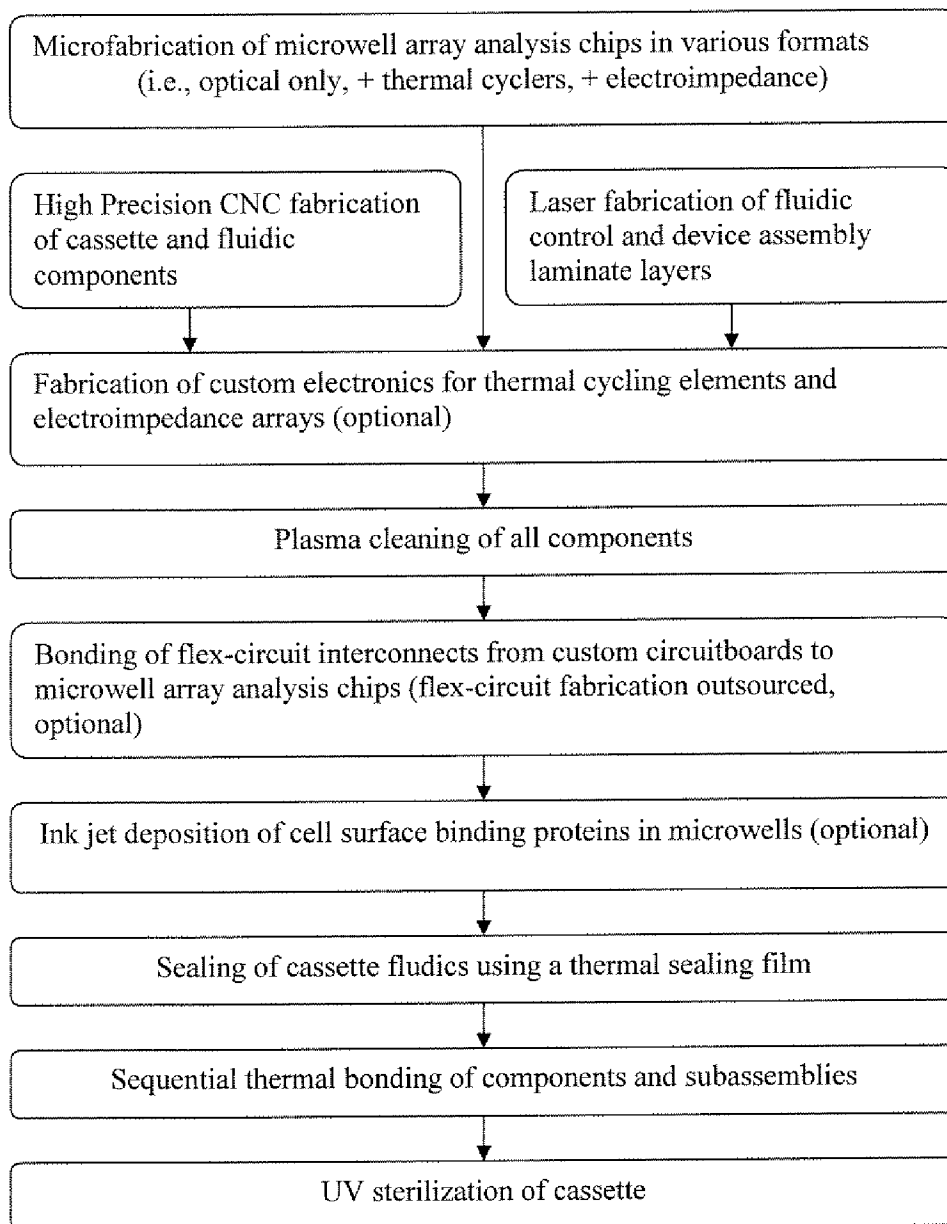


Figure 19A

Sheet 36/54

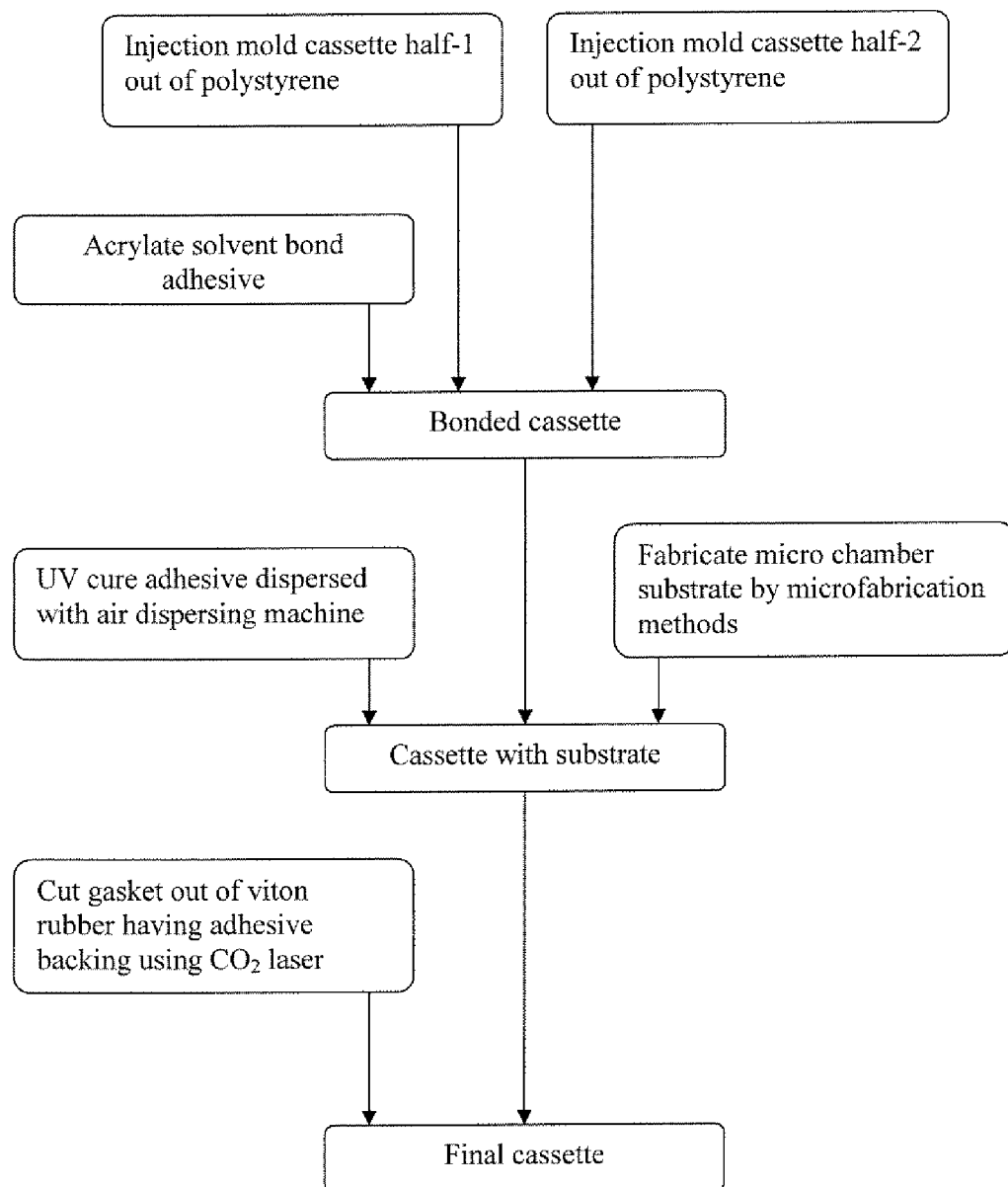
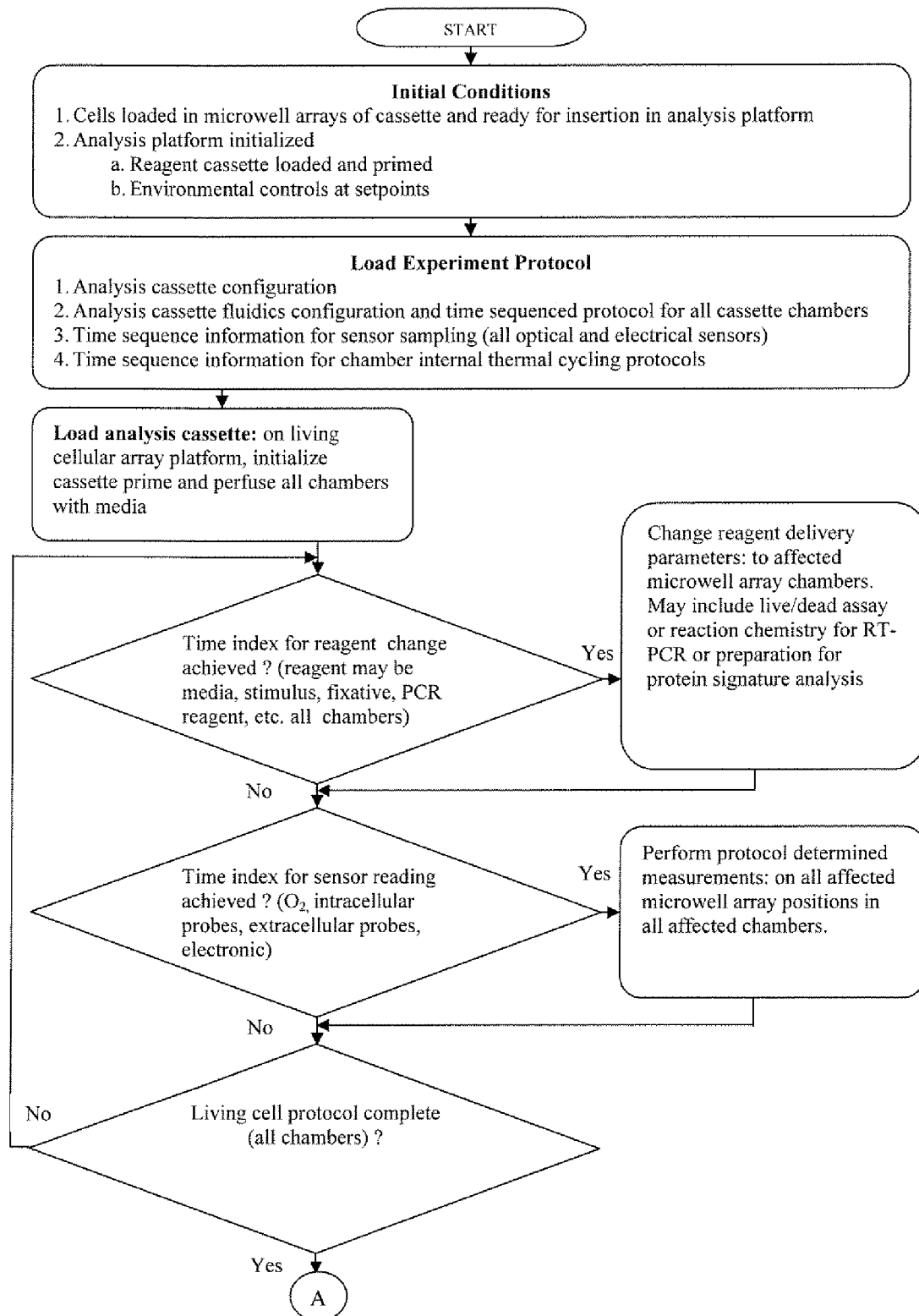


Figure 19B

Sheet 37/54



Sheet 38/54

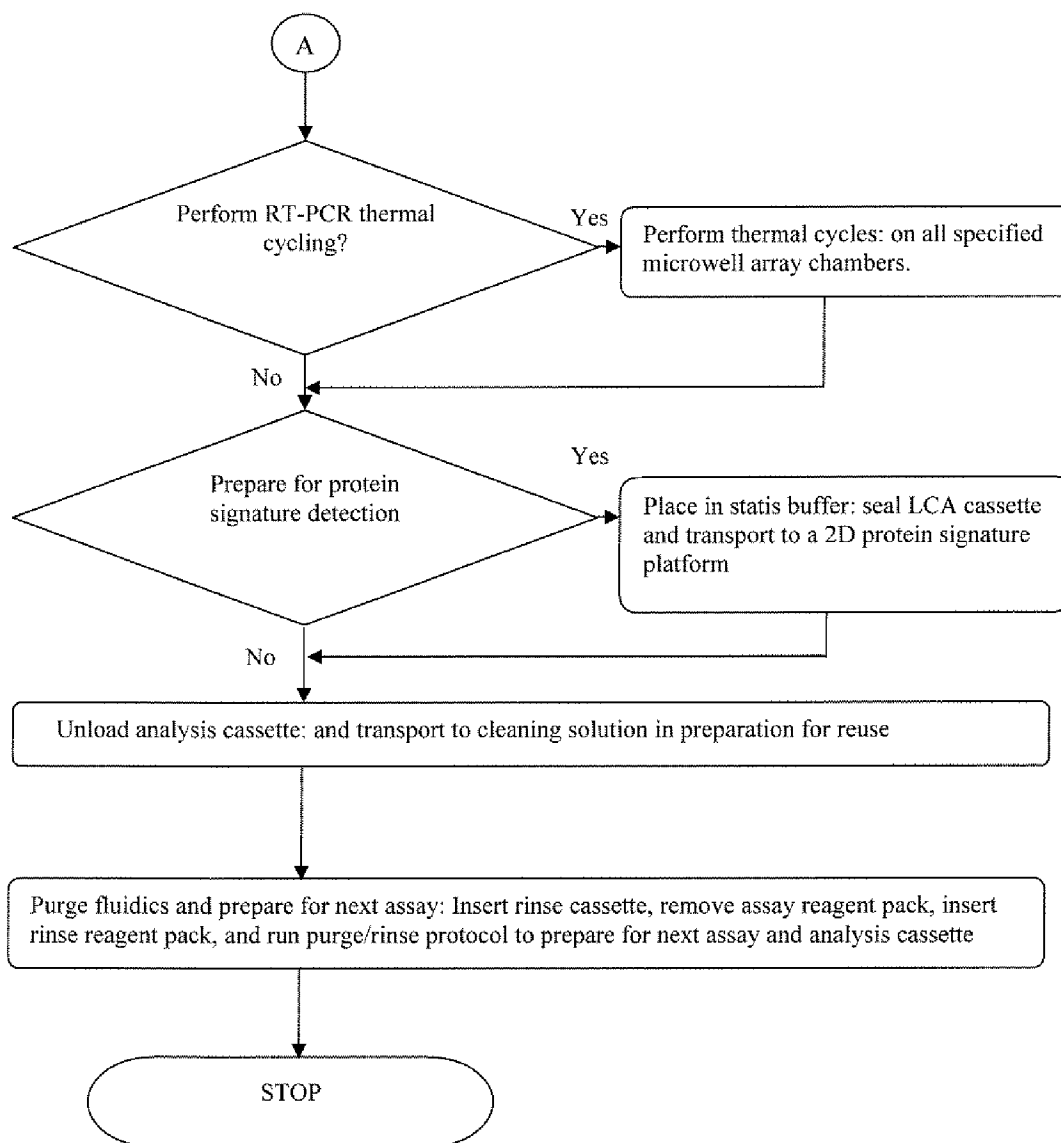


Figure 20 (con't)

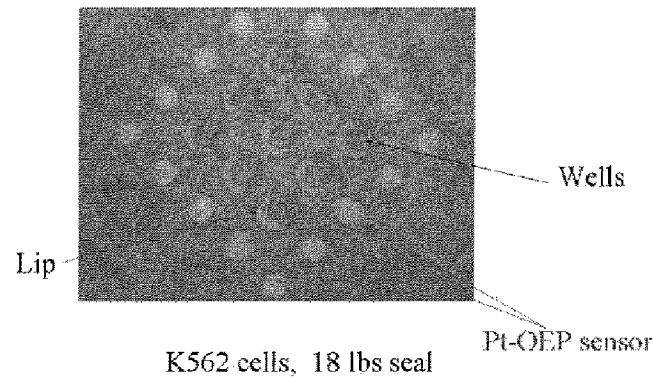


Figure 21

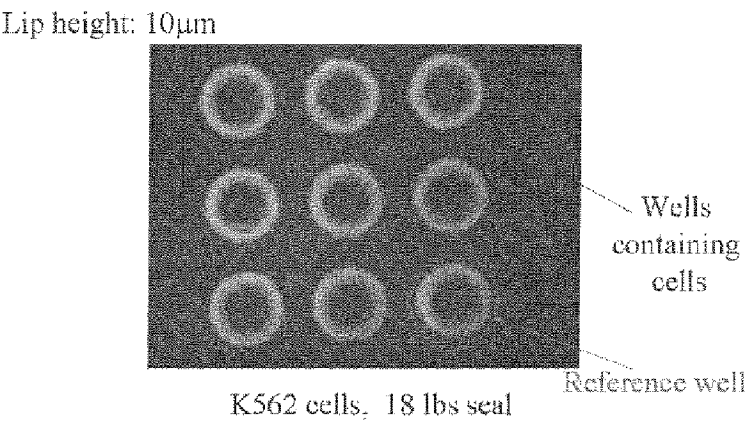


Figure 22

Sheet 40/54

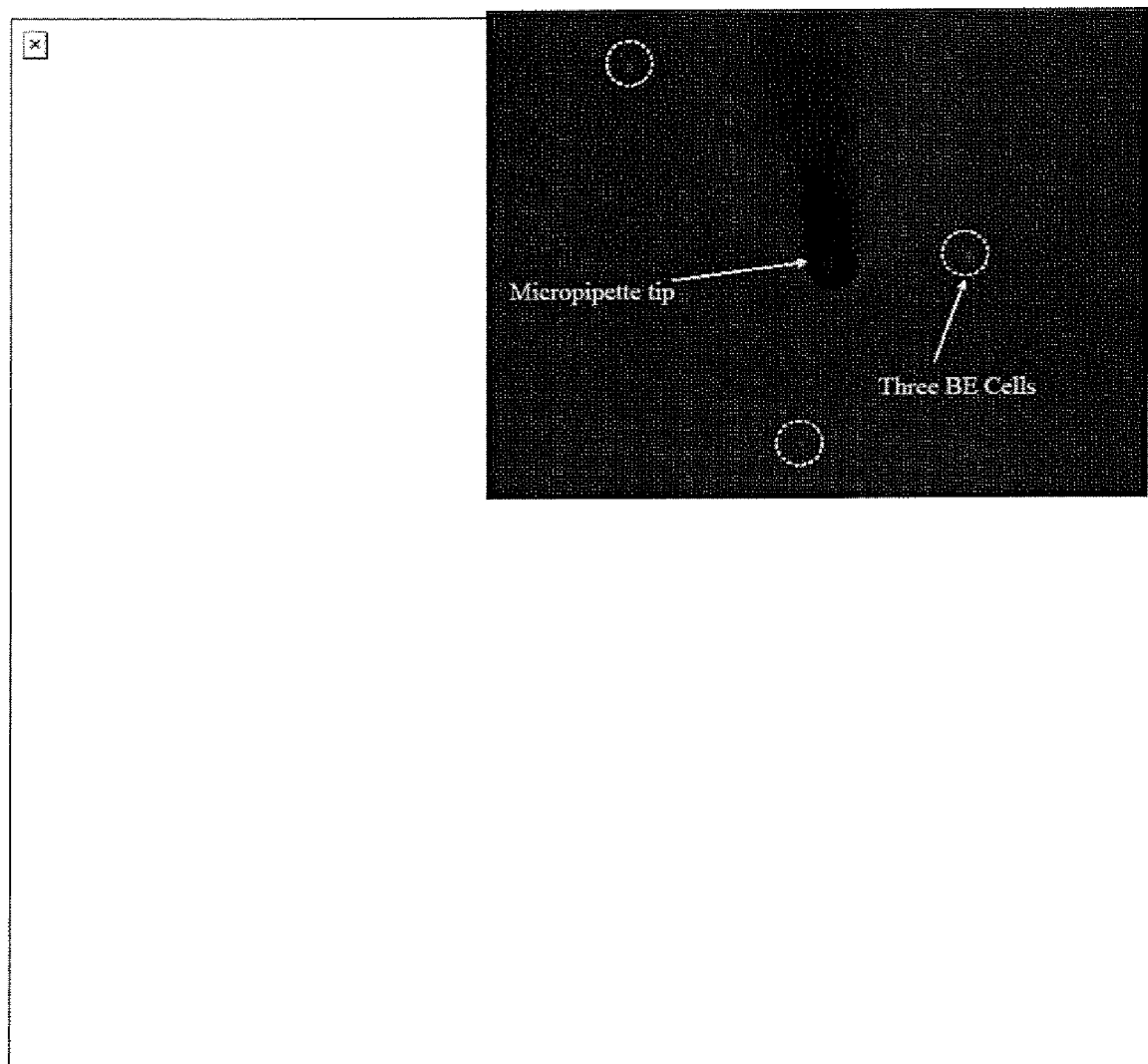


Figure 23

Sheet 41/54

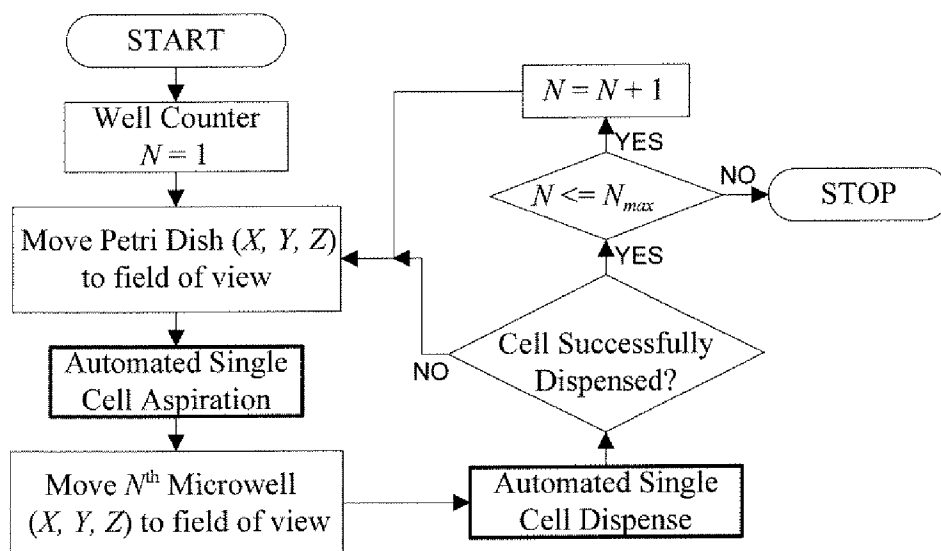


Figure 24

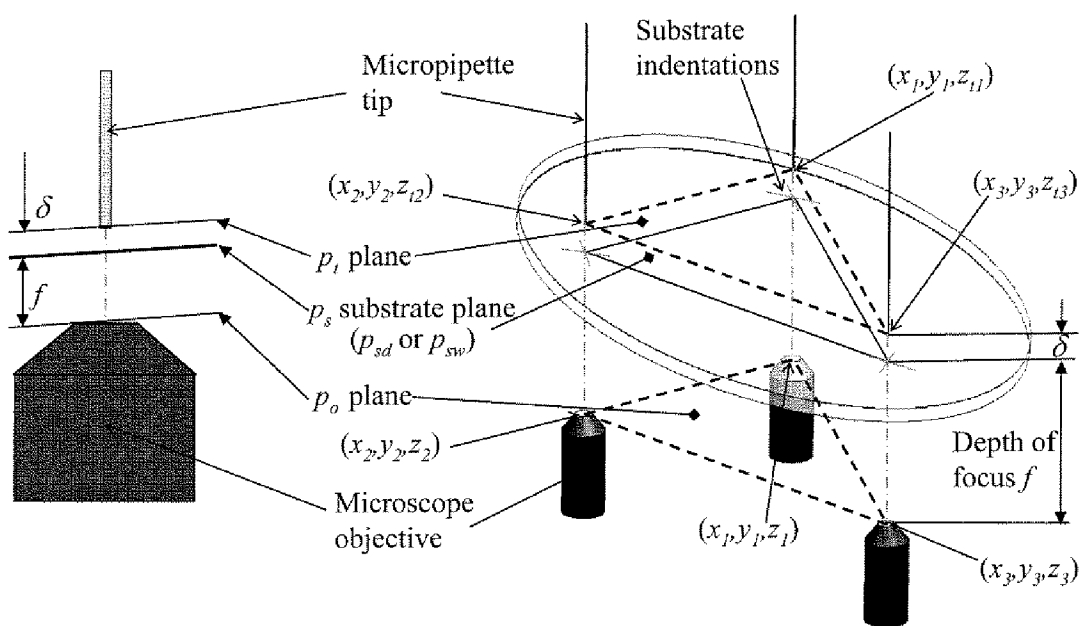


Figure 25

Sheet 42/54

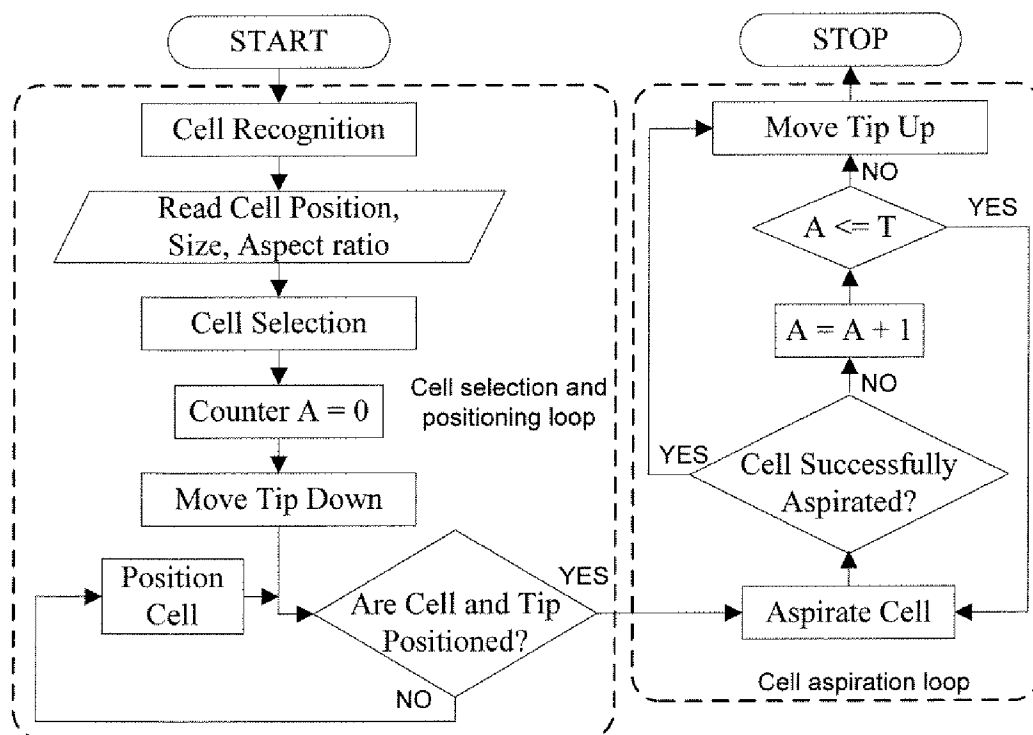


Figure 26

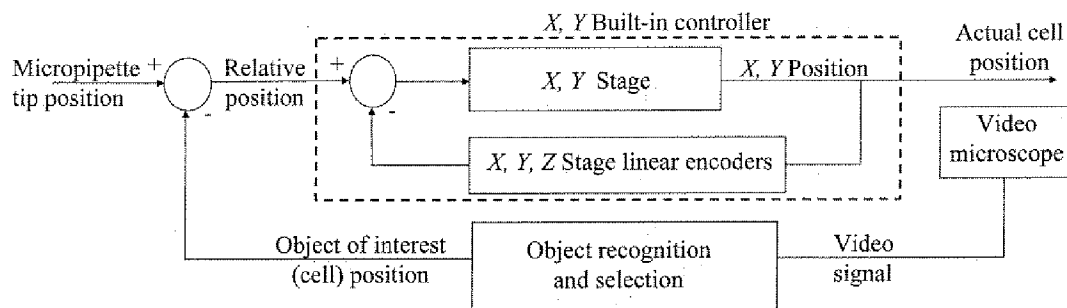


Figure 27

Sheet 43/54

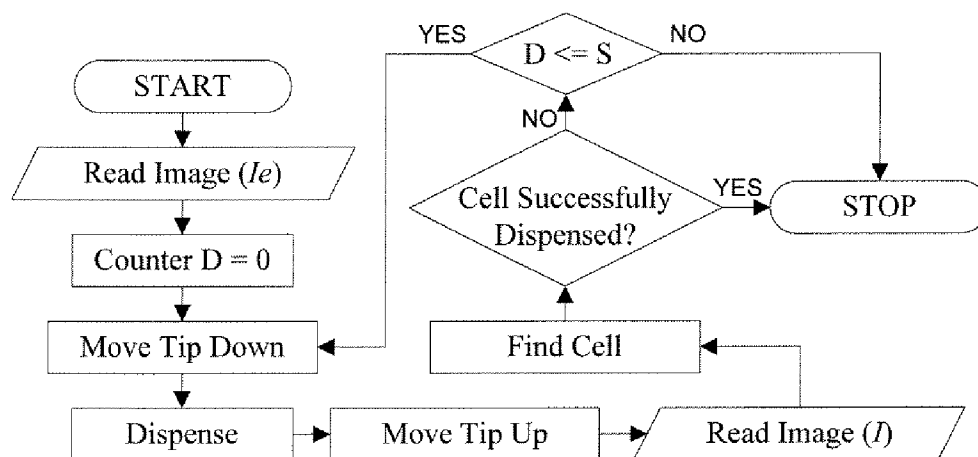


Figure 28

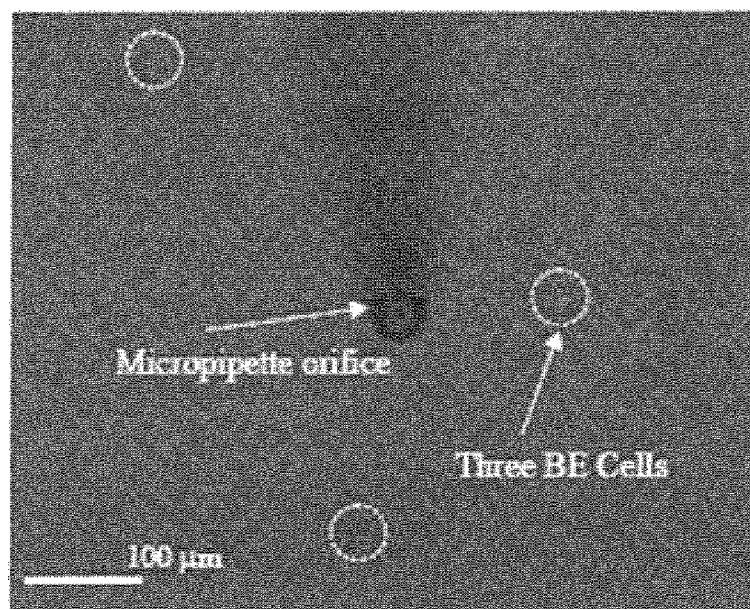


Figure 29A

Sheet 44/54

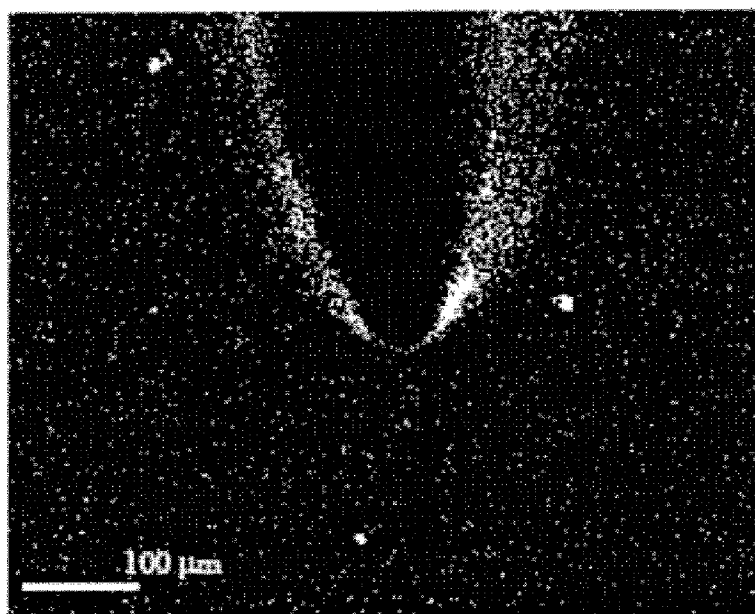


Figure 29B

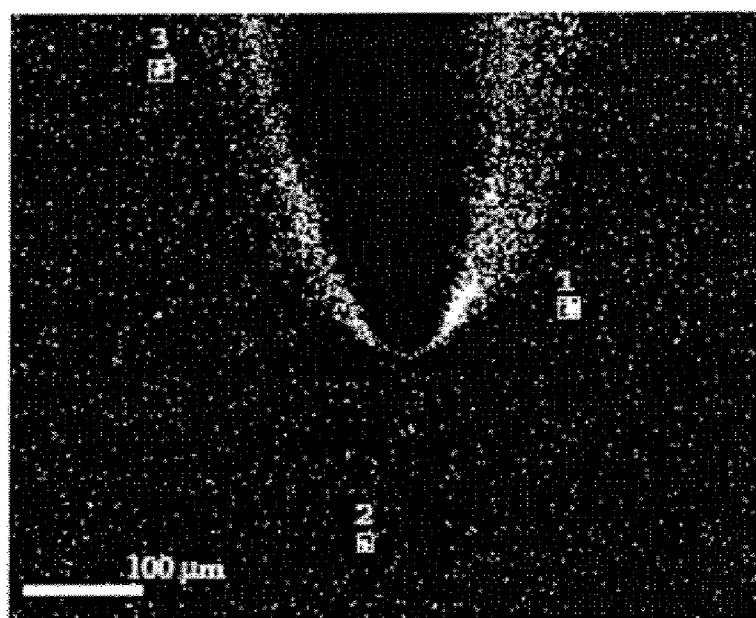


Figure 29C

Sheet 45/54

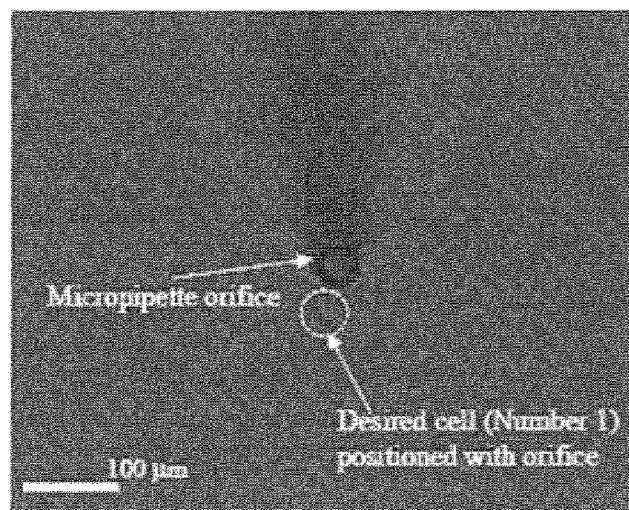


Figure 29D

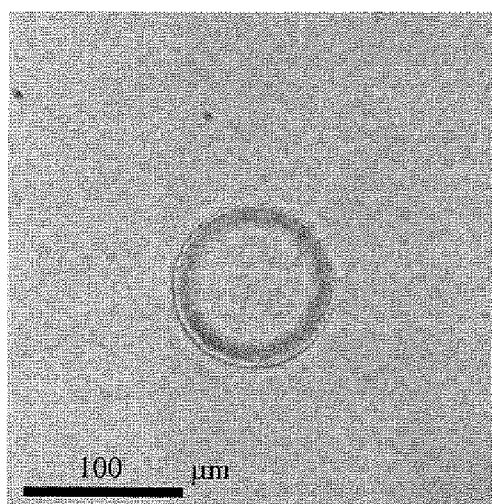


Figure 30A

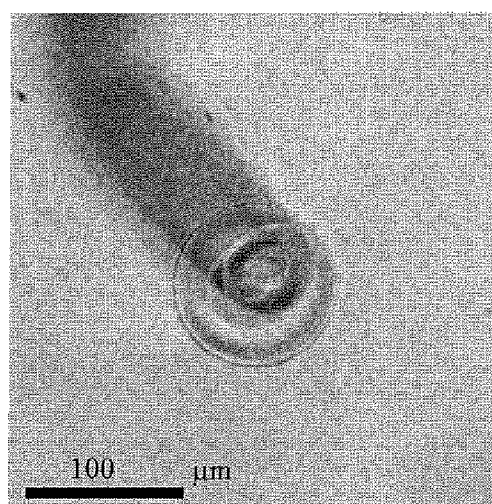


Figure 30B

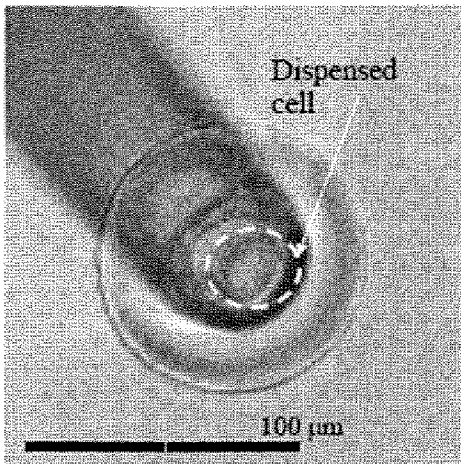


Figure 30C

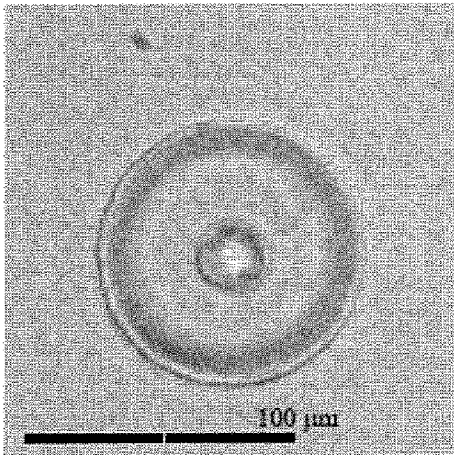


Figure 30D

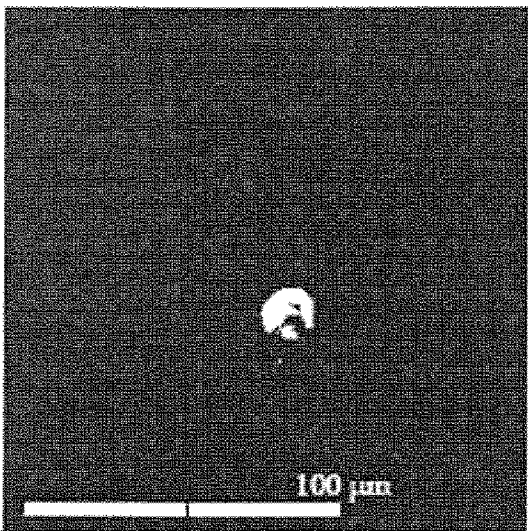


Figure 30E

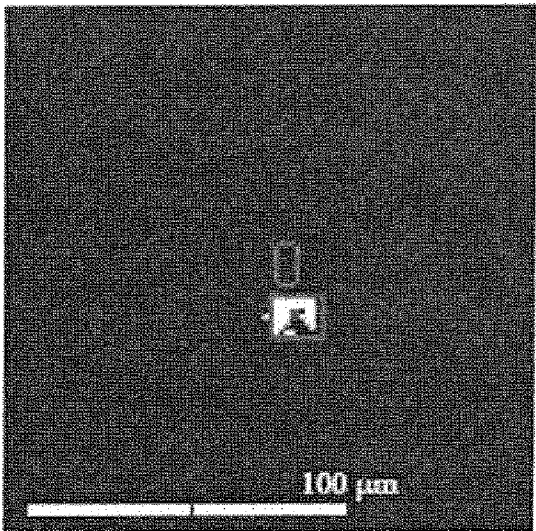


Figure 30F

Sheet 47/54

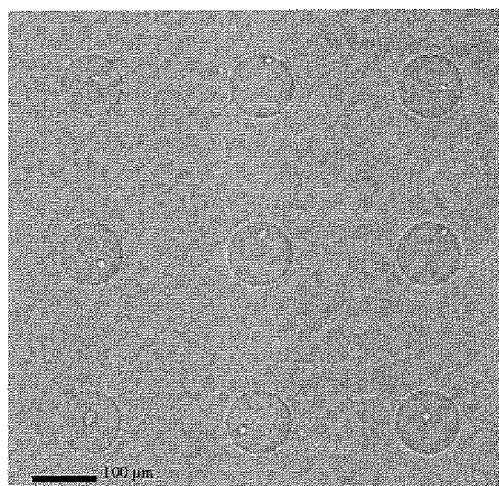
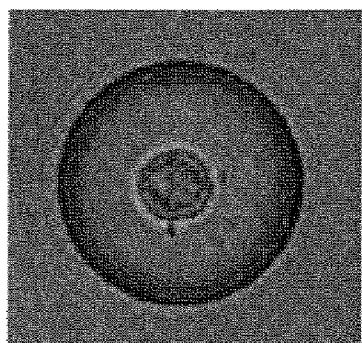
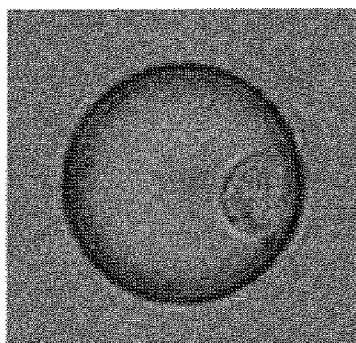


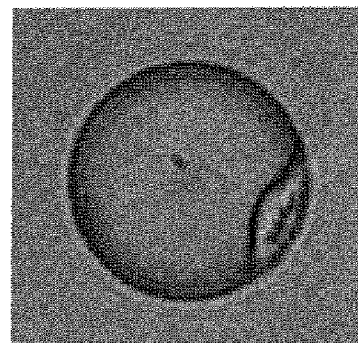
Figure 31



A



B



C

Figure 32

Sheet 48/54

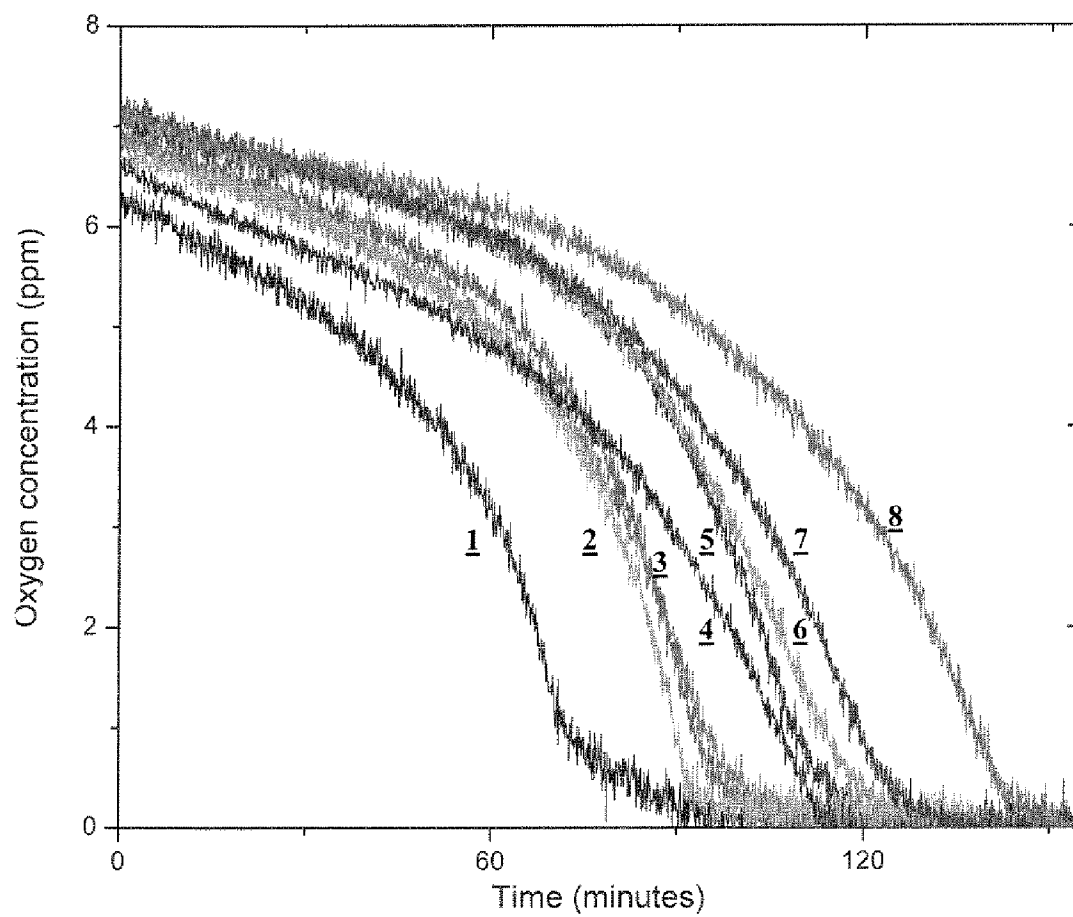


Figure 33A

Sheet 49/54

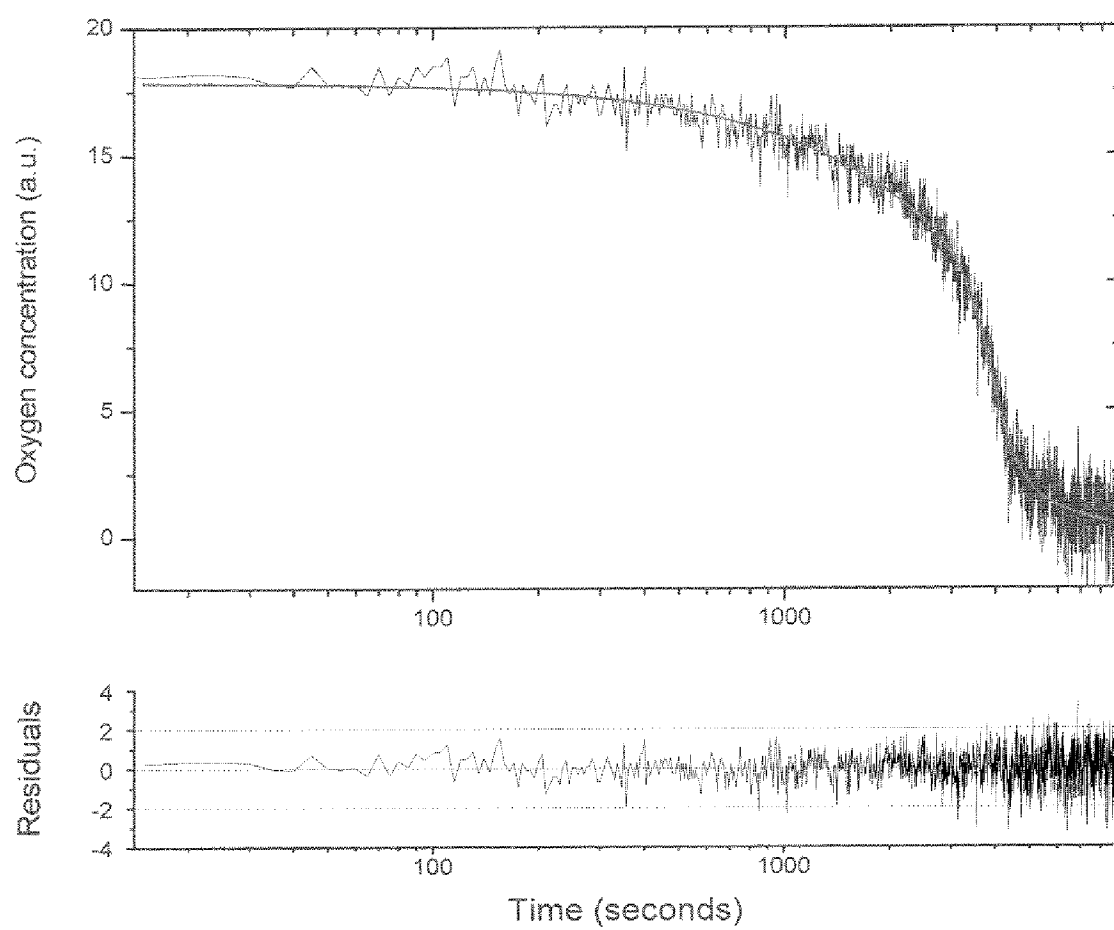


Figure 33B

Sheet 50/54

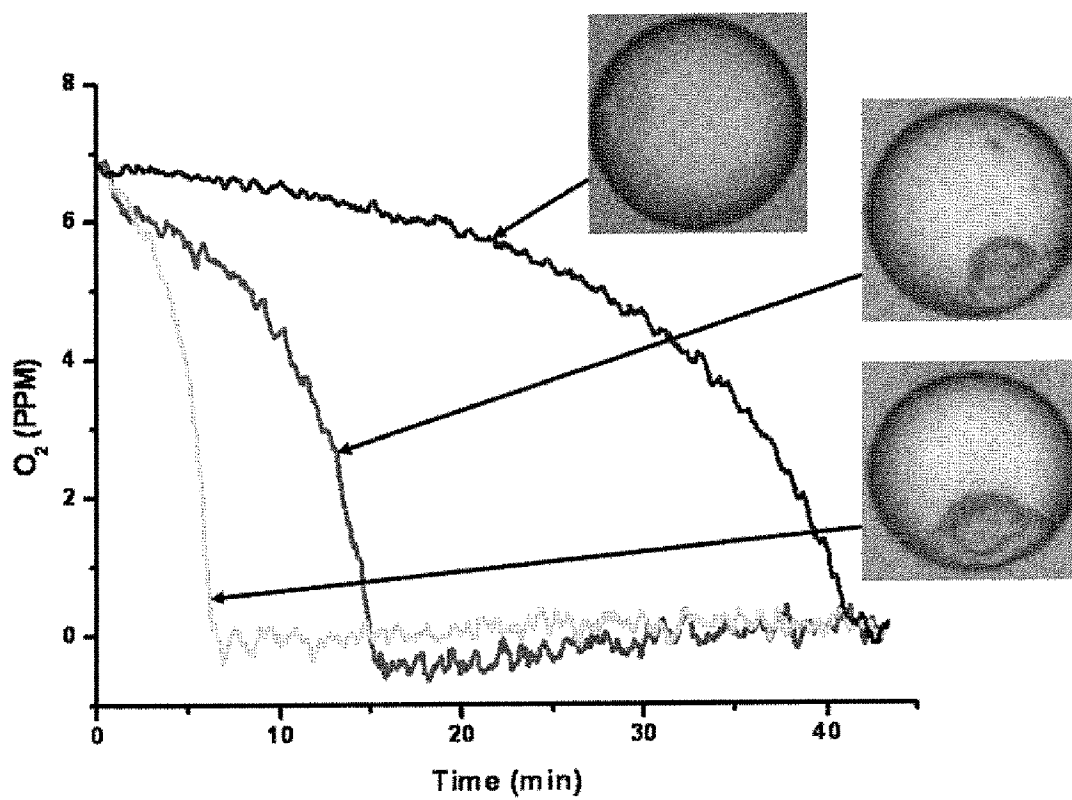


Figure 34A

Sheet 51/54

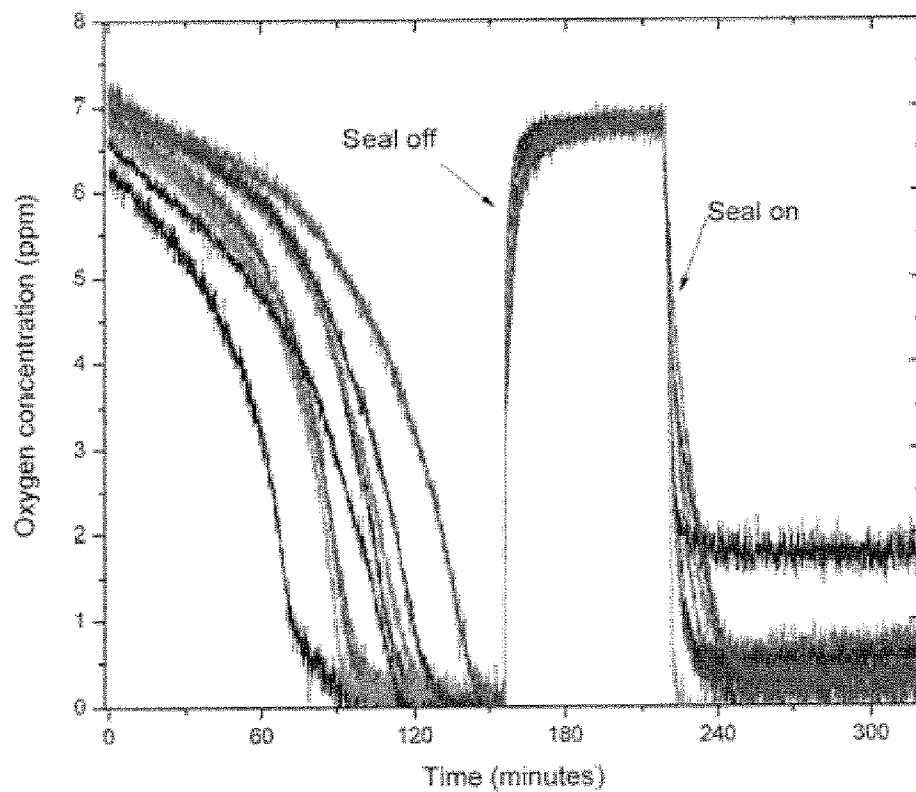


Figure 34B

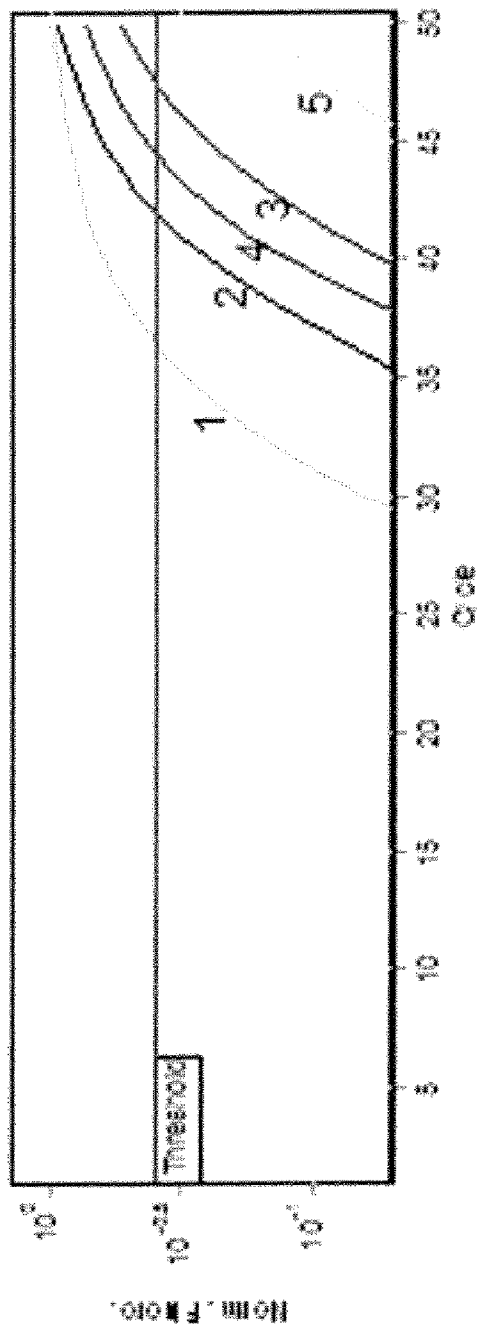


Figure 35A

Sheet 53/54







Number	Shade	ample	Ct
1		mRNA	36.60
2		single-cell	42.07
3		single-cell	47.56
4		single-cell	44.57
5		single-cell	
6		negative	

Figure 35B

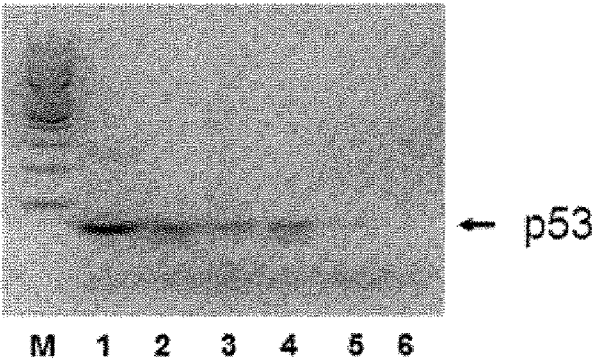


Figure 35C

Sheet 54/54

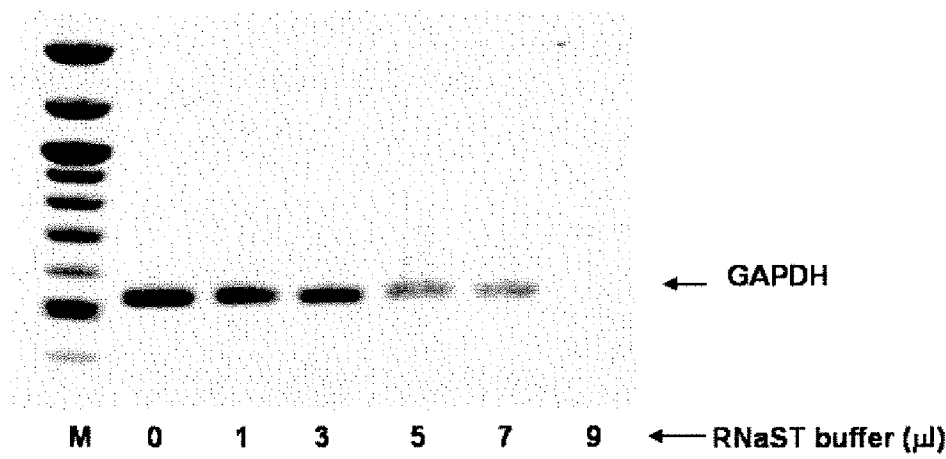


Figure 36A

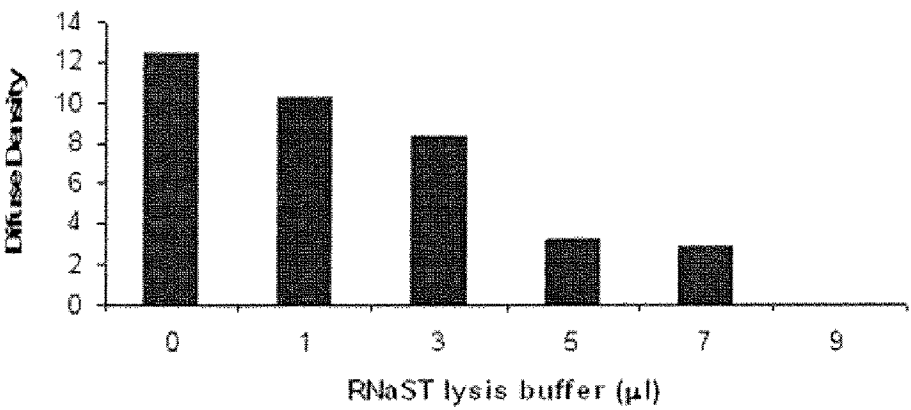


Figure 36B